Aero- and Hydrodynamic Performance Analysis of a Speed Kiteboarder

Breaking the World Speed Sailing Record

Rolf van der Vlugt
October 2009

Master Thesis Report

TUDelft Delft University of Technology

asset
Aerospace for Sustainable Engineering and Technology

Challenge the future

Delft University of Technology

Aero- and Hydrodynamic Performance Analysis of a Speed Kiteboarder

Breaking the World Speed Sailing Record

Master Thesis Report by Rolf van der Vlugt

Graduation committee:

Prof.Dr. W.J. Ockels
Prof.ir. A. Beukers
Dr.-Ing. R. Schmehl
A. de Wachter MSc

October 28th, 2009

Delft University of Technology
Faculty of Aerospace Engineering

Preface

The magical 50 knots barrier fell as the outright sailing record fell twice in 24 hours at the Luderitz Speed Challenge over the weekend. Kitesurfers demonstrate they are currently the fastest sailors on the planet. Source: www.sailing.org, 7 October 2008

50 knots has been referred to as the sailing equivalent of the sound barrier for many years. The big question was: Who would be the first one to break this barrier? Sailboats and windsurfers had been involved in this battle for many years, but it was a kitesurfer who finally broke the elusive 50 knot barrier.

I started windsurfing sixteen years ago and had my first kitesurfing experience nine years ago. I have been involved in different competitions both at national and international level. I became fascinated by the simplicity of the equipment that enables a kitesurfer to obtain record breaking velocities. In 2007 I entered my first speed kitesurfing competition. My best results since include two times a second place in a world cup competition. During the Luderitz Speed Challenge of 2008 I obtained my personal speed record of 47.36 knots, counting as the official Dutch National Speed Sailing Record.

Unfortunately I was not the one breaking the 50 knots barrier. But the battle is not over. There will always be a new magical barrier. I see it as the ultimate challenge to add the engineering skills I obtained in Delft, to my kite- and windsurfing experience. And attempt to beat the world's fastest sailing craft and break the Outright Speed Sailing World Record.

WORLD SAILING SPEED RECORD COUNCIL
AUTHORIZED BY THE INTERNATIONAL SAILING FEDERATION
I S A F

PERFORMANCE CERTIFICATE

YACHT *Xtreme 153: Airush Speed Prototype kite 7 sq.m*

OWNER / SKIPPER *Rolf van der Vlugt NED*

CREW *Singlehanded*

This is to certify that on

9th October 2008 at Luderitz, Namibia

the above achieved a performance for

The Dutch National Speed Sailing Record

DISTANCE *501 metres* AVERAGE SPEED *47.36 kts.*

CHAIRMAN OF THE COUNCIL   SECRETARY WSSRC

THIS CERTIFICATE OF ACHIEVEMENT WAS ISSUED ON *5th February 2009*

This document is the final report of my master thesis at the ASSET chair, faculty of Aerospace Engineering at the Delft University of Technology. The reader should at least have a basic knowledge of aerodynamics.

There are a number of people I would like to thank for their help and support:

- First of all I would like to thank my professor Wubbo Ockels for his support and enthusiasm and for giving me the opportunity to use the subject of speed kitesurfing for my thesis.
- I would like to thank both Wubbo Ockels and Aart de Wachter, my graduation supervisors, for their guidance and their valuable comments on my draft report.
- Roland Schmehl, for taking place in my graduation committee and for his comments on my draft report.
- Professor Adriaan Beukers, for taking place in my graduation committee.
- Rene Oudeman, for building three subsequent load cell logger versions. The load cell logger has been of enormous value for my thesis.
- John, Roland and Aart again, for their help on the beach during experiments.
- The Young Wild Ideas commission for giving me a Young Wild Ideas Award to support my research.
- And my girlfriend Katja, for reviewing parts of my report and for luring me out of bed on so many days with a hot cup of tea and a bowl of fresh fruit and yogurt.

Rolf van der Vlugt
October 28th, 2009
Delft, The Netherlands

Summary

Motivation

Speed sailing can be seen as the ultimate challenge for a sailing craft. Kiteboarders have recently shown to be capable of extremely high sailing speeds using a relatively cheap and simple combination of a kite and a board. They proved to be the world's fastest sailing crafts during a record attempt in October 2008, in September 2009 the record was broken again by a large hydrofoil trimaran. Only little is known about the performance characteristics of a kiteboarder. Research is required to investigate the possibilities to further increase the sailing speed and reach the maximum speed potential of a kiteboarder.

Problem statement

This thesis aims to obtain a general understanding of what properties are of importance to obtain a high kiteboarding velocity and to understand how each component contributes to the finally obtained velocity.

Approach

A kiteboarder can be seen as a sailing system. It is first explained how to calculate the sailing velocity when wind velocity and both the aerodynamic and hydrodynamic efficiency is known. The kiteboarder is divided into four components; the board, the rider, the lines and the kite. Each component is separately analyzed. The aerodynamic forces on the rider and the lines are estimated using available theory. A special effort is made to investigate the kite's lift and drag coefficients. A new kite testing method is proposed. The test is based on steering the kite in a horizontal path from one side to the other while constantly monitoring kite velocity, line tension and wind velocity. The hydrodynamic properties of the board are analyzed using available empirical results and by analyzing measured data from a kiteboarding session.

Two steady state models are built to combine all the obtained knowledge. In the first model the sailing velocity is one of the input parameters. This model serves to provide an overview of all forces involved in a realistic sailing situation. Variations of wind velocity over height are taken into account. Two cases are described and worked out to obtain an overview of the drag distribution over the kiteboarder. The second model serves to predict the improvement in velocity after improving one of the components and is used to optimize line length and sailing direction.

Results

It is found that during record sailing conditions 20 to 21 percent of the total drag is created by the kite, 13 to 18 percent by the rider, 3 to 6 percent by the lines and 56 to 63 percent by the interaction of the board with the water. Research focused on the board could thus lead to a large velocity increment. It is also found that optimizing line length and sailing direction could result in substantial velocity increments.

Contents

Nomenclature

AR	=	Aspect ratio [ ]
BL%	=	Percentage of the total line tension that acts on the back/steering lines [%]
$(C_{D,c})_{\beta=0}$	=	Cross flow drag coefficient for a flat plate [ ]
C	=	Sutherland's constant for air [120 K]
Cd	=	Drag coefficient [ ]
$C_{D,basic}$	=	Line drag coefficient for a line perpendicular to the flow [ ]
$C_{D,line}$	=	Line drag coefficient [ ]
$C_{D,line,k}$	=	Line drag coefficient based on the dynamic pressure at the location of the kite (ρ_a $v_{a,k}/2$) and defined over the total line surface area S_{line}. [ ]
$C_{D,S}$	=	Board drag coefficient based on the principal wetted area [ ]
C_{D0}	=	Zero lift drag coefficient [ ]
$C_{Dk,I}$	=	Aerodynamic drag force coefficient of the kite in sweep number i [ ]
C_{Dkl}	=	Kite drag coefficient after correcting for line drag [ ]
C_f	=	Friction coefficient [ ]
$C_{L,line}$	=	Line lift coefficient [ ]
$C_{L,S}$	=	Board lift coefficient based on the principal wetted area [ ]
$C_{Lk,I}$	=	Aerodynamic lift force coefficient of the kite in sweep number i [ ]
C_{Lkc}	=	Kite lift coefficient after centrifugal force correction [ ]
$C_{N,line}$	=	Line normal force coefficient [ ]
$C_{Rk,I}$	=	Aerodynamic resultant force coefficient of the kite in sweep number i [ ]
d	=	Diameter [m]
D_a	=	Total aerodynamic drag force [N]
D_{board}	=	Board drag force [N]
$D_{friction}$	=	Board friction drag force [N]
D_h	=	Total hydrodynamic drag force [N]
D_k	=	Kite aerodynamic drag force [N]
d_{line}	=	Line diameter [m]
$D_{line,i}$	=	Drag of line section i [N]
$D_{line,k}$	=	Line drag result on the kite [N]
D_{rider}	=	Aerodynamic drag force acting on the rider [N]
dv/dt	=	kite acceleration [m/s^2]
e	=	Oswald factor [ ]
F	=	Mechanical contact force [N]
F_{board}	=	Contact force between board and rider [N]
F_{cent}	=	Centrifugal force acting on the kite during sweep [N]
Fr	=	Froude number [ ]
g	=	Gravitational constant [9.81 m/s^2]
h	=	Height [m]
h_{kite}	=	Height of kite position [m]
$h_{line,I}$	=	Height of line section i [m]
h_{rider}	=	Height of rider center of gravity [m]
L	=	Length [m]
L_a	=	System total aerodynamic lift force [N]
$L_{a,h}$	=	Horizontal component of total aerodynamic lift force [N]
L_h	=	System total hydrodynamic lift force [N]
$L_{h,h}$	=	Horizontal component of total hydrodynamic lift force [N]
l_i	=	Length of line section i [m]

L_k	=	Kite aerodynamic lift force [N]
$L_{line,l}$	=	Lift of line section i [N]
m_k	=	Mass kite [kg]
m_k	=	Kite mass [kg]
$M_{line,l}$	=	Moment around the origin introduced by line section i [N m]
p	=	Absolute pressure in the observed system. [Pa]
p_d	=	Partial pressure of dry air [Pa]
p_{sat}	=	Saturation vapor pressure [Pa]
p_v	=	Partial pressure of water vapor [Pa]
r	=	radius [m]
R_a	=	System total resulting aerodynamic force [N]
$R_{a,h}$	=	Horizontal component of total resulting aerodynamic force [N]
R_{board}	=	Resultant hydro- and aerodynamic force on the board [N]
R_d	=	Specific gas constant of dry air [287.05 J/(kg K)]
Re_{line}	=	Reynolds number with reference to a kite line [ ]
Re_{rider}	=	Reynolds number with reference to a rider dimension [ ]
R_h	=	System total resulting hydrodynamic force [N]
$R_{h,h}$	=	Horizontal component of total resulting hydrodynamic force [N]
r_i	=	Moment arm between the section element and the origin [m]
R_{kite}	=	Resultant aerodynamic force on the kite [N]
R_{lines}	=	Resultant aerodynamic force on the lines [N]
R_{rider}	=	Resultant aerodynamic force on the rider [N]
R_v	=	Specific gas constant of water vapor [461.495 J/(kg K)]
S_k	=	Kite surface area [m^2]
S_{line}	=	Frontal surface area of the combination of all lines [m^2]
S_{wet}	=	Wetted surface area of the board [m^2]
T	=	Temperature [K]
T_0	=	reference temperature [291.15 K]
T_{back}	=	Line tension on the backlines [N]
T_{line}	=	Mechanical contact force between line and rider [N]
$T_{line,k}$	=	Exact total line tension at the location of the kite [N]
T_o	=	Tether tension component in the direction of the origin [N]
T_{tot}	=	Total tension force of all lines [N]
v_a	=	Apparent wind velocity, as experienced by a moving object [m/s]
v_s	=	Sailing velocity [m/s]
v_t	=	True wind velocity, as measured by a non moving object [m/s]
$v_{t,n}$	=	True wind velocity at height n [m/s]
v_w	=	True Wind Velocity as used in the context of kite testing [m/s]
W	=	System gravitational force [N]
W_{rider}	=	Gravitational force of the rider [N]
z_0	=	Aerodynamic roughness length, related to the landscape [m]
z_n	=	Height n [m]

Underlined symbols refer to the vector representation of that symbol.

Greek Symbols

α	=	Angle of attack [rad]
α_{board}	=	angle between F_{board} and the horizontal plane [rad]
α_{kite}	=	angle between T_{line} and the horizontal plane [rad]
α_{va}	=	angle between the apparent wind vector $\underline{v}_a$ and the positive x-axis [rad]
β	=	$\varepsilon_a + \varepsilon_h$, total system glide angle [rad]
β_e [rad]	=	Dead rise angle, angle between the v shaped bottom surface and the horizontal [rad]
γ	=	Sailed course as compared to the wind , 180 degrees is straight downwind [rad]
ε_a	=	atan($D_a/L_{a,h}$) , aerodynamic glide angle [rad]
ε_h	=	atan($D_h/L_{h,h}$) , hydrodynamic glide angle [rad]
ε_k	=	atan(D_k/L_k) , glide angle of the kite [rad]
ε_m	=	atan(D_{tetjer}/T_o) [rad]
ε_t	=	atan(D_{tetjer}/T_o) [rad]
θ	=	Kite sweep angle, ranging from 0˚ to 180˚ with 90˚ straight downwind [rad]
θ_p	=	Kite pitch angle [rad]
μ	=	Dynamic viscosity at temperature T [Pa*s]
μ_0	=	Reference viscosity at reference temperature T_0 [18.27E-6 Pa*s]
μ_w	=	Dynamic viscosity of water [Pa*s]
ν	=	Kinematic viscosity [m^2/s]
ρ_a	=	Humid air density [kg/m^3]
ρ_d	=	Dry air density [kg/m^3]
ρ_v	=	Water vapor density [kg/m^3]
ρ_w	=	Water density [kg/m^3]
τ	=	Board angle of attack [rad]
ϕ	=	Relative humidity [ ]

1 Introduction

Speed sailing can be seen as the ultimate challenge for sailing craft. Speed sailing records have been officially registered since 1972. Sailing speeds climbed with sailboats of different configuration and with the developments achieved by windsurfers. Kiteboarders have only recently entered the speed sailing arena. Despite of the fact that the sport is still young, kiteboarders have already shown to be capable of extremely high speeds using a relatively cheap and simple combination of a kite and a board. They proved to be the world's fastest sailing crafts during a record attempt in October 2008. In September 2009 the record was broken again by a large hydrofoil trimaran. Only little is known about the aero- and hydrodynamic performance characteristics of a kiteboarder as a whole and especially of the used kites and kite boards. Research is required to investigate the properties of each component of the kiteboarder and find possibilities to further increase the sailing speed. The ultimate goal is to reach the maximum speed potential of a kiteboarder.

This thesis aims to obtain a general understanding of what properties are of importance to obtain a high kiteboarding velocity and to understand how each component contributes to the finally obtained velocity.

This report presents an analytical approach to obtain the performance characteristics of a speed kiteboarder. The kiteboarder is first approached as a complete system. Then the system is divided into four components; kite, lines, rider and board. There is a strong focus on describing a method to analyze the characteristics of the kite.

The report is structured as follows. In chapter 2 the necessary background is given on the subjects of high altitude wind power, kiteboarding and speed sailing. In chapter 3 a two dimensional method is described to analyze the performance of a sailing craft in general. In the same chapter a more sophisticated three dimensional method is introduced to account for variations of wind velocity over height.

Chapter 4 to 7 each zoom in on a component of the system. In chapter 4 it is explained how to estimate the aerodynamic line drag. A theoretical approach is found to be sufficient as enough literature on the subject is available. Chapter 5 contains an analysis of the rider. The drag coefficient is estimated. Pictures are analyzed to obtain the total frontal area and to obtain realistic values for the forces acting on the rider by both the lines and the board. In chapter 6 a method to test the aerodynamic properties of a kite is described. The method is based on flying kites along a certain path in the sky and keeping track of the flying speed, wind speed and resulting line tension. Although the idea of testing kites by analyzing their crosswind flight behavior is not completely new, no reports where available on the subject. The test was exclusively designed and set up for this thesis work. Experimental results are presented in the same chapter. Chapter 7 describes the obtained hydrodynamic performance properties of the board. A test is conducted using the same setup as used in the kite test. This test is done during actual kitesurfing. Both the line tension and the position of the kite with respect to the rider is logged and analyzed. Empirical results on the subject of planing plates are used to verify whether the obtained results are realistic.

1 Introduction

In chapter 8 all obtained knowledge is fed into an extensive model that verifies if the total of all forces on each part of the system results in equilibrium. Using the results of this model a distribution of the drag over all four system components is given. In the same chapter a sensitivity analysis is performed to illustrate the effect of improving each of the components. Chapter 9 contains conclusions on what is learned about the aerodynamic performance of a kiteboarder and recommendations on how to improve both the used analysis and the performance of a kiteboarder.

2 Background

This thesis aims to obtain more knowledge about how to increase the sailing velocity of a speed kiteboarder. Nevertheless it needs to be mentioned that the work done in this thesis applies to a much broader field than speed sailing. Especially the kite testing method, presented in this thesis, is of relevance to other fields. Firstly it needs to be mentioned that a large part of the modeling, approach and results can be employed in kite power research. Research focused on producing electrical energy with the use of kites and on using kites for ship propulsion can profit from obtained results. Secondly the existing kite industry, currently a multimillion dollar business, could use the described methods to test and improve different kite and board designs.

Generally speaking a kite can be used as a device to obtain energy. This can be mechanical energy as in the case of using kites for propulsion. The propelling application can vary from recreational use by a single human being to professional use on large cargo ships. Obtained mechanical energy can also be transformed into electrical energy. This work aims to be of use for all applications in which kites are used as a means to obtain energy. This is why in the first paragraph a general explanation will be given of how a kite can be used to obtain energy. For those who don't know what kitesurfing is, a short introduction to kitesurfing will be given in the second paragraph. In the third paragraph of this chapter it will be explained what speedsailing is, what the rules are for setting a new record and which competitors can be found in the field of speed sailing.

2.1 High altitude wind power

In different dictionaries (1)(2) the definition of a kite can be found as: "A light frame covered with some thin material, to be flown in the wind at the end of a long string."

Flying an object at the end of a long string requires a tension force in this string. When this force initiates a motion, energy is being transferred. This wind energy can be used for propulsion, creating electric energy or any other mechanical work (i.e. pumping water).

Wind energy has been around for a long time and the use of wind turbines is growing rapidly. Still a conventional wind turbine is only able to reach a fraction of the energy available in the atmosphere. Research shows that in the first kilometer of the earth boundary layer the available energy grows rapidly. The available energy keeps growing up to a height of around 9 km where a decrease in air density causes the available energy to decrease with height. This is illustrated in Figure 1. Conventional wind turbines can only subtract energy from the lower layers of the earth boundary layer. With the use of kites it is possible to subtract energy from higher layers and increase the potential of wind energy as a clean energy source.

To this date high altitude wind energy has not been applied on a commercial scale. Different demonstrations show the feasibility of the concept, but more research is required to realize the large scale use of high altitude wind power. Some of the results obtained in this thesis are directly applicable to research in this direction. Further, using a kite to break the speed sailing world record is a strong demonstration of the potential of kite energy.
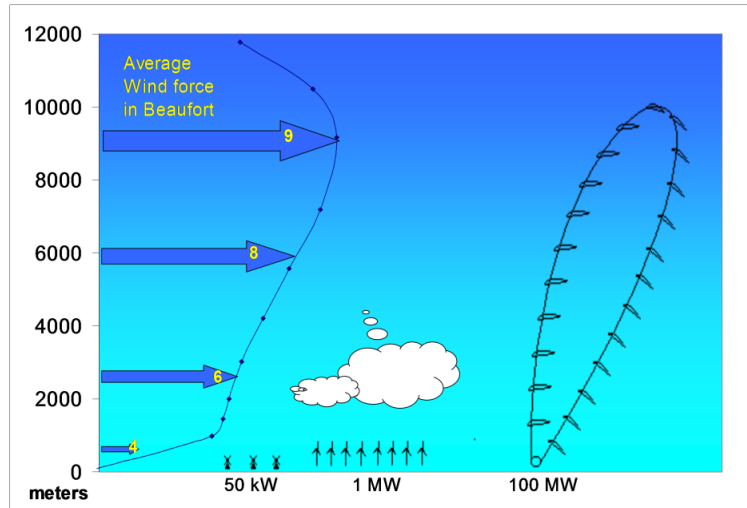
Figure 1, Schematic representation of wind variation over height. Source: Wubbo Ockels

2.2 Kiteboarding

Kiteboarding or kitesurfing is a water sport similar to windsurfing and sailing. The wind is used to propel oneself over the water. When comparing kiteboarding to sailing one could say that a board is used instead of a boat, a kite is used instead of a sail. A set of strong thin lines (Dyneema fiber) is used to control the kite and would be the equivalent of the mast and rigging. With the kite and the board weighing less than 3 kg each, a kitesurfer is the lightest sailing craft available today.

Figure 2, A kitesurfer is a sailing system with four components; Board, Rider, Lines and Kite. Picture: Ian Edmondson

Throughout this work a kitesurfer with his equipment is seen as a system that can be split up into four system components:

- The board
- The rider
- The lines
- The kite

Each of these components has its own function and its own set of forces working on it.

The board

The board forms the interface with the water. Unlike sailing boats a kiteboard is normally not able to support the weight of the rider while at rest. The lifting force from the kite will bring the board to speed and help the rider to stand up on the board. A small amount of velocity is enough for the board to produce enough lift to remain above the water surface. Normal board lengths range from 1.2 meter for a short freestyle board to about 2 meter for a large race board or surf/waveride board. The average width is between 30 and 50 centimeter.

The rider

The rider could also be called the kitesurfer, the kiteboarder, the sailor or in more technical terms the system operator. The rider forms the link between the lines and the board and controls the whole system. It takes some practice to control both the board and the kite and stay in balance at the same time. An interesting aspect in kitesurfing is that the rider is an integral mechanical part of the system. As the rider forms a mechanical connection between the kite and the board, the presence of the rider is required for the system to work.

The lines

The lines link the kite to the rider and are used to steer the kite. The most frequently used line length is around 25m for all kite sizes. Line lengths shorter than 20m and longer than 30m, are not often used. Still, line lengths outside this range are certainly possible. Normally the used line thickness is around 1.3mm. Each line can carry around 300kg.

The kite

There are two types of kites that are used in kiteboarding. The one that is most frequently used is called the tube kite and uses a structure of tubes that need to be inflated before launching the kite. The second type is called the ram air inflatable kite. This kite uses the stagnation pressure of the oncoming flow to inflate itself.

Commercially available surf kites are made in many different sizes. A $5m^2$ kite can be seen as a storm kite that can be used up to wind speeds of 9 Beaufort by expert riders, but can also be used in more moderate winds as a trainer kite or as a kite for people with a low body weight. In light winds sizes from $12m^2$ up to $19m^2$ are used.

Overview

In its most general form, a sailing system (sailboat, catamaran, windsurfer, kitesurfer, ice sailor, land sailor) interacts with two media with each a different velocity. The media can be air and water, air and ice, air and ground or even two layers of air. It is only possible to sail when both media are moving with respect to each other. By creating a mechanical system that interacts with both media it becomes possible to move into almost any direction and theoretically with any velocity. The word theoretically is used here, as in practice the sailing velocity and direction will be limited by the total of aero- and hydrodynamic drag forces on all parts of the system.

A kiteboarder can be seen to form a connection between water and air. The hydrodynamic force runs through the board into the rider, the rider exerts a tension load on the lines, which on their turn connect to the kite and its aerodynamic force. This is displayed in Figure 3.

Water ⬌ Board ⬌ Rider ⬌ Lines ⬌ Kite ⬌ Air
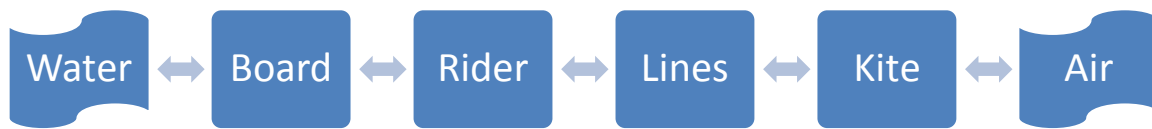
Figure 3, Schematic interaction scheme of a kiteboarder.

Disciplines

There are five different disciplines that can be recognized in kitesurfing, they are listed in Table 1. Each discipline has its own specialized boards and kites and each discipline (except freeriding) has its own competition.

Discipline	Characteristics
Freeriding	Cruising around over the water.
Freestyling	Doing tricks e.g.: Jumps, grabs, loops, kiteloops and handle passes.
Waveriding	Surfing waves.
Racing	Sailing a set trajectory around buoys with a number of competitors.
Speed	Trying to go as fast as possible in a straight line.

Table 1, Disciplines in kitesurfing.

2.3 Speed Sailing

The WSSRC

The World Sailing Speed Record Council (WSSRC) was established by the International Yacht Racing Union (now renamed the International Sailing Federation) in 1972. The object was to provide impartial results for increasing numbers of claims to high speed sailing craft (on water: never on ice nor land!). Early on the decision was made to base such speed ratifications on a one-way leg of exactly 500 meters. Meetings were held every year, often several meetings a year, in various suitable places in the world and speeds climbed with boats of various configurations and with sailboards. Reference(3)

Any sailing craft can attempt to break the world speed sailing record. Historically the ultimate record is set on a 500m course but records can be obtained over different distances. Examples are the nautical mile, the 24 hour distance and the transatlantic record. Apart from the world record also national records are listed.

Rules

The 500 meter record is originally sailed on a course with a start and a finish line. The sailors are allowed to accelerate before arriving at the starting line such that they enter the course at full speed. On both lines a camera is placed such that it is aligned with the corresponding line. Both cameras are connected to a central point where all images are collected. Only the runs that are potential speed records are accurately processed by manually setting both start and end times.

Currently record ratification is also possible using a GPS track. The used GPS receiver has to meet strict conditions with respect to accuracy. The only GPS system that is approved in the year 2009 is the Trimble GPS survey system.

Competitors

In 2009 there are different competitors trying to break the sailing speed record. Five competitors that have proved to be capable of breaking records are listed below.

Figure 4, Hydroptere training in the harbour of Hyères, France. Copyright C. Levy – Hydroptère.

Name: Hydroptère
Type: Hydrofoil trimaran
Record speed: 51.36 knots (95.12 km/h)
Estimated wind during record: 24 knots

Figure 5, Alex Caizergues is currently the fastest kiteboarder. Source: http://kitesquad.com.

Name: Alex Caizergues
Type: Kitesurfer
Record speed: 50.57 knots (93.66 km/h)
Estimated wind during record: 46 knots

Name: Macquarie Innovations
Type: Planing Tripod with rigid wing
Record speed: 50.07
Estimated wind during record: 24 knots

Figure 6, Macquarie Innovations. Picture: Steb Fisher

Name: Antoine Albeau
Type: Windsurfer
Record speed: 49.09 knots (90.91 km/h)
Estimated wind during record: 45-50 knots

Figure 7, Antoine Albeau during his record run. Source: www.sail-world.com

Name: Vestas SailRocket
Type: Planing craft with rigid wing
Record speed: 47.36 knots (87.71 km/h)
Estimated wind during record: 22.6 knots

Figure 8, Sailrocket. Source: www.Yachtpals.com

3 Sailing performance

The objective of this chapter is to define the performance of a sailing system that sails over water. No distinction is made between a sail boat, a windsurfer or a kitesurfer. They all work with the same principles. The main question here is: What makes a sailing craft go fast?

3.1 Basic Aspects of Sailing

For a mass to accelerate a resultant force is required. For the mass to remain at a constant velocity all forces need to be in equilibrium. Independent of what the type of sailing craft one is looking at one can always divide all forces into three groups. Gravitational forces, aerodynamic forces and hydrodynamic forces. Sailing at constant velocity is only possible when these three groups are in equilibrium.
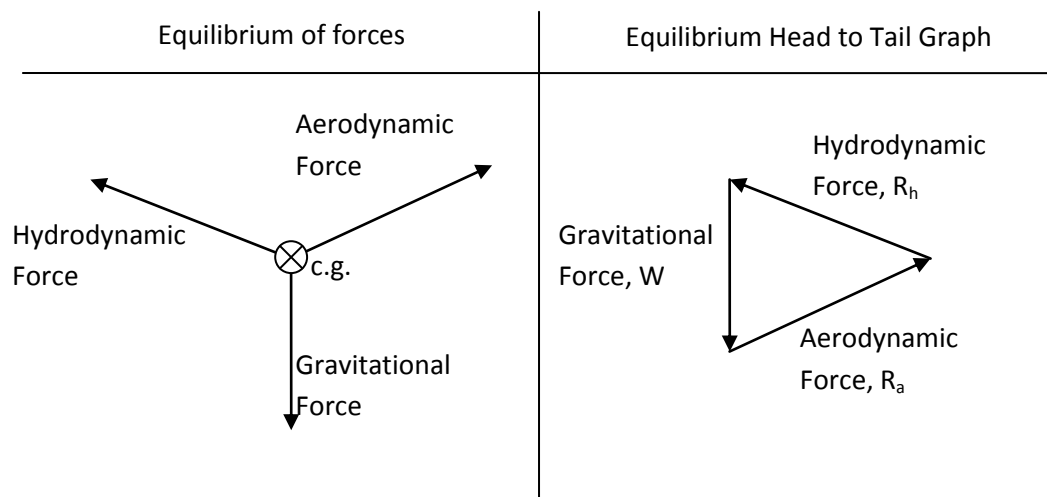

Figure 9, For equilibrium, the aerodynamic, hydrodynamic and gravitational forces need to be balanced.

A first requirement for a sailing craft to sail in a straight line at a constant speed is that all forces are balanced in vertical direction. As gravity always works in the downward direction this means that the combination of aerodynamic and hydrodynamic forces always needs to provide enough upward force to bring the system to balance.

Note that increasing the system's weight while keeping the magnitudes of both the hydrodynamic and aerodynamic forces fixed results in decreasing horizontal components. Only the horizontal component of a force can help to obtain a horizontal velocity. This explains why making the system lighter is in principle good for the system's efficiency.

Horizontal equilibrium

In the horizontal plane, gravity doesn't play a part. This means that for horizontal equilibrium the only requirement is that the horizontal component of the sum of all aerodynamic forces is in balance with the horizontal component of the sum of all hydrodynamic forces.

Conclusion

It can be concluded that for equilibrium the weight vector of the whole system $\underline{W}$ needs to be balanced with the sum of all aerodynamic forces $\underline{R}_a$ and the sum of all hydrodynamic forces $\underline{R}_h$.

$$\underline{W} + \underline{R}_a + \underline{R}_h = \underline{0}$$

(3.1)

3.2 Sailing theory in 2D
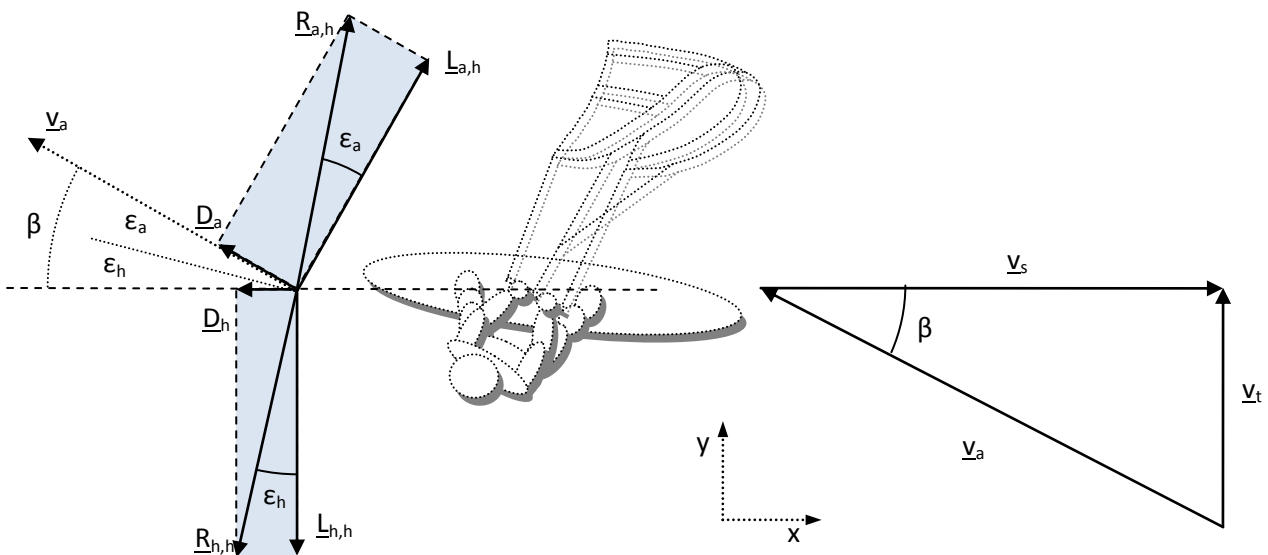
Figure 10, Top view of a sailing kiteboarder. Both the horizontal component of the total aerodynamic force $\underline{R}_{a,h}$ and the horizontal component of the total hydrodynamic force $\underline{R}_{h,h}$ have been decomposed into their horizontal lift and drag components.

When looking at the equilibrium situation in the horizontal plane, displayed in Figure 10, the aerodynamic and hydrodynamic force vectors can be decomposed into a lift and a drag component. The aerodynamic drag component $\underline{D}_a$ is defined as parallel to the apparent wind direction $\underline{v}_a$. The aerodynamic lift component $\underline{L}_a$ is perpendicular to the aerodynamic drag.

The hydrodynamic drag component $\underline{D}_h$ is defined as always opposed to the direction of the sailing speed $\underline{v}_s$. The hydrodynamic lift $\underline{L}_h$ is always perpendicular to the hydrodynamic drag.

In Figure 10 it is shown how the aerodynamic glide angle ε_a and the hydrodynamic glide angle ε_h depend on the lift to drag ratio of respectively the aerodynamic and hydrodynamic forces.

$$\varepsilon_a = \arctan\left(\frac{D_a}{L_a}\right) \rightarrow with: 0 < \varepsilon_a \le \frac{\pi}{2}$$

(3.2)

$$\varepsilon_h = \arctan\left(\frac{D_h}{L_h}\right) \rightarrow with: 0 < \varepsilon_h \le \frac{\pi}{2}$$

(3.3)

Figure 10 also shows that the system can only be in equilibrium when the sum of ε_a and ε_h is equal to the angle β between $\underline{v}_s$ and $\underline{v}_a$. So for equilibrium:

$$\beta = \varepsilon_a + \varepsilon_h \rightarrow with: 0 < \beta \le \pi$$

(3.4)

β can be seen as a value for the efficiency of the total system. The higher both the aerodynamic and hydrodynamic lift over drag, the lower the value of β.
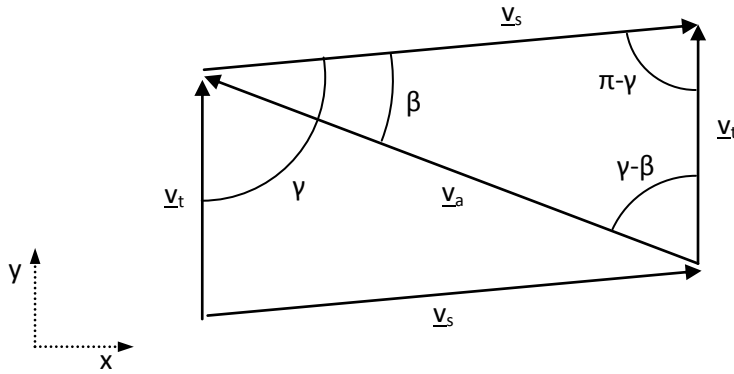

Figure 11, Sailing velocity triangle. The sailed course is represented by the angle γ between the true wind vector and the sailing velocity vector.

Looking at Figure 11 a relation between v_s and v_t can be obtained using the sine law. Rearranging results in an expression for the sailing velocity ratio v_s/v_t (the ratio of sailing velocity over wind velocity):

$$\frac{v_s}{\sin(\gamma - \beta)} = \frac{v_t}{\sin\beta} \Rightarrow \frac{v_s}{v_t} = \frac{\sin(\gamma - \beta)}{\sin\beta}$$

$$where:$$
$$0 < \gamma \le \pi \wedge 0 < \gamma - \beta < \pi$$
$$so:$$
$$\beta < \gamma \le \pi$$

(3.5)

Using equation 3.5 it is possible to plot a speed polar for different values of β.
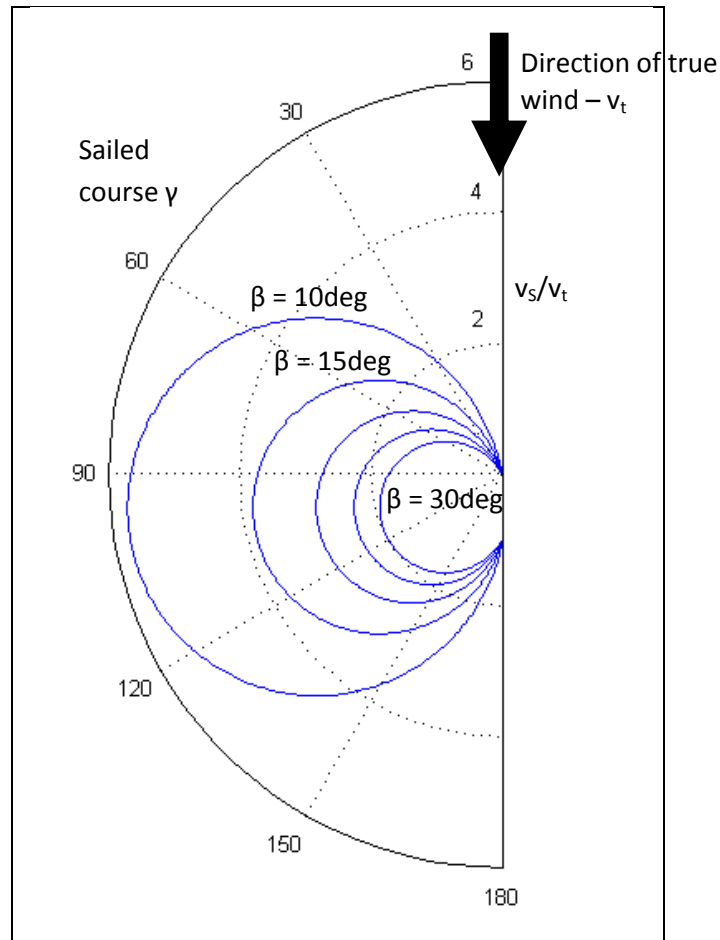
Figure 12, Speed polar for different values of β. From β = 10 deg to β = 30 deg in steps of 5deg. This shows how with a certain wind speed v_t, different sailing speeds v_s can be obtained by varying the course. Depending on the value of β different maximum speeds in all directions are obtained.

To determine at which sailing course γ the system will obtain its maximum velocity, 3.5 needs to be differentiated and solved for γ.

$$for: 0 \leq \gamma \leq \pi$$

$$\frac{d}{d\gamma}\left(\frac{v_s}{v_t}\right) = \frac{d}{d\gamma}\left(\frac{\sin(\gamma - \beta)}{\sin \beta}\right) = \frac{\cos(\gamma - \beta)}{\sin \beta} = 0 \qquad \textbf{(3.6)}$$

This gives:

$$\gamma - \beta = \frac{\pi}{2} + k \cdot \pi$$

$$now\ for: \beta < \gamma < \pi \vee 0 < \beta < \frac{\pi}{2} \qquad \textbf{(3.7)}$$

$$\gamma = \frac{\pi}{2} + \beta$$

This means that for a known β between 0 and π/2 the optimal sailing course is at 90˚ with respect to the wind plus β in downwind direction. Note that this means that at the optimal course, the angle between $\underline{v}_t$ and $\underline{v}_a$ is exactly 90 degrees. This is illustrated in Figure 13.
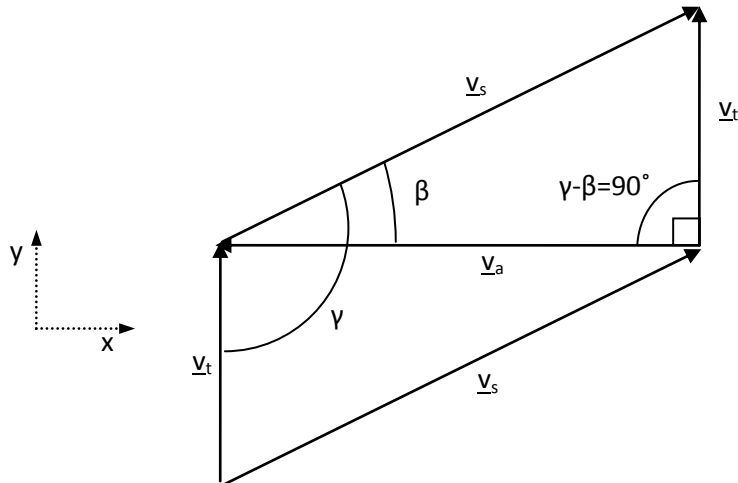
Figure 13, Sailing velocity triangle at optimal sailing course

At the fastest course we find:

$$\frac{v_s}{v_t} = \frac{\sin\left(\pi/2 + \beta - \beta\right)}{\sin\beta} = \frac{1}{\sin\beta}$$

(3.8)

The ratio of obtained sailing speed over true wind speed at the optimal course is thus given by:

$$\left[\frac{v_s}{v_t}\right]_{max} = \frac{1}{\sin\beta}$$

(3.9)
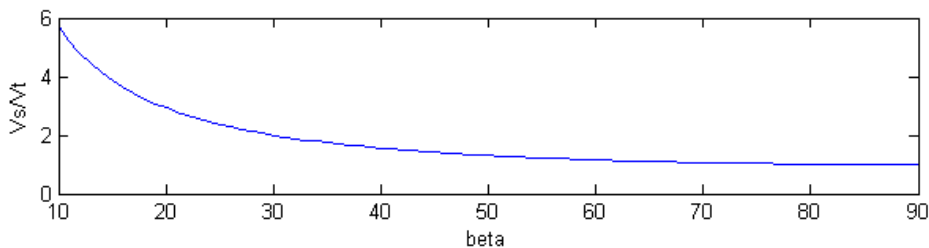
Figure 14, Sailing speed ratio, v_s/v_t against β [deg].

Here one can clearly see that by making β as small as possible, the maximum velocity will be as high as possible. This means that ε_a and ε_h should be both as small as possible and so for high speeds the aerodynamic and hydrodynamic lift to drag ratio, as well as the wind velocity, need to be as high as possible.

Variable β

Until now it was assumed that β is a constant value for all different sailing speeds and sailing courses. This makes it easy to find the optimal course for speed. In reality β can vary with speed and with the course that is sailed. Different reasons can be given for this. Recall that a variation in β actually

means a variation in either the aerodynamic or hydrodynamic lift to drag ratio. For example the board could show variations in lift to drag ratio with variations in speed or when the rider shifts his position when sailing on a different course. The kite could be trimmed at a different angle of attack for each different course. This could result in both a variation in the kite's lift force and the kite's lift to drag ratio. In strong wind it is very common to decrease the angle of attack of the kite (this is often called depowering) when sailing upwind and increase the angle of attack at a more downwind course.

To deal with variations in β, β could be a function of for example the course sailed and the true wind velocity. Experimental work would then be required to find the relation between β, sailed course, sailing velocity and maybe also other variables. This work is left for further research.

3.3 Sailing theory in 3D model
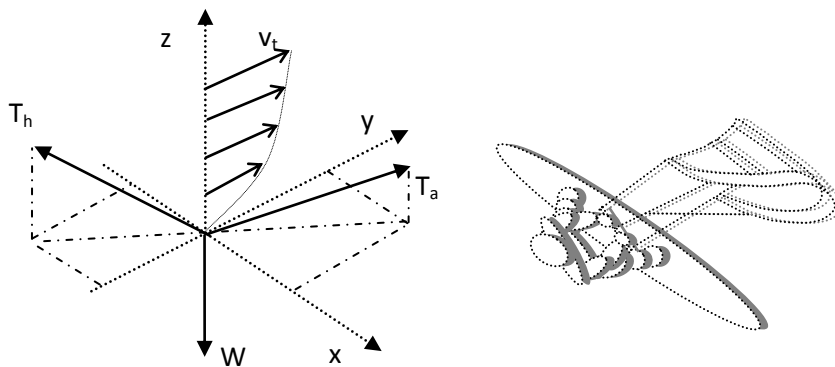
Figure 15, 3D visualization of the forces working on a kitesurfer sailing in the x direction with wind in the y direction.

The above presented two dimensional sailing theory is instructive and useful when it comes to a simple analysis. In 2D the vertical equilibrium is assumed to be automatically satisfied and the true wind velocity is equal at all heights. For this thesis it is decided that a more detailed model is required. The main reason for this decision is that neglecting the wind gradient (variation of wind velocity over height) is too simplistic. For example increasing the length of the kite lines could be beneficial as it enables the kiter to use the stronger wind at higher altitude. On the other hand a longer line produces more drag and could also result in a lower speed. It is thus expected that there is an optimum line length. The 2D model is not useful for finding the optimal line length, it will always conclude that less line results in less drag and so that no line at all is the best solution. The 3D model was build to take the wind gradient into account. Introducing the wind gradient means that the 2D theory presented before does not directly apply anymore. This paragraph serves to clarify the method that was used to build the 3D model. Results obtained with this model are presented in chapter 8.

The 3D model of a kitesurfer was build in order to provide insight in the efficiency of all parts of the system. The approach could be used for any given sailing system, and the model could easily be modified into a different sailing craft. However, this model is specifically tailored for kitesurfing and includes a board, a kite, lines and a rider. The model is used in two different ways and for two different purposes: 1) Parameter estimation and 2) speed prediction and optimization.

The first objective for using the model is parameter estimation. As will be shown there are many parameters involved in the modeling of a kitesurfer. A number of these parameters can be measured. Examples are sailing velocity, wind velocity and sailing direction. Other parameters can be estimated accurately enough with the use of theory and literature. For example the aerodynamic drag on the lines and the rider. Some parameters remain that can be estimated when all others are known. The board's lift and drag coefficients were selected for this.

The second objective for the model is speed prediction. When all parameters are known with enough accuracy, the question will be what will happen on changing one of the parameters. Does a certain increase in kite efficiency result in a large velocity increment? What would happen if the board drag would be reduced by 10%?

In this chapter it is shown how the model is basically build up and what parameters are taken into account. The used approach to model of the four system components is clarified in chapters 4 to 7.

3.4 Parameters to include in the model

This paragraph serves to outline which parameters are of importance when building a model of a kiteboarder. Looking at a sailing craft one could state that one is looking at two systems interacting with each other. The craft acts on the surroundings and the surroundings act on the sailing craft. This division in two systems is the first step that is used to investigate which parameters are of interest to include in the model.


Figure 16, Sailing craft inside its surroundings.

Fistly the surroundings will be closely examined, secondly the sailing craft. In a brainstorm all parameters linked to each part of the system are collected.

3.4.1   Surroundings

The surroundings of a kitesurfer could be devided into three groups. Air, water and gravity. Each of these subparts has a number of properties that could be of interest when building a model.

```
                          ┌─────────────────┐
                          │   Surroundings  │
                          └─────────────────┘
                                   │
        ┌──────────────────────────┼──────────────────────────┐
   ┌─────────┐               ┌─────────┐              ┌──────────────────┐
   │   Air   │               │  Water  │              │ Gravitational    │
   └─────────┘               └─────────┘              │ field            │
        │                         │                   └──────────────────┘
                                                               │
```

Air	Water	Gravitational field
Temperature	Temperature	Gravitational constant
Density	Density	
Viscosity	Viscosity	
Pressure	Pressure	
Humidity	Wave height	
Wind velocity	Wave period	
Wind direction	Wave shape	
Wind gradient	Current	
Wind twist	Depth	
Gust/turbulence factor	Cavitation	
	Ventilation	
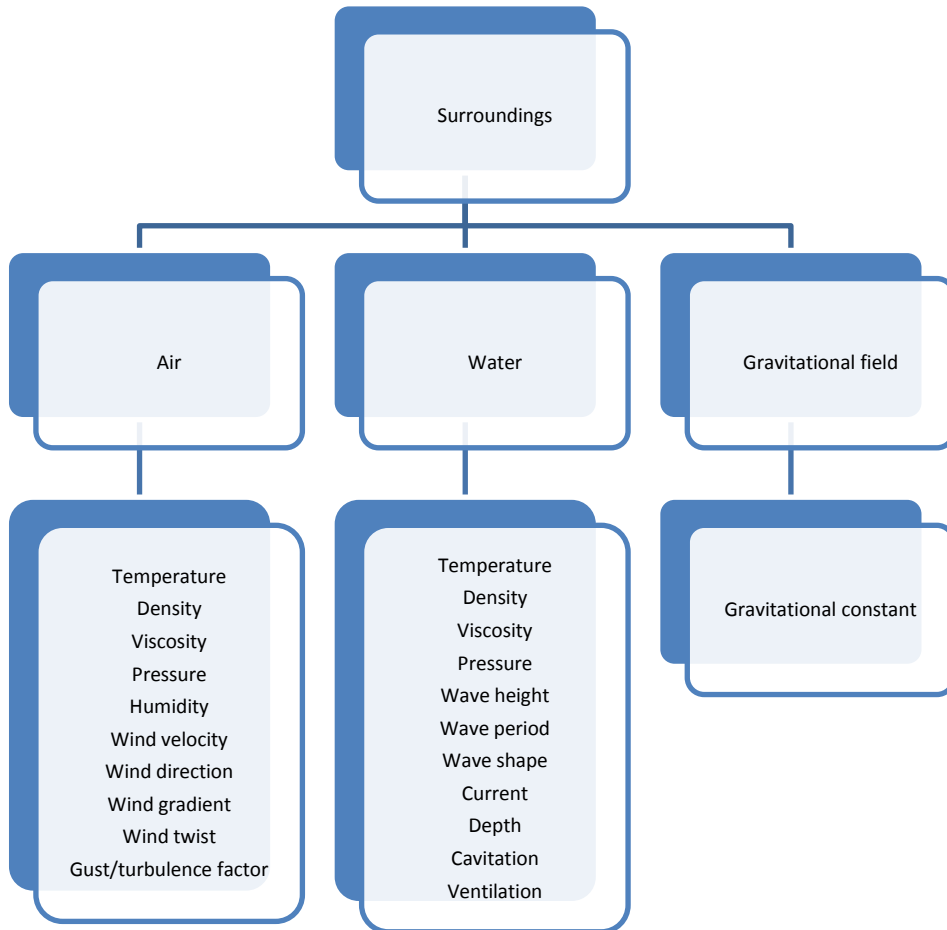
Figure 17, Brainstorm of all parameters and phenomena related to the surroundings.

Looking at the air group it is noted that temperature, pressure and humidity are of importance as they are required to obtain the air density and viscosity. The effects of gusts are outside the scope of this work. Wind velocity variations over height or wind gradient and wind twist need to be discussed.

Looking at the water section there is a relation between temperature and viscosity that needs to be taken into account. Pressure and temperature could be important in relation to cavitation. Cavitation could be initiated on the surface of the small fins used under a kiteboard, its effect will propably be limited. Unfortunaly time constraints prohibit including cavitation effects in this research. Issues related to waves and water depth also fall outside the scope of this research.

It will now be explained how to calculate the required environmental parameters.

Air density

The density ρ_a of humid air is given by the ideal gas law:

$$\rho_a = \rho_d + \rho_v = \frac{p_d}{R_d \cdot T} + \frac{p_v}{R_v \cdot T}$$

(3.10)

Where:
ρ_a = Humid air density [kg/m^3]
ρ_d = Dry air density [kg/m^3]
ρ_v = Water vapor density [kg/m^3]
p_d = Partial pressure of dry air [Pa]
R_d = Specific gas constant of dry air [287.05 J/(kg K)]
T = Temperature [K]
p_v = Partial pressure of water vapor [Pa]
R_v = Specific gas constant of water vapor [461.495 J/(kg K)]

The partial pressure of dry air is given by:

$$p_d = p - p_v$$

(3.11)

Where:
p = Absolute pressure in the observed system [Pa]

The partial water vapor pressure is calculated as:

$$p_v = \phi \cdot p_{sat}$$

(3.12)

Where:
ϕ = Relative humidity [ ]
p_{sat} = Saturation vapor pressure [Pa]

The saturation vapor pressure of water depends only on temperature:

$$p_{sat} = 610.78 \cdot 10^{\frac{7.5T - 2048.625}{T - 35.85}} \, [Pa]$$

(3.13)

Air viscosity

The dynamic viscosity of air can be derived by using Sutherland's formula:

$$\mu = \mu_0 \frac{T_0 + C}{T + C} \left(\frac{T}{T_0} \right)^{3/2}$$

(3.14)

Where:
μ = dynamic viscosity at temperature T [Pa*s]
μ_0 = reference viscosity at reference temperature T_0 [18.27E-6 Pa*s]
T = air temperature [K]
T_0 = reference temperature [291.15 K]
C = Sutherland's constant for air [120 K]

Wind Shear and Wind Gradient

Due to friction between the atmosphere and the earth's surface the wind velocity shows a variation over height in both direction and magnitude. In general the variation of the wind direction over the first 100 meters can be neglected (4). The velocity, on the other hand, shows a variation that becomes more and more severe when approaching the earth surface. Unless one chooses to use an extremely long tether, the kite of a kitesurfer always stays within the first 100 meters from the earth's surface. In normal sailing condition the height of the kite can be expected to be around 10 to 15 meter.

Roland B. Stull (4) explains how the earth is surrounded by what is called the Atmospheric Boundary Layer (ABL). The ABL is defined as the region that experiences the effects of the daily cycle of heating and cooling. This also includes daily variations in humidity, wind and pollution. For the ABL three forms of so called static stability are recognized:

- Unstable air refers to light wind and a surface that is warmer than the air.
- Stable layers of air are also associated with light winds, but with a surface that is cooler than the air.
- Neutral conditions can be found at moderate to strong winds where there is little effect of cooling or heating by the surface.

Clearly for speed kitesurfing the wind needs to be strong and the conditions can be called neutral. For neutral conditions the bottom 5% (50 to 100m) of the boundary layer can be called the surface layer. Here wind speeds increase roughly logarithmically with height.

Governing equation

The true wind velocity v_t is always zero at the ground (actually at height equal to the surface roughness length). The shape of the profile depends on the surface roughness length z_0 [m]. If the wind speed $v_{t,1}$ at height z_1 is known then the wind speed $v_{t,2}$ at height z_2 is given by:

$$v_{t,2}(z_2) = v_{t,1} \frac{ln(z_2/z_0)}{ln(z_1/z_0)}$$

(3.15)

Z$_0$ (m)	Classification	Landscape
0.0002	Sea	Sea, paved areas, snow-covered flat plain, tide flat, smooth desert
0.005	Smooth	Beaches, pack ice, morass, snow-covered fields
0.03	Open	Grass prairie or farm fields, tundra, airports, heather
0.1	Roughly open	Cultivated area with low crops & occasional obstacles (single bushes)
0.25	Rough	High crops, crops of varied height, scattered obstacles such as trees or hedge-rows, vineyards
0.5	Very rough	Mixed farm fields and forest clumps, orchards, scattered buildings
1.0	Closed	Regular coverage with large size obstacles with open spaces roughly equal to obstacle heights, suburban houses, villages, mature forests
≥2	Chaotic	Centers of large towns and cities, irregular forests with scattered clearings

Table 2, Davenport-Wieringa roughness length classification. Source: Meteorology for Scientist and Engineers, Roland B. Stull (4)

While sailing, the kitesurfer including the lines and the kite, moves through this wind profile. This movement always creates an apparent wind, the wind as experienced by the moving object. Looking at this apparent wind, while taking the wind gradient into account, results in an apparent wind that varies dramatically over height in both direction and magnitude. In the model the true wind $\underline{v}_t$ is defined as always in the direction of the positive y-axis but as explained with a variation over height.
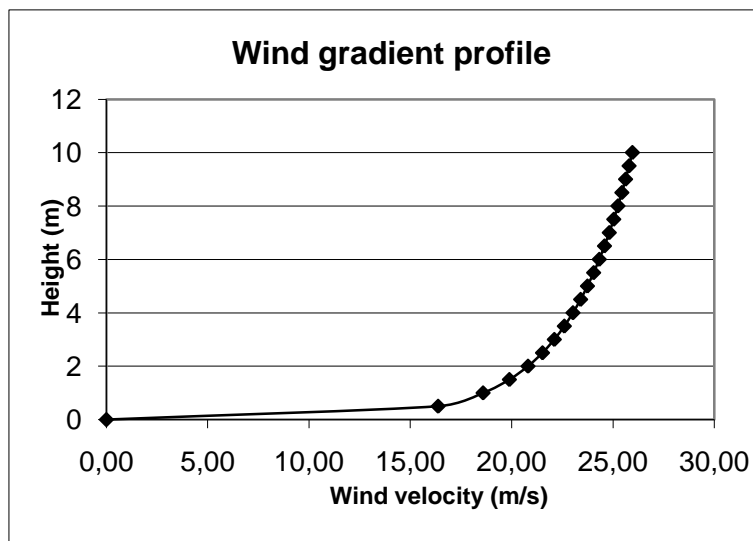

Figure 18, Wind gradient profile for v_t = 25 m/s at 10m height. The assumed roughness length is 0.005 meter.

Water density

Water density ρ_w changes with temperature although variations are relatively small. Fresh water at 25˚C has a density of 997 kg/m^3 at 4˚C it has its highest density at 1000 kg/m^3. The density of seawater at the surface of the ocean ranges between 1020 and 1029 kg/m^3 depending on temperature and salinity. Unless more detailed information is at hand the average density of 1025 kg/m^3 will be used for sea water.

Water viscosity

The dynamic viscosity of water μ_w as a function of temperature:

$$\mu_w = A \cdot 10^{B/(T-C)}$$

(3.16)

Where:
A = 2.414E-5 [Pa*s]
B = 247.8 [K]
T = Water temperature [K]
C = 140 [K]

Gravity

The gravitational constant used in this research is always g = 9.81 m/s^2.

3.4.2 Kitesurfer

For the kitesurfer a similar approach as for the environment is used. The components board, rider, lines and kite are used. For each component a set of possibly interesting properties is found.

```
                            Kitesurfer

        ┌──────────────┬──────────────┬──────────────┐
      Board          Rider        Kite Line         Kite

   Velocity        Velocity       Velocity        Velocity
   Lift coefficient Drag coefficient Lift coefficient Lift coefficient
   Drag coefficient Frontal Area   Drag coefficient Drag coefficient
   Frontal Area    Mass           Length          Surface Area
   Wetted Surface                 Thickness       Mass
   Mass                           Number
   Volume                         Density
                                  Frontal Area
```
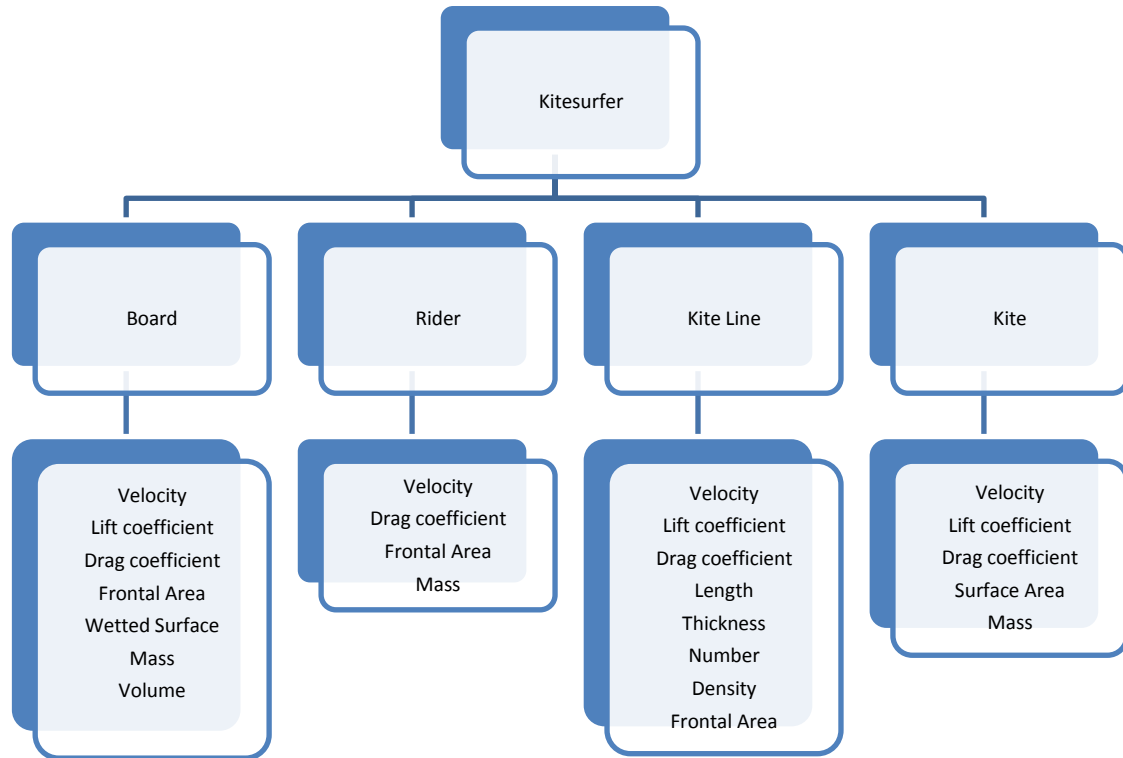
Figure 19, Brainstorm of the kitesufer with all its possibly interesting properties for modeling.

As said before, when modeling the kitesurfer the goal is to find the equilibrium situation. The acceleration towards this situation is left for future research. In the equilibrium situation the system moves as a rigid body in a straight line without any rotation. This means that the velocities of the board, the rider, the lines and the kite are all equal in magnitude and direction. This parameter is called sailing velocity or system velocity vector $\underline{v}_s$.

When the sailing velocity $\underline{v}_s$ and the true wind velocity $\underline{v}_t$ are known it is possible to calculate the apparent wind velocity vector $\underline{v}_a$ at each height h.

$$\underline{v}_a = \underline{v}_t(h) - \underline{v}_s \tag{3.17}$$

For equilibrium it is required that for each component of the system the combination of body forces W, aero- and hydrodynamic surface forces R and mechanical contact forces F results in a null vector.

$$\left(\underline{W}+\underline{R}+\underline{F}\right)_{board} = \left(\underline{W}+\underline{R}+\underline{F}\right)_{rider} = \left(\underline{W}+\underline{R}+\underline{F}\right)_{lines} = \left(\underline{W}+\underline{R}+\underline{F}\right)_{kite} = \underline{0} \tag{3.18}$$

The model that was build estimates the body forces, aero- and hydrodynamic surface forces and mechanical contact forces of all four components. Feeding enough information into the model allows the model to estimate the missing forces. In the case of using the model for velocity prediction the model can search for the velocity where a steady state is obtained.

The required information for building the model of each component is gathered in chapter 4 to 7.

4 Component 1: Lines

It was decided to treat the forces on the kite lines first so that the results can be used in the following chapters. In literature the word tether is often used as a replacement for a line, a rope, a cable or a string. In this document the words line and tether can be used interchangeably.

In normal usage there are four forces acting on the kite lines. The largest two are mechanical contact forces between the kite and the lines on one end and the rider and the lines on the other. Thirdly there are aerodynamic surface forces acting on the lines. The fourth force exists of gravitational body forces. For clarity the forces are listed below:

- Mechanical contact forces from kite and rider
- Aerodynamic surface force
- Gravitational body force

The forces are illustrated in the free body diagram given in Figure 20. The diagram represents the general 3D situation of a line immersed in a fluid continuum.
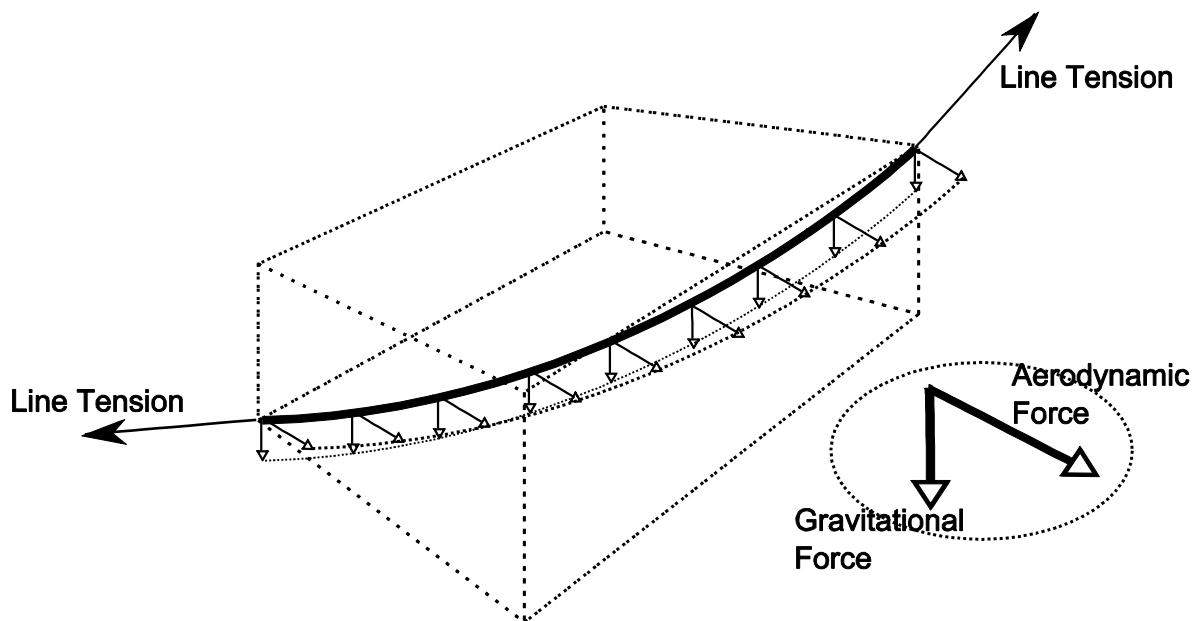
Figure 20, Free body diagram of a kite line

4.1 Flow situations

In this thesis work there are two different situations where the line forces need to be taken into account. The situation while sailing and the situation during crosswind testing (details on the crosswind test are found in chapter 6). Both situations are introduced in this paragraph.

Firstly there is a situation where the kitesurfer is moving across the surface of the water. Looking at this situation in its steady form, so no accelerations or rotations, it is seen that the whole system moves through space as one. Every point of the system has the same velocity and moves in a purely translational motion.

In the second case the kite line is attached to the ground and the kite flies on the spherical surface, defined by the used line length, at a fixed radius from this attachment point. During the crosswind test explained in chapter 6 the kite flies at constant height above the ground. This motion is purely rotational around a vertical axis at the line attachment point.

In order to be able to estimate the aerodynamic drag acting on the lines an estimation of the expected Reynolds number is required. The line diameter could vary between 1 and 2 mm. The apparent wind velocity is estimated to range between 15 and 30 m/s. A kinematic viscosity of $v = 1.47E\text{-}5$ m^2/s (15˚C, Standard Atmospheric Pressure) is assumed. The Reynolds number can thus be expected to be in the range:

$$\text{Re}_{line} = \frac{v_a d}{v} = \frac{15 \cdot 10^{-3}}{1.47 \cdot 10^{-5}} ...to... \frac{30 \cdot 2 \cdot 10^{-3}}{1.47 \cdot 10^{-5}} = 1 \cdot 10^3 ...to... 4 \cdot 10^3 \qquad (3.19)$$
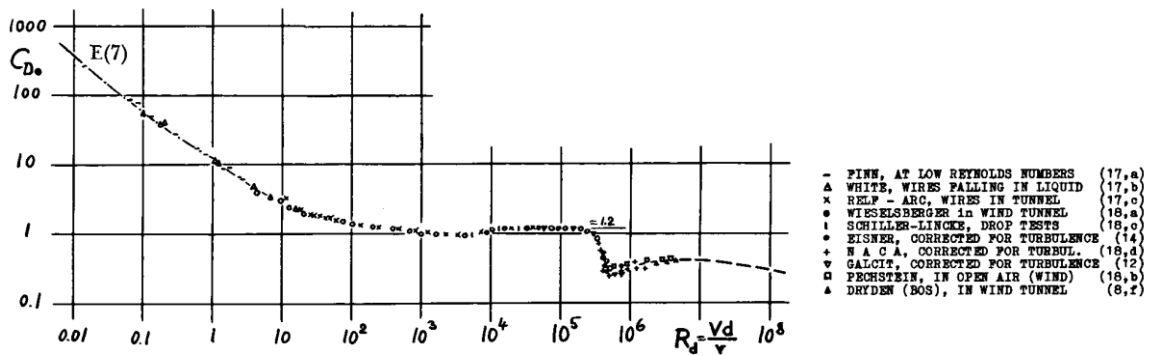
Figure 21, Drag coefficient of the circular cylinder in a flow normal to the axis (between walls), as a function of Reynolds number. Source: (5)

In Figure 21 Hoerner (5) shows how the drag coefficient of a circular cylinder varies for Reynolds numbers in a range from 10^{-2} to 10^8. The Reynolds number is referenced to the cylinder diameter. At a Reynolds number of say 3 times 10^5 the drag coefficient drops sharply, this is called the critical Reynolds number. Note that for the lines the expected Reynolds number lies on the plateau before the critical point.

4.2 Governing lift and drag equations

The so called cross flow principle describes how to calculate drag and lift coefficients for a cylinder under different angles of attack α. The governing equations are given by Hoerner (5) and Melkert (6).
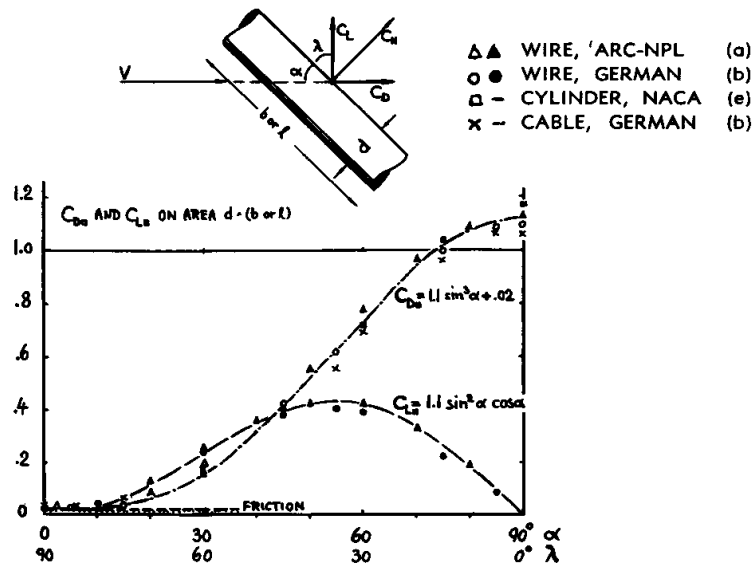
Figure 22, Drag and lift coefficients (on area "d" times axial length "l") of circular cylinders, wires and cables; inclined against the direction of the flow. At Reynolds numbers below the critical. Source: Hoerner (5).

The flow pattern and aerodynamic pressure forces on an inclined cylinder correspond only to the velocity component normal to the cylinder axis. The normal force coefficient (on area 'd' times axial length 'l') is given by:

$$C_{N,line} = C_{D,basic}\,\sin^2(\alpha)$$

(4.1)

The basic drag coefficient $C_{D,basic}$ is given to be 1.1. $C_{N,line}$ is then decomposed into a force coefficient perpendicular to the flow $C_{L,line}$ and a force coefficient parallel to the flow $C_{D,line}$:

$$C_{L,line} = C_{N,line}\,\cos(\alpha) = 1.1\sin^2(\alpha)\cos(\alpha)$$

(4.2)

A constant friction coefficient $\pi\,C_f = 0.02$ is added to the drag coefficient

$$C_{D,line} = C_{N,line}\,\sin(\alpha) + \pi\,C_f = 1.1\sin^3(\alpha) + 0.02$$

(4.3)

In some cases it can be assumed that both the flow direction and velocity are constant over the whole length of the line. Calculation of line lift and drag is then straight forward. In other cases the angle of attack α and the velocity of the flow will vary along the line. Calculation of line lift and drag is then done by numerical integration over the length of the line.

4.3 Line material properties

The kite lines are made from Dyneema. This material is perfect for kitesurfing as it has a very high tensile strength. Still it is lighter than water, assuring it to float. It is also possible to use non floating lines, but this would introduce the risk of the line sinking and getting stuck around an underwater object (e.g. a stone). This would be inconvenient and could be potentially dangerous.

Other reasons for Dyneema to be popular amongst kitesurfers are its excellent resistance to abrasion, UV light, folding and bending, moisture, sharp bends and peak loading. Due to a high material stiffness, control inputs are transferred directly into the kite. Due to the low mechanical friction coefficient of the material the kite remains controllable with multiple twists in the line.

The density of Dyneema is on average specified at 970 kg/m^3. This refers to solid Dyneema. It can be expected that a woven Dyneema line contains a certain volume of air trapped between the yarns. No literature values where found for this air fraction. As a high degree of accuracy is not required here, it is assumed, after inspecting a 2 mm cable, that the air fraction is around 10%. This means that one line with a length of 25 meter and a thickness of 2mm has a mass of around 69 gram. This could already indicate that the mass of the kite lines can be neglected in most of the analysis.

The tensile strength of Dyneema is specified to be between 1400 and 3090 MPa (7). The modulus of elasticity between 55 and 172 GPa (7).

4.4 Line drag while sailing

This paragraph serves to describe the used method to account for tether drag implemented in the kitesurfing model.

While sailing, the tether runs from the rider to the kite. Normally this means that the rider end of the line is at a height of about 1 meter above the surface. The kite end of the line is normally at 10 to 15 meter above the surface, depending on where the rider decides to position the kite. As explained in paragraph 3.4.1 the wind velocity will vary over height due to friction with the earth's surface. Due to this wind gradient the line will experience a different apparent wind vector at each height. To accurately estimate the tether drag this variation in apparent wind velocity should be carefully taken into account.

The simplest method to estimate the resulting total tether drag would be by selecting a reasonable height at which the apparent wind is calculated. This apparent wind vector can then be used to obtain an estimation of the tether drag and lift.

For this thesis it was decided to introduce an extra step to increase the accuracy. The tether was divided into 9 equal sections. Section one starts at the estimated height of the center of gravity of the rider h_{rider}. Section nine ends at the estimated height of the kite h_{kite}. The average section height above the ground $h_{\text{line},i}$ for each section is obtained by:

$$h_{\text{line},i} = h_{rider} + \left(i - \frac{1}{2} \right) \frac{h_{kite} - h_{rider}}{9}$$

(4.4)

The apparent wind velocity at each section $\underline{v}_a$ is now obtained using the true wind velocity $\underline{v}_t$ as a function of height described in equation 3.15 and the sailing velocity $\underline{v}_s$:

$$\underline{v}_a(h_{line,i}) = \underline{v}_t(h_{line,i}) - \underline{v}_s$$

(4.5)

The drag of each section can now be calculated using:

$$\underline{D}_{line,i} = \frac{\underline{v}_a}{|\underline{v}_a|} \frac{1}{2} \rho_a |\underline{v}_a|^2 C_{D,line} d_{line} l_i$$

(4.6)

Where d_{line} represents the section diameter and l_i represents the section length. The lift of each section can be calculated using:

$$\underline{L}_{line,i} = \begin{bmatrix} 0 & -1 \\ 1 & 0 \end{bmatrix} \frac{\underline{v}_a}{|\underline{v}_a|} \frac{1}{2} \rho_a |\underline{v}_a|^2 C_{L,line} d_{line} l_i$$

(4.7)

The line drag coefficient can be obtained when the angle of attack of each section is known. In order to simplify this part of the analysis it was decided to use a single drag and lift coefficient for all sections. To estimate the used values, an acceptable value for the line angle of attack has to be found first.

While sailing the kite position will depend on the apparent wind vector. The kite will be in a position almost normal to the apparent wind vector. This means that the line angle of attack α will always be close to 90 degrees. A downwind deflection from the 90 degrees angle is caused by the L/D value of the kite. The magnitude of this deflection is equal to:

$$\varepsilon_{kite} = \arctan\left(\frac{1}{[L/D]_{kite}}\right)$$

(4.8)

Thus the line angle of attack can be calculated by

$$\alpha = \frac{\pi}{2} - \arctan\left(\frac{1}{[L/D]_{kite}}\right)$$

(4.9)

For a L/D of say 5 the value of α will be 79 degrees. This results in a line drag coefficient of 1.06 and a line lift coefficient of 0.20.

4.5 Line drag during crosswind sweep

This paragraph serves to outline the method that was used to estimate the line drag during the crosswind test that is explained in chapter 6. While steering the kite through the wind from one side to the other an aerodynamic drag force acts on the lines. In order to be able to account for this force it is required to create a model that estimates the magnitude of the force. It is noted that the amount of line drag is not depending on the kite that is used. It only depends on the line's velocity vector and the true wind velocity vector.

2 D assumption

This part of the analysis will be purely 2 dimensional. This means that in top view the kite sweeps from one side to the other at ground level. This is a good approximation of the real crosswind test as the kite is always flown at low altitude (about 6 m high) with long lines (50 m). This results in a small angle between the lines and the horizontal plane.
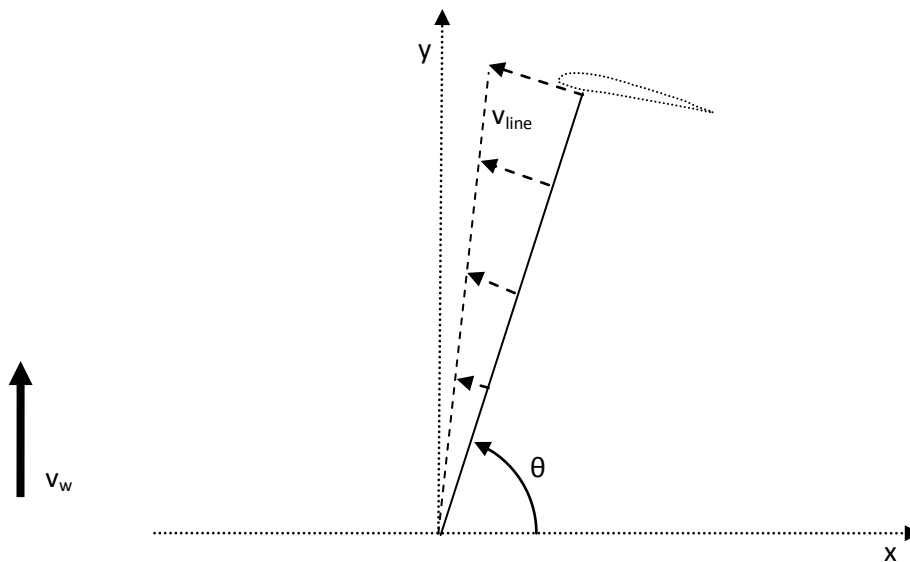
Figure 23, Schematic top view representation of the crosswind test. The kite flies from one side to the other.

Straight line assumption

A second assumption in calculating line drag is that all kite lines run in a straight line from the ground attachment point to the kite. This means that sagging effects due to line mass and due to drag are neglected when it comes to determining the shape of the line. In practice the line sag amounts to a maximum deviation of about 0.5 meters from the straight line. With a line length of 50 meter this is clearly only a very small deviation from the straight line situation.

Rigid rotating body

The lines always rotate around the attachment point to the ground. This is why it is chosen to always refer to this point as the origin. The whole problem can be expressed in terms of a rotation around the origin. No translations are required. All forces applied to the system are regarded in terms of their moment around the origin. The aerodynamic forces on the line result in a moment M_{line} around the origin.

Drag calculation

In order to compute the drag on the lines the lines are divided into a finite number of segments. For each segment the apparent wind velocity vector is calculated.

$$\underline{v}_a = \underline{v}_t - \underline{v}_{line,i}(\underline{r}_i)$$

(4.10)

The apparent wind vector is then used to determine the drag and lift force vectors per segment. The line drag is always in the direction of $\underline{v}_a$.

$$\underline{D}_{line,i} = \frac{\underline{v}_a}{|\underline{v}_a|} \frac{1}{2}\rho_a |\underline{v}_a|^2 C_{D,line} d_{line} l_i$$

(4.11)

The line lift is always perpendicular to $\underline{v}_a$. On must be careful with the direction of this vector rotation.

$$\underline{L}_{line,i} = \begin{bmatrix} 0 & 1 \\ -1 & 0 \end{bmatrix} \frac{\underline{v}_a}{|\underline{v}_a|} \frac{1}{2}\rho_a |\underline{v}_a|^2 C_{L,line} d_{line} l_i$$

(4.12)

Here $C_{D,line}$ and $C_{L,line}$ are defined as before, but for vector implementation purpose, each with a small sign modification.

$$C_{L,line} = sign(\theta - \alpha_{va})1.1 \sin^2(\theta - \alpha_{va})\cos(\theta - \alpha_{va})$$

(4.13)

and

$$C_{D,line} = abs(1.1 \sin^3(\theta - \alpha_{va})) + 0.02$$

(4.14)

Here θ is defined as the angle between the tether and the positive x-axis. α_{va} is defined as the angle between the apparent wind vector $\underline{v}_a$ and the positive x-axis.
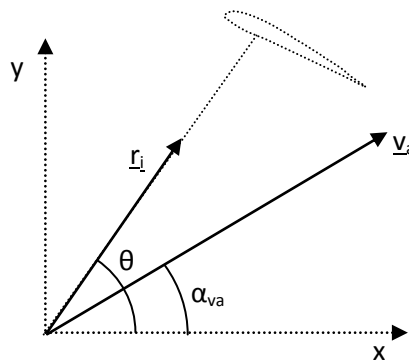
Figure 24, Schematic representation of the kite in crosswind sweep including the defined angles.

Line Lift and Drag vectors during sweep in x y topview
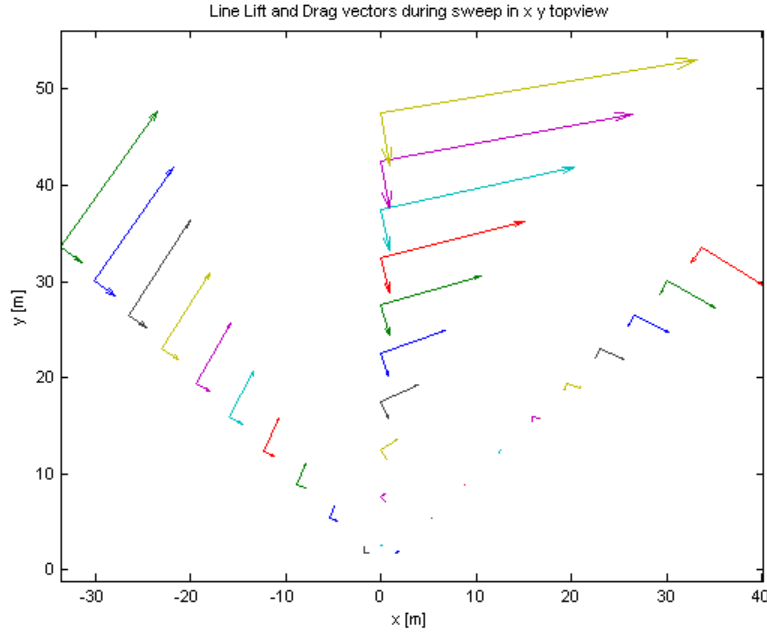
Figure 25, Local lift and drag values on different positions on the kite line during sweep. Vector lengths are in Newton times 10. The line length is 50m and is divided over 10 steps. At the middle position (θ = 90 deg) the kite velocity is 25 m/s. At both the side positions (θ = 45 and 135 deg) the kite velocity is 15 m/s. The used wind velocity is 5 m/s.

For each line section the local lift and drag is calculated. Using moment arm r_i between the section element and the origin the moment around the origin introduced by each section is calculated.

$$M_{line,i} = \underline{r}_i \times \underline{D}_{line,i} + \underline{r}_i \times \underline{L}_{line,i}$$

(4.15)

All section moments are summed to form the total line drag moment.

$$Line\ Drag\ Moment = \sum_{i=1}^{n} M_{line,i}$$

(4.16)

The goal here is to compensate for the effect of the line drag on the kite's velocity. The arm of the total line drag moment is equal to the line length. This is why the total line drag moment is divided by the line length to form the line drag result on the kite.

$$D_{line,k} = \frac{Line\ Drag\ Moment}{Total\ Line\ Length}$$

(4.17)

It would now be convenient to define a constant line drag coefficient that is based on the dynamic pressure at the location of the kite ($\rho_a v_{a,k}^2 / 2$) and defined over the total line surface area S_{line} (length times diameter).

$$C_{D,line,k} = \frac{2 D_{line,k}}{\rho_{air} v_{a,k}^2 S_{line}}$$

(4.18)

It will now be determined whether it is possible to define a constant line drag coefficient $C_{D,line,k}$ over the entire sweep. This is why $C_{D,line,k}$ is plotted as a function of the kite´s velocity and position in the sweep.
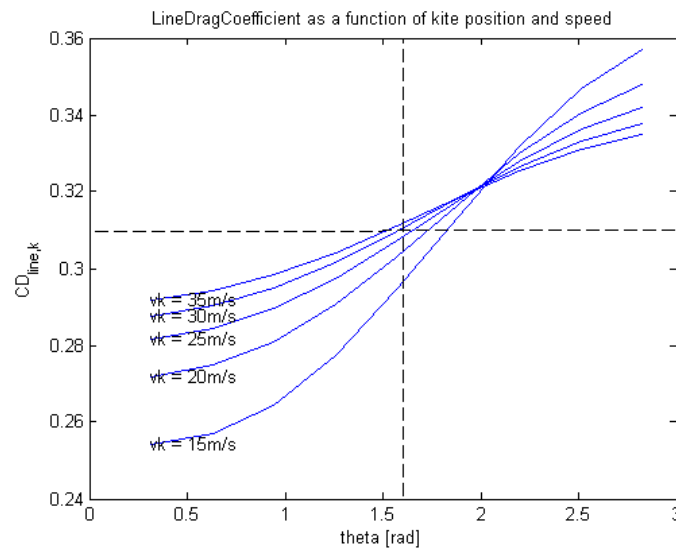
Figure 26, Line Drag Coefficient as a function of kite velocity and position. [Setup: Total line length: 50m, Line thickness: 2mm, Number of Lines: 3 in first 25meter and 4 in last 25 meter.]

$C_{D,line,k}$ becomes more constant at higher kite velocities. This can be expected as the variation is initiated by the difference in apparent wind velocity between the start of the sweep (were the line moves with the wind) and the end of the sweep (were the line moves into the wind). The expected top speeds during a crosswind sweep are between 20 and 25 m/s. The location of the highest speed is usually a few degrees before straight downwind.

It is concluded that a constant value of $C_{D,line,k}$ = 0.31 can be used for the crosswind sweep experiment with an accuracy of around ±10%. It would be most accurate to use the full integrating calculation to determine the line drag in each sweep, but for clarity and simplicity of the line drag correction method it was decided to use the obtained constant drag coefficient in this project.

5 Component 2: Rider

The second component of the system that will be considered is the rider. While sailing, the rider stands on the board, balancing between the force of the kite and the force of the board. The objective of this chapter is to define a method to model the forces that act on the rider. An approximation of the expected magnitude of the mechanical contact forces introduced by the lines and the board is given.

Figure 27, Typical stance for a speed kitesurfer. The rider's hair gives some indication of the apparent wind direction at the location of the rider's head.

The rider is defined as:

- The person standing on the board and steering the kite
- The handle bar that is used for steering the kite
- Everything the rider is wearing (harness, wetsuit, impact vest, cap)

There are four forces acting on the body of the rider.

- Gravitational body force (W_{rider}).
- Contact force from the board acting on the soles of the rider's feet (F_{board}).
- Contact force from the lines acting on the handle bar and on the harness of the kitesurfer (T_{line}).
- Aerodynamic drag force (D_{rider}).

All four forces need to be investigated to get a good impression of what can be expected during speed sailing. A fifth force could be given but has purposely been omitted as it should not be present if the rider has found the right stance. This fifth force is an impact force from water spraying against the ankles of the rider.

5 Component 2: Rider

A free body diagram has been drawn showing all four forces.
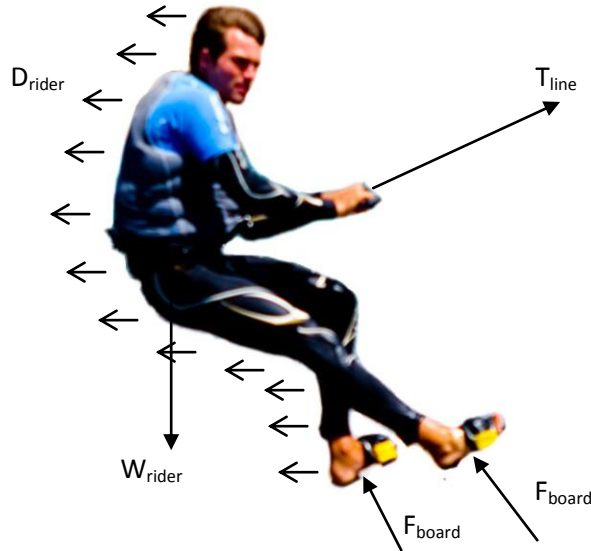
Figure 28, Free body diagram with all forces acting on the rider.

5.1 Gravitational force

The first force that will be discussed is the gravitational force. The component rider contains the largest part of the system's total mass. This is why it is important to give a good overview of how the rider mass is build up. In order to estimate the total mass of the rider each component of the rider is listed in Table 3 with its mass.

Component	Mass [kg]
Human Body	80
Wetsuit, wet	3
Impact vest, wet	1
Harness	2
Handle bar	0.5
Total	**86.5**

Table 3, Mass breakdown of all components of the rider.

The total body force W_{rider} is thus estimated at 9.81*86.5 = 850 N.

5.2 Aerodynamic drag on the rider

The second force that will be discussed is the aerodynamic drag on the rider. This paragraph serves to investigate how this force can be correctly introduced into the model.

A first estimate of the aerodynamic drag can be given when the apparent wind velocity and density are known. For this the frontal area needs to be estimated and a certain drag coefficient needs to be assumed. The drag force can then be calculated using:

$$D_{rider} = \frac{1}{2}\rho_{air}v_a{}^2 S_{rider}C_{D,rider} \tag{5.1}$$

The frontal surface area of the rider is first estimated using Figure 27. This picture was chosen because the camera position is estimated to be almost exactly in line with the apparent wind vector. This means that a good first estimate of the frontal area can be deduced from this picture.
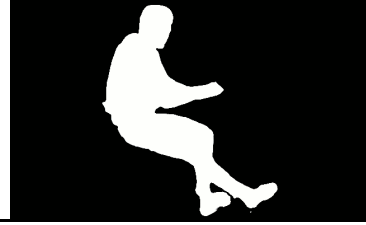
Number of white pixels	37498 pix
Measured pixel size	277 pix/m
Pixel area	76729 pix/m^2
White area is frontal area	0.489 m^2

Table 4, Estimation of the frontal surface area using image pixels

To be able to give a first estimate of the drag coefficient it is first required to estimate the expected Reynolds number. For this the human body is regarded as a composition of different sized circular cylinders. The smallest cylinder diameter is found at the location of the wrists and is estimated at 0.05m. The largest diameter is found on the chest and is estimated at 0.25m. Thus the reference length is estimated as L_{min} = 0.05m to L_{max} = 0.25m.

The apparent wind velocity is estimated to range between 15 and 30 m/s. A kinematic viscosity of v = 1.47E-5 m^2/s (15˚C, Standard Atmospheric Pressure) is assumed. The Reynolds number can thus be expected to be in the range:

$$\mathrm{Re}_{rider} = \frac{v_a L}{v} = \frac{15 \cdot 0.05}{1.47 \cdot 10^{-5}}...to...\frac{30 \cdot 0.25}{1.47 \cdot 10^{-5}} = 5 \cdot 10^4...to...5 \cdot 10^5 \tag{5.2}$$

It is now investigated what drag coefficient can be expected at this range of Reynolds numbers.
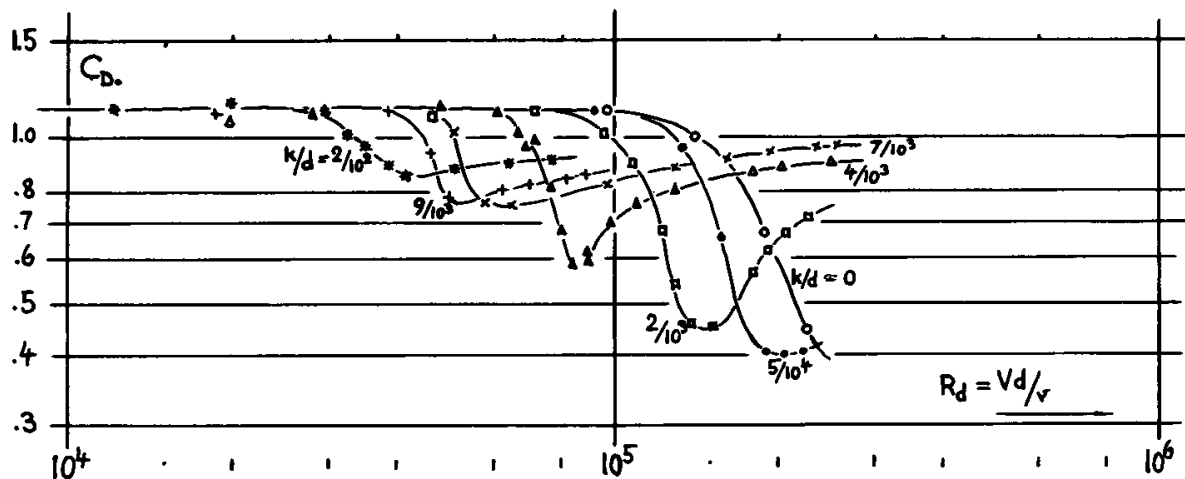
Figure 29, Drag coefficient of cylinders having various degrees of surface roughness (sand-grain size "k" as against diameter "d"). Source: (5)

The drag coefficient of a two dimensional circular cylinder as a function of Reynolds number is shown in Figure 29. The location where the drag coefficient drops rapidly is called the critical Reynolds number. The critical Reynolds number varies with surface roughness and free stream turbulence and can be expected somewhere between $4 \cdot 10^4$ and $4 \cdot 10^5$. It is noted that the critical Reynolds number lies inside the expected range of Reynolds numbers and thus needs to be carefully considered.

For a rider wearing a standard wetsuit the surface is expected to be rough as compared to a polished surface. The sand-grain size "k" over diameter "d" is estimated at 1/100. Using this roughness in Figure 29 it can be seen that the drag coefficient remains between 0.85 and 1.15 in almost the whole region of Reynolds numbers between 10^4 and 10^6. When a single drag coefficient with reference to the frontal area needs to be used over for the entire rider it is proposed to use 1.0 ± 0.15.

In reality the cross section of a human body is not perfectly circular, also it needs to be taken into account that it is not a two but a three dimensional shape. The result above is compared to literature values for the human body drag.

It is found in Hoerner's Fluid Dynamic Drag (5) that the drag area D/q of an average man with a mass of 75 kg equals 5 ft^2 or 0.47 m^2 while standing upright and facing sideways in a 30 to 60 m/s airflow (Figure 30). Note that the flow velocity related to this literature value is up to twice the expected flow velocity. Still it can be said that this is in conformity with the drag area given by the results obtained above. Multiplying a drag coefficient of 1.0 with a frontal area of 0.49m^2 results in a drag area of 0.49m^2 for a 80 kg kiteboarder.
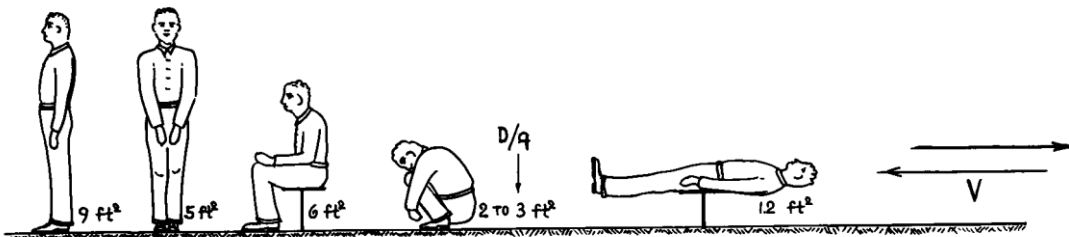
**Figure 30, Drag areas (D/q in ft^2) of an average man in various positions, tested in a wind tunnel at speeds between 100 and 200 ft/sec (30 and 60 m/s). Specifications: W = 165 lb (75 kg); h = 5.9 ft (1.8 m); Volume = 2.6 ft^3 (7.4E-2 m^3). Source (5)**

In the text above a single flow velocity and direction is applied to the complete component called rider. In reality the presence of a wind gradient complicates this analysis. In chapter 4 this was already explained for the case of the lines. Recapitulating, the apparent wind vector $\underline{v}_a$ as felt by the rider results by subtracting the sailing velocity vector $\underline{v}_s$ from the true wind velocity vector $\underline{v}_t$.

$$\underline{v}_a(h) = \underline{v}_t(h) - \underline{v}_s$$

(5.3)

Introducing the wind gradient, results in a true wind velocity, and thus an apparent wind velocity, that varies as a function of height. The apparent wind varies in both magnitude and direction. In the first two meters above the water surface the true wind velocity shows a steep variation over height. Due to this the apparent wind shows a steep variation in both magnitude and direction. To illustrate this effect, velocity vectors v_s, v_t and v_a are plotted in 3D over the first two meters above the water.
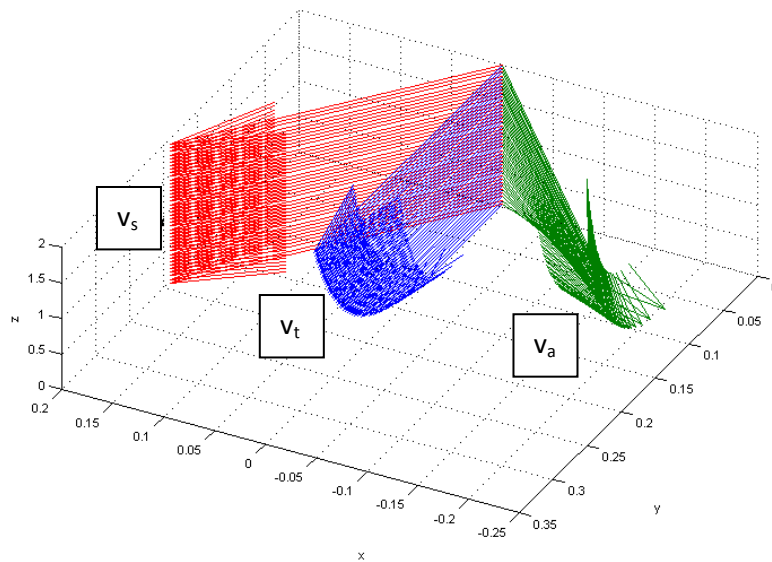

Figure 31, Velocity vectors v_s, v_t and v_a as a function of height. Sailing speed v_s=25m/s at a 135 degree downwind course. The wind speed v_t = 25m/s at 10m above the surface. The apparent wind changes magnitude and direction over height.

In order to account for the variation in $\underline{v}_a$ over height it was decided to split the rider into different sections. For each section the local apparent wind vector $\underline{v}_a$ is calculated using equation 5.3. Also the frontal area and the drag coefficient of each section are estimated. Addition of all section drag forces results in a total resultant drag force.
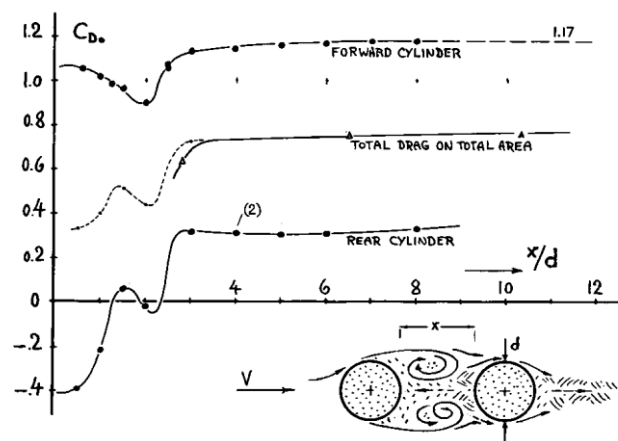

Figure 32, Drag coefficients of two circular cylinders, one placed behind the other. Re = 10^5. Source (5)

It is noted that in Figure 27 the body of the rider is positioned such that the left arm travels in the wake of the right arm. The distance between the arms is estimated at four times the radius. Hoerner shows in Figure 32 that the expected drag coefficient over the total of the two frontal areas is estimated at Cd = 0.74.

The upper legs are also more or less in aligned position. Here the estimated distance between the cylinders is equal to the radius. It is read from Figure 32 that the expected drag coefficient could be as low as Cd = 0.4 but taking into account that the legs are not perfectly aligned it is found more realistic to use a slightly higher value. Cd = 0.6 is seen as a best educated guess. The lower legs are seen as two separate cylinders without interference effects, this means Cd = 1.0 is used.

	L [m]	D [m]	Nr	S [m2]	Cd	Cd*A [m2]	H [m]
Feet	0.26	0.06	2	0.031	1	0.031	0.05
Lower Legs Low	0.25	0.09	2	0.045	1	0.045	0.17
Lower Legs High	0.25	0.11	2	0.055	1	0.055	0.37
Upper Legs	0.5	0.15	2	0.150	0.6	0.090	0.5
Hips and Belly	0.25	0.25	1	0.063	1	0.063	0.63
Chest	0.25	0.25	1	0.063	1	0.063	0.88
Lower Arms	0.3	0.07	2	0.042	0.74	0.031	0.63
Upper Arms	0.3	0.08	2	0.048	0.74	0.036	0.88
Head	0.25	0.17	1	0.043	1	0.043	1.13
Sum				**0.539**		**0.455**	

Table 5, the body is regarded as a composition of differently size cylinders. This allows calculation of the drag contribution of each part as a result of the local flow conditions. L = part length, D = part diameter, Nr = Number of parts, S = frontal surface area, H = height above ground to calculate v_a.

Table 5 shows the drag areas that are used in the model and the heights that are used to calculate the apparent wind velocity. Results from this approach are presented after combining all components of the sailing system in chapter 8.

Wind tunnel testing and CFD analysis where considered, but fall outside the scope of this thesis. The amount of work involved is too large, and it is expected that accurate results cannot easily be obtained with these methods. The non homogeneous flow caused by the wind gradient is not easily constructed in both wind tunnel and CFD analysis.

5.3 Line Tension and Board Force
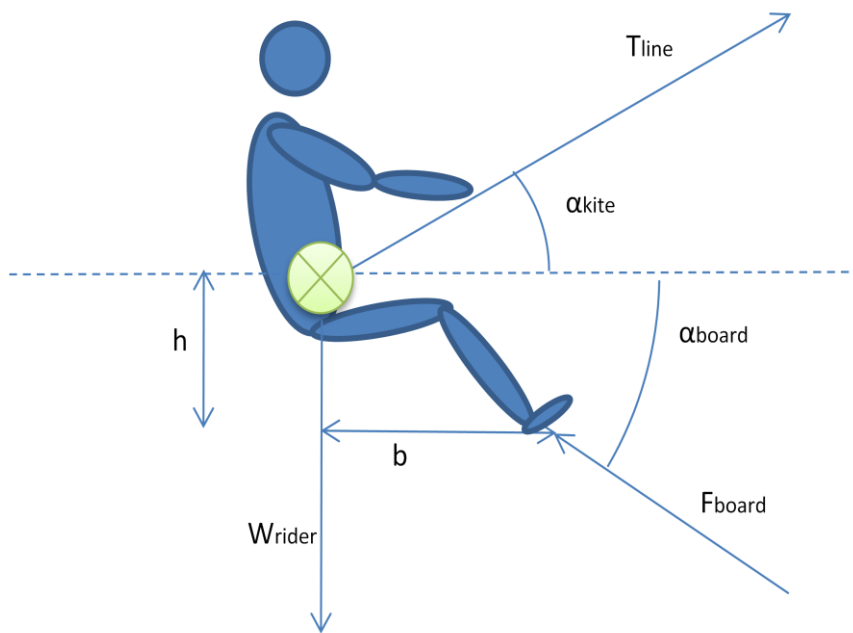
Figure 33, Schematic figure of balanced forces on the rider.

Looking at the free body diagram of the rider four forces where recognized. Gravitation and aerodynamic drag where treated in paragraph 5.1 and 5.2, the last two forces will be treated in this paragraph:

- Line tension contact force T_{line}, always tension and slightly up.
- Contact force between board and rider F_{board}, always introducing a compression force in the legs.

Both forces are limited by the weight and strength of the rider. In order to obtain a realistic estimate of the magnitude of both forces it was decided to investigate five selected pictures. All pictures were taken in Luderitz, Namibia, during the 2008 Luderitz Speed Record Attempt. This is an event where kitesurfers and windsurfers can aim to break both personal records and the outright speed sailing world record. The former outright world sailing record of 50.57 knots as well as the current Dutch outright sailing record of 47.36 knots where set during this event.

Five pictures (Figure 34) were selected. For each picture the center of mass location was estimated. The horizontal and vertical distance to the longitudinal center line of the board is also estimated. This information is used to obtain the total line tension T_{line} and total board contact force F_{board} in that situation. For this calculation the drag force on the body of the rider is neglected. This is seen as a valid approach for the following reason. The drag force is always in the direction of the apparent wind. The apparent wind is more or less perpendicular to the plane of the picture in all five cases, while F_{board}, T_{line} and W_{rider} are working by estimate in the plane of the illustration.

5 Component 2: Rider

The line tension is calculated using the formula:

$$T_{line} = \frac{W_{rider}}{\sin(\alpha_{kite}) + \dfrac{h}{b}\cos(\alpha_{kite})}$$

(5.4)

The hydrodynamic force is calculated using the formula:

$$F_{board} = W_{rider}\sin(\alpha_{board}) + T_{line}\cos(\alpha_{kite} + \alpha_{board})$$

(5.5)

Figure 34,Selected pictures for estimating line tension and board force.

Figure 34 shows the pictures that were used as sample cases. For each picture the ratio between the vertical and horizontal distance between the board and the center of gravity h/b is obtained. Also the angle between the kite lines and the horizontal α_{kite} is obtained. The obtained results are shown in the following table:

CASE	h/b	α_{board} [deg]	W_{rider} [N]	α_{kite} [deg]	T_{line} [N]	F_{board} [N]
1	0.68	34	850	28	797	850
2	1.07	47	850	22	624	845
3	1.03	46	850	33	603	726
4	0.93	43	850	14	745	985
5	0.75	37	850	32	731	773

Table 6, Case study results. In five pictures the moments around the board were balanced.

It is noted that it can roughly be estimated that the line tension during a record speed run is between 70% and 95% of the body weight. The board contact force is found to be between 85% and 116% of the body weight.

6 Component 3: Kite (Crosswind Kite Test)

The properties of the components lines and rider were studied in the previous two chapters. This chapter will serve to study the aerodynamic properties of the component kite.

The kite provides the propelling force of the system. In chapter 3 on sailing performance it became clear that the higher the lift to drag ratio of the kite the higher the speed potential of this kite will be. This means that information about the lift to drag ratio at different flight conditions is of great importance. Also the possibility to use a large range of different lift coefficients can be an important asset. In kitesurfing this is normally called a large depower range. This enables the kitesurfer on one hand to use the kite at a low lift coefficient when the apparent wind velocity is high (normally on a square course), resulting in a moderate force and good control. On the other hand it enables the kitesurfer to use maximum power when racing downwind and going for the ultimate record. The lift to drag ratio and lift coefficient are regarded as the two most important required parameters.

For a performance analysis of a kiteboarder a thorough examination of the kite's properties is clearly of great importance. The availability of experimental results for different kites is limited. It is thus decided to study the kite properties experimentally. Therefore the first objective of this chapter is to obtain an experimental method to test the kite properties. The second objective is to describe the obtained experimental results.

Different possible methods for testing kites are discussed in paragraph 6.1. A method referred to as crosswind testing is selected as the most appropriate. The exact procedure of testing was worked out further in paragraph 6.2. The required components of the test setup are described in paragraph 6.3. A sample of the obtained raw results is presented in paragraph 6.4. The used theoretical methods for working out the results are described in paragraph 6.5. The obtained results are presented and discussed in paragraph 6.6. Sources of error are discussed in paragraph 6.7. Conclusions and recommendations concerning the kite test are given in paragraph 6.8.

6.1 Kite testing methods

This paragraph serves to investigate which methods could be used to test the aerodynamic properties of a kite and to select the method that is used in this thesis.

In literature only little can be found on the specific subject of kite performance testing. Justin Stevenson(8), (9) shows his proceedings with car traction testing and circular testing. Aart de Wachter (10) performed wind tunnel tests with a Ram Air inflated kite. As cited from Barlow's book on Low-Speed Wind Tunnel Testing(11):

Experimental information useful for solving aerodynamic and hydrodynamic problems may be obtained in a number of ways: from flight experiments; drop tests; rocket sleds; water tunnels; whirling arms; shock tubes; water tables; rocket flights; flying scale models; road tests; ballistic ranges; subsonic, near sonic, transonic, super sonic, and hypersonic wind tunnels; and other methods leading to an almost endless list. Each device has its own sphere of superiority, and no one device can be called "best". Source: (11)

In a trade off on which way of obtaining performance characteristics is most appropriate, eight different testing methods that seem feasible for kites are compared to each other:

1. Wind tunnel testing
2. Car traction testing
3. Circular testing
4. Dynamic flight testing/Crosswind testing
5. Static flight test
6. Gliding test
7. Water tank testing
8. Riding test (Riding on land, water or ice)

Each of the proposed testing methods is described in the following section.

1) Wind tunnel testing

Since the start of experimental aerodynamics, wind tunnels have been of great value to provide accurately controlled and monitored testing conditions. The huge amount of wind tunnel testing experience available today enables engineers to obtain very accurate experimental data. Testing kites in a wind tunnel can give accurate experimental data, but there are also a few limitations.

Firstly the size of the tunnel test section limits the size of the kite that can be tested. The larger the wind tunnel the more expensive it is to operate. Testing a small surf kite in a wind tunnel is possible but will already be a very costly occupation. A frequently used way to test a large structure in a small wind tunnel is by using a scale model. Building a scale model of a kite is not impossible but it will be a challenge to produce exactly the same structure. Scaling down seams, wrinkles and fabric thickness could even prove to be impossible due to material constraints. The flexible shape of the kite will inevitably change when load is applied. It can't be guaranteed that the model reacts similar to the full sized kite. Besides, a model will be more expensive than a standard production surf kite. Finally it can be said that testing dynamic behavior is not possible in a wind tunnel.

2) Car traction testing

Kites could be tested by mounting a scale or load cells on a car or on a truck. By adjusting the driving speed it is possible to adjust the velocity of the airflow that passes the kite. The cost of such a test will be moderate if a testing truck is already available. As explained by Stevenson (8), obtaining accurate data with this method is a challenge. Accurately measuring the angle between the free-stream direction and the direction of line tension will be of great importance to obtain accurate lift to drag ratios. The availability of a large test field is very important. A large beach or airfield would be ideal. Most importantly the field has to be long enough to accelerate to the desired velocity, perform a test and decelerate again. A smooth test field will be favorable for the results as every bump can disturb the stable situation of the kite and introduce a small load peak. As this test is performed outdoors the favorability of the testing conditions will depend on the weather.

3) Circular testing

As argued by Stevenson (8),(9), circular testing could provide a more accurate method then car traction testing. Circular testing could also be called a whirling arm experiment. A rotating device is placed in the middle of the test ground. The kite lines are connected to the device at a certain distance from the center of rotation. Due to the rotation of the system the kite whirled around and flies in large circles around the center of rotation. This enables the kite to fly in a windless environment. Higher accuracy is due to the fact that the test can be performed indoors and that the circular movement increases the sensitivity of the angle that needs to be measured to obtain the lift to drag ratio of the kite.

A large indoor facility would be optimal for testing, preferably with a free test ground with a diameter of more than 40 meters. In that case the line length could be around 15 meters long. Finding this test ground could be difficult and using it could be expensive. A test device with the function of a large whirling arm should be build for testing large kites at high velocities. Stevenson shows that it is also possible to perform the test while walking backwards in a circle, this is undoubtedly the least expensive way of testing but also limited to small kites.

4) Dynamic flight testing/ Crosswind testing

In normal use one can fly a kite while standing on the beach. If the kite is steerable one can steer from one side to the other. While flying from one side to the other the kite will obtain a certain velocity and produces a certain tension in the lines. Both velocity and tension give information about the kite's properties. By accurately tracking the movements and forces of the kite in combination with accurate environmental data one could obtain the required aerodynamic kite properties. Inaccuracies could be minimized by averaging over and extended flying time. The more data the more accurate the results will be.

A large advantage of this testing method is that there is no limitation to the size of the kite. Even a 500 m^2 energy producing monster that will never fit into any wind tunnel can be tested full scale using this method. Kites can obtain high velocities in moderate wind. This is due to the large wing loading introduced by the line tension. No additional energy apart from the available wind energy is required. This means that it is not needed to wait for a storm to test the kite at high velocity. Independent of whether it is a large or a small kite the test location and testing method stays the same, possibly the size of the load sensors needs to be adapted to the expected loads.

A limitation could be that when flying a kite from one side to the other in strong wind, the tension could become so large that the kite could be damaged. The velocity of flight is depending mostly on the lift to drag ratio of the kite and the wind velocity. This means that testing at low velocity could require such light winds that it is not possible to launch the kite.

This can be seen as a relatively cheap way of testing kites of all sizes, but always depends on the actual weather conditions. An undisturbed and constant wind will be favorable to achieve reliable results.

5) Static flight test

Similar to the crosswind kite test, but here the kite would be launched and kept at a fixed position. By accurately monitoring the position of the kite and the tension in the lines it produces, one can obtain the required aerodynamic constants. One of the easiest ways is probably to place the kite directly overhead and determine the position by analyzing photographs. Many methods of determining the position of the kite are possible.

A disadvantage of this method is that kites can only be tested at the available wind velocity. The expected accuracy is moderate due to vulnerability to atmospheric turbulence.

6) Gliding test

It could be possible to launch the kite from an elevated position and let it glide down, similar to a paraglider. By determining the glide angle, the lift to drag ratio can be determined. By changing the payload the flying velocity can be controlled. Testing at high velocity would require a large payload. Monitoring the velocity of flight one can obtain the lift coefficient. Outdoor testing is possible but indoor conditions could provide a more controlled environment. A good elevated starting possibility will be critical for performing tests. Steering the kite while in flight would probably require a form of radiographic control. Possibly the kite will fly straight enough without any form of control.

7) Towing tank or water tunnel testing

Water tunnels tend to be physically smaller then wind tunnels while achieving the same Reynolds numbers. Testing kites under water could provide a good way of testing but will probably require the use of scaled models. Water tunnels are in general much smaller then wind tunnels. Using a towing tank could possibly provide a somewhat larger test section, but is still restricted to small scale models. Water tank and water tunnel testing will probably be expensive and impractical.

8) Riding test

Instead of testing kites while standing still on the beach one could also test kites while letting the kite propel the test operator or test rider over land, ice, or water. When all forces are accurately monitored as well as the velocity of wind rider and kite, one can obtain the required aerodynamic characteristics.

A drawback of this method is that many unknown parameters have to be estimated in order to obtain the required values. This could decrease the accuracy of the obtained data.

The method could be fairly cheap and when looking at kite surfing, ice kiting and buggy kiting it is the equivalent of airplane flight testing. For kitesurfing the board drag forms a large unknown factor and could make this way of testing kites unreliable. With accurate knowledge about the board properties this method could be interesting.

Conceptual analysis

The different test concepts were examined and compared on different points.

- Testing cost
- Complexity
- Accuracy
- Kite limitations
- Requirements for testing conditions
- Need for a special testing facility
- Possible other problems

An overview of the conceptual analysis is given in Table 7.

	Wind tunnel testing	Car traction testing	Circular testing	Flight/cross wind testing	Static test	Gliding test	Towing tank test	Riding test
Testing cost	High	Medium	High	Low	Low	Low	High	Low
Complexity	Medium/ Low	Medium	Medium/High	Medium	Low	Medium	Medium	Medium
Accuracy	High	Low	Medium	Medium	Low	Low	Low	Low
Kite Limitations	Limited by test section size. Only small kites.	Limited by car's power. Large surf kites are possible.	Limited by power and moment of test device. Also limited by size of the test facility.	All sizes. Only steerable kites.	All kites	All sizes. Possibly limited by size of testing facility.	Only non floating scale models.	The kite has to fit the wind conditions.
Weather require-ments	All weather (if in doors)	All weather	Indoors = All weather Outdoors = no wind	6 to 12 knots	6 knots +	In doors = All weather Outdoors = no wind	All weather	Good sailing weather.
Special testing facility	Wind tunnel facility	Testing car + large testing terrain	Circular testing device + preferably large indoors facility (min 50m x 50m x 15m)	Large testing terrain with "clean" wind.	No	Preferably large indoors facility (20m wide x 30m long x 20 m high)	Towing tank facility	No
Problems	Influence of walls	Very accurate angle measurement is needed	Position tracking of the kite.	True wind measurement needs to be very accurate	Efficient kites become un-stable	How to make a gliding kite stable?	A scale model of the kite is needed	On water all instrumen tation needs to be sealed.

Table 7, Considered kite test methods and their score on each examination point.

For all test methods it is required to obtain information on both the magnitude and the direction of the aerodynamic forces on the kite. Especially the determination of the direction can be seen as a challenge. The accuracy with which the angle between the direction of the aerodynamic force and the direction of the apparent wind can be obtained, determines how accurately the lift to drag ratio can be obtained.

In deciding which testing method is most appropriate for this thesis work, cost was an important factor. It was seen as a large advantage to be able to use a testing method which is easily available and does not involve large additional costs while testing. The use of scale models was seen as an

important negative aspect, as one of the aims of the test is to select the best speed kite available on the market. Building scale models of existing kites would result in high costs and low reliability. It was concluded that the crosswind test was the most promising method for kite testing during this thesis.

6.2 Description of crosswind kite testing setup

As explained in the previous paragraph, the selected test method is based on flying kites horizontally from one side to the other while recording flight data. This paragraph serves to explain the used process of testing kites in more detail and to clarify which instrumentation is required to gather all the data.
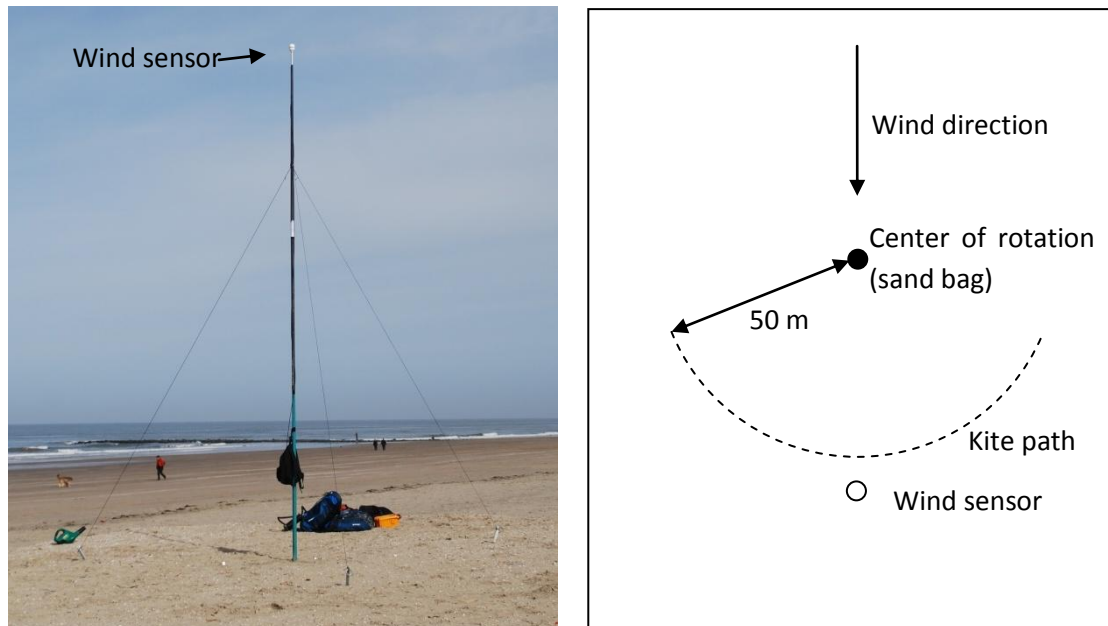
Figure 35, Left: Mast with wind sensor mounted in the top. Right: Schematic representation of the crosswind test setup.

Firstly the test requires a large open field, preferably in combination with undisturbed wind. It was decided that for this thesis the beach provided the most suitable test ground. Beaches provide a lot of freely available space in combination with undisturbed wind, especially when the wind is parallel to the beach or any onshore direction.

Secondly an anchoring point is required that is strong enough to distribute the large aerodynamic kite forces into the ground. For this reason the test setup includes a large bag that can be filled with sand and serve as an anchor. Advantages of using a bag include the ability to install it at any location on the beach and include an automatic overload security. Overloading the bag will cause it to slowly slide into a new position, reducing the potential danger caused by a failing construction.

Thirdly a device is required that records the resulting aerodynamic forces. The most favorable position for this device is seen to be in the lines and close to ground. Hanging a large sensor package into the kite could add drag and disturb the normal flying behavior. A standard kite handlebar is attached to the bag for steering the kite. Above the handle bar there are three lines that run to the kite. Two steering lines and one depower line. Each line is fitted with a load cell and each load cell is connected to a logger module. At a distance of 25 meters from the bar the depower line splits into two 25 meter lines which each run to their standard connection point on the kite. This results in a 50 meter total line length. This line length allows the kite enough space to accelerate to its maximum

velocity and is still comfortable in use. Longer lines introduce larger line drag and so a larger compensation for line drag could decrease the accuracy of the method. Quantification of the line drag contribution follows in paragraph 6.5.3.

The fourth requirement is to track the velocity of the kite while moving through each sweep. The kite velocity is required firstly to obtain the velocity of the air flow interacting with the kite. Secondly the kite velocity is required to calculate the lift to drag ratio of the kite. Roughly speaking the maximum velocity of the kite divided by the wind velocity equals the lift to drag ratio of the kite. A more accurate explanation of this principle can be found in paragraph 6.5. To measure the kite velocity, the use of GPS technology was found to be most suitable. Accurate data can be obtained by a small separate unit. The specifications will be clarified in the next paragraph.

Finally environmental information is required. Most importantly an accurate wind sensor is essential for obtaining accurate experimental results. It was decided to mount a wind sensor on a 6m high pole to allow for undisturbed wind measurement. It was aimed to fly the kite in straight lines parallel to the ground at exactly the height of the wind sensor.

6.3 Materials

In this paragraph a more detailed description of the used components is given. It is described what sensors are used and what accuracy can be expected. Also it is described which components needed to be self fabricated and which kite was selected for testing.

6.3.1 Load cell data logger

Figure 36, Picture of loadcell logger version 1. The principle of version 2 and 3 remained the same. Only the electronics where improved in subsequent versions.

In order to record the tension of the lines a configuration of three load cells is used, two installed in the steering lines and one in the depower line. A load cell consists of a metal body that deforms elastically when a load is applied. The small elastic deformations are registered by so called strain gages, wired patches that change their electrical resistance upon deformation. The used load cells

are produced by transducer techniques. The two cells measuring the steering line tension are rated as 300 pound tension/compression load cells. The one attached to the depower lines is rated as a 1000 pound tension/compression load cell.

In the course of the project, three subsequent logger versions where build and calibrated. The final version is able to log at 10 Hz and includes a GPS for accurate time stamps.

6.3.2 GPS

Recording the kite velocity is done using a handheld GPS device mounted to the kite. Other methods, like tracking the kite movements using photo sequences and using a radar gun, where considered, but were considered to be less accurate and more laborious than using a GPS. Advantages of GPS include: light weight, easy to process the data, cheap unit, good sample rate and continues tracking. The device is turned on at the start of the testing day and tracks all movements during the day.

A second handheld GPS was used on the ground. This device was used to provide an accurate time on the ground during the experiment. Also the location of the ground anchor could be logged and marked as the center of rotation.

The GPS outputs a number of parameters. Only five of the available parameters where used in this project. The first is time, as each data point requires a time stamp. The second and most important one is velocity. This is the magnitude of the 3 dimensional velocity vector and is frequently called the Doppler velocity. Shortly said, the frequency of the signal received from each satellite changes as a result of moving into or away from the direction of the satellite. Combining the Doppler shift of each signal, results in a velocity. Most importantly this method is more accurate than differentiating between the obtained points in space (track points). The last three parameter that were used form the track point coordinates; latitude, longitude and height.

The two handheld GPS units that were used during the experiment are the GT-31 by Locosys and the Qstarz BTQ1300.

Figure 37, Locosys GT-31 on the left and Qstarz Q1300 on the right.

GT-31

The GT-31 is kept on the ground and used as an accurate system to read the time. Also it is used to record the location of the ground anchor with respect to the kite.
Output frequency: 1 Hz

Qstarz BT Q1300

The BT Q1300 is mounted to the kite, this is the GPS that tracks all the movements of the kite.
Output frequency: 5 Hz
Accuracy position: 3.0m 2D-RMS
Accuracy velocity: 0.05 m/s with the aid of DGPS
Size: 62 x 38 x 7 mm
Weight: 22 g

6.3.3 Wind sensor

There are many methods to measure the wind velocity. While selecting the most suitable method for this thesis, a number of measuring principles were considered. A list of available principles is given below:

Flat plate

Probably one of the oldest and simplest means of measuring wind velocity is by hanging a flat plate normal to the wind direction. As the wind blows against the plate the plate gets deflected in the direction of the wind. The amount of deflection is a measure for the wind velocity. This method is seen as too rough and is immediately discarded.

Cup or mill anemometer

The so called cup and mill anemometers are rotating devices similar to a small wind turbine. There are two versions. The cup anemometer has a vertical axis of rotation and uses rotating cups. As the cups have a higher drag coefficient when the wind blows into the cup then when it blows from the bottom side of the cup, a rotating motion is initiated. An advantage of the cup anemometer is that alignment with the flow direction is not required. The device is completely rotation symmetric. The mill anemometer has a horizontal axis that needs to be aligned with the wind direction. This can be done with a wind vane. For both systems the velocity of rotation is a measure for the wind velocity.

Pitot tube

The pitot tube is a tube that needs to be aligned with the direction of flow. The wind velocity is determined by comparing the static pressure and the dynamic pressure. This method is frequently used in airplanes and wind tunnels.

Sonic

The sonic sensor (also called ultrasonic sensor) uses the principle of sound being carried into the direction of the air flow. Sound pulses can be transmitted and received in multiple directions, either in a 2D plane or in 3D. By comparing the times that the sound takes to travel from the transmitters to the receivers both the wind velocity and direction can be deduced.

RASS

RASS (Radio Acoustic Sounding) can be used to sense both temperatures and wind velocities from a distance. This means that only a relatively small (fitting in the back of a pickup truck) ground station is needed to obtain the wind profile up to a height of a few hundred meters. The principle is based on the detection of echoes of radar waves. The radar waves are scattered by acoustic waves, both are transmitted by a station on the ground.

SODAR

Sonic detection and ranging works with a ground based instrument that sends acoustic pulses into the air. By analyzing the reflected signal, wind velocity and direction information can be obtained.

LIDAR

Light Detection and Ranging works similar to SODAR but now with a ground based station sending light pulses into the air. The light is reflected from natural aerosols like dust, salt crystals, water droplets or pollution. By analyzing the reflected light a complete image of wind speed and direction can be obtained. This is generally seen as a very promising method that can measure up to higher altitude than SODAR.

Used Device: Sonic Sensor

Figure 38, Ultrasonic Wind Sensor CV3F by LCJ capteurs. Source: LCJ capteurs.

Both a mill anemometer and a sonic sensor were readily available and could be tested. The sonic sensor showed higher sampling frequency and higher resolution. It was thus decided to use the sonic sensor for the final experiment.

The device is named the CV3F, manufactured by LCJ capteurs. The accuracy as specified by the manufacturer is 5% of the measured wind velocity. The sensor can be used to measure velocities from 0.5 to 99.5 knots. The wind direction is measured with a resolution of 1 degree and a sensitivity of plus or minus 1.5 degree. For accurate directional data the sensor needs to be installed with high accuracy. The operating temperature is from -10 °C (without iceing) to 50°C. The output frequency is 1.87 Hz or 533 ms cycle time.

In order to be able to obtain undisturbed wind information the sensor was placed on a 6 meter high mast that was constructed from 3 old windsurfing masts. The sensor needs to stay clear of the path of the kite and the lines but should be positioned as close to kite as possible. It was decided to position the sensor straight downwind from the position of the anchor point at a distance of 5 meters from the path of the kite.

6.3.4 Used Line Setup
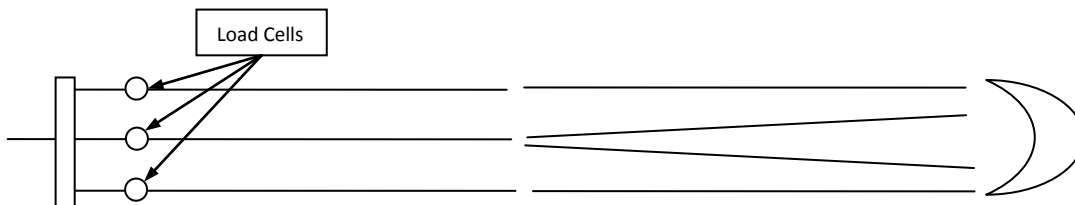
Figure 39, Schematic drawing of the used line setup.

The used line set is composed of seven Dyneema lines with a thickness of 2mm and a length of 25m. The lines are carefully spliced at the ends in order to allow a strong connection. From the bar up, a set of 3 lines is used. After 25 meter the middle line splits into 2 lines. Also the steering lines are extended with another 25 meter each. The load cells are positioned 1 meter above the steering bar.

6.3.5 Tested Kite

Multiple kites where tested and the data has been processed and analyzed. In order to provide a clear presentation, the methods which are used to process the obtained data are illustrated using the results of a selected kite. The Flysurfer Pulse2 6m^2 was selected as a lot of knowledge about this kite was already obtained in the work of de Wachter (10).

Manufacturer	Flysurfer
Model	Pulse2 6.0
Area Flat [m2]	6.0
Area Projected [m2]	5.2
Aspect Ratio	3.85
Root cord [mm]	1340
Mass [kg]	1.6

Table 8, Properties of the kite that is used for the experiment, as specified by the manufacturer.

6.4 Observations and Data

The experiment was conducted as described in paragraph 6.2. The resulting raw data is presented in the current paragraph. As the amount of data is too large to display in a single graph, it was decided to choose three subsequent crosswind sweeps that are representative for the whole experiment. With the use of these three sweeps the obtained data will be presented and discussed.

There are three sensors from which data is obtained, the GPS logger, the load cell logger and the wind sensor. Each sensor produces a number of parameters:

The GPS logger (5 Hz):

- Time
- Longitude
- Latitude
- Height
- Velocity

The Load cell logger (10 Hz):

- Time (using a separate GPS receiver)
- Load cell 1 tension
- Load cell 2 tension
- Load cell 3 tension

The wind sensor (1.876 Hz):

- Wind velocity
- Wind direction
- Temperature

Also the ambient air pressure and the relative humidity are used from the KNMI website. (http://www.knmi.nl/klimatologie/daggegevens/index.cgi) When testing on Scheveningen beach, the weather station of Hoek van Holland, at a distance of 20 km from Scheveningen, is selected as the most representative weather station.

6.4.1 GPS Data

A sample of the obtained GPS data is given below. The three sweeps are easily recognized in the kite velocity parameter due to the high peak velocities.
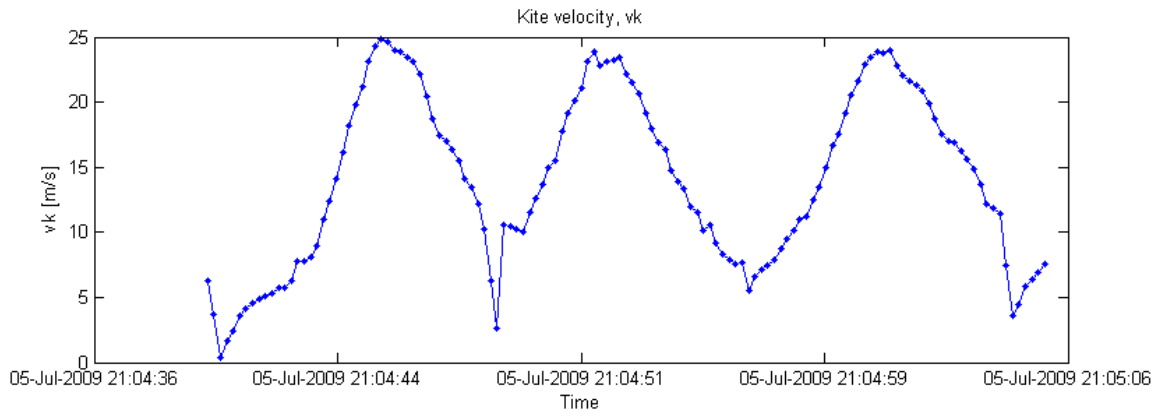
Figure 40, Kite velocity data, obtained with the GPS data logger. Selected sample of three sweeps.

Latitude, longitude and height provide positional information to track the movements of the kite.
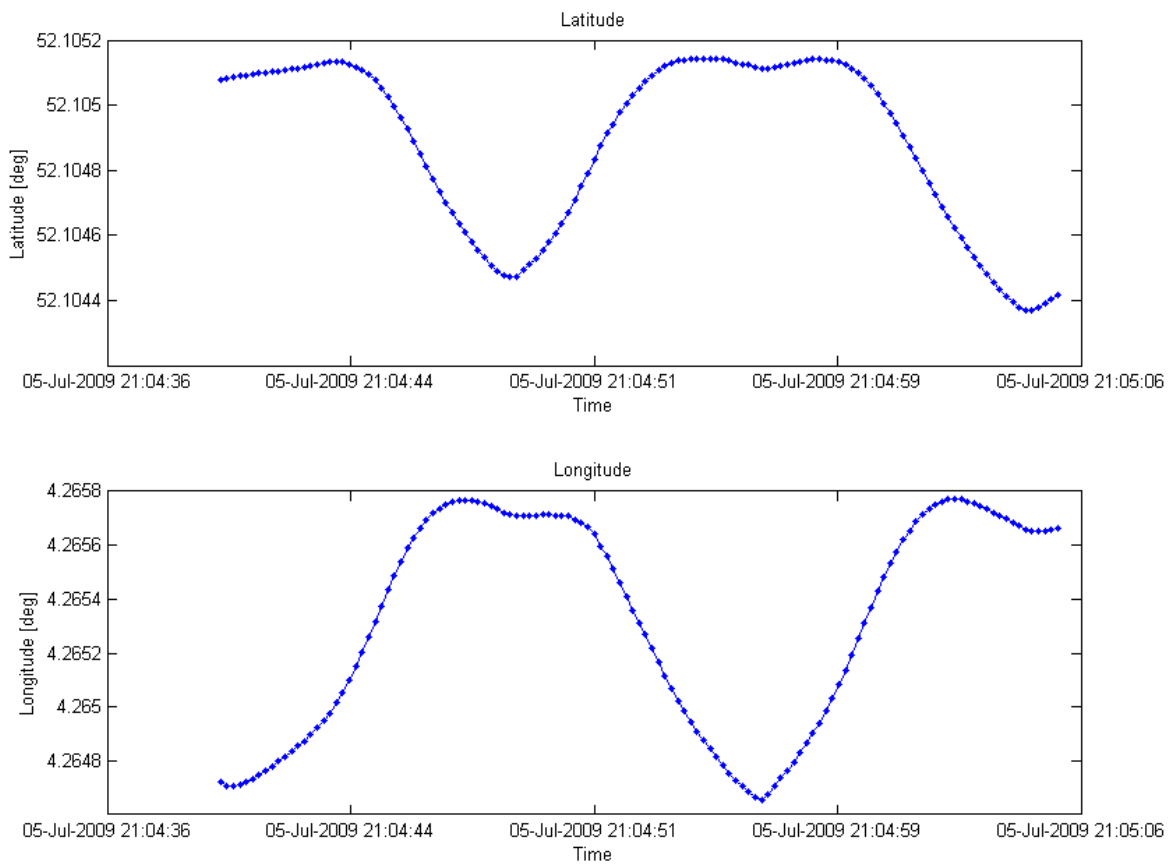
Figure 41, Latitude and longitude data, obtained with the GPS data logger. Selected sample of three sweeps.
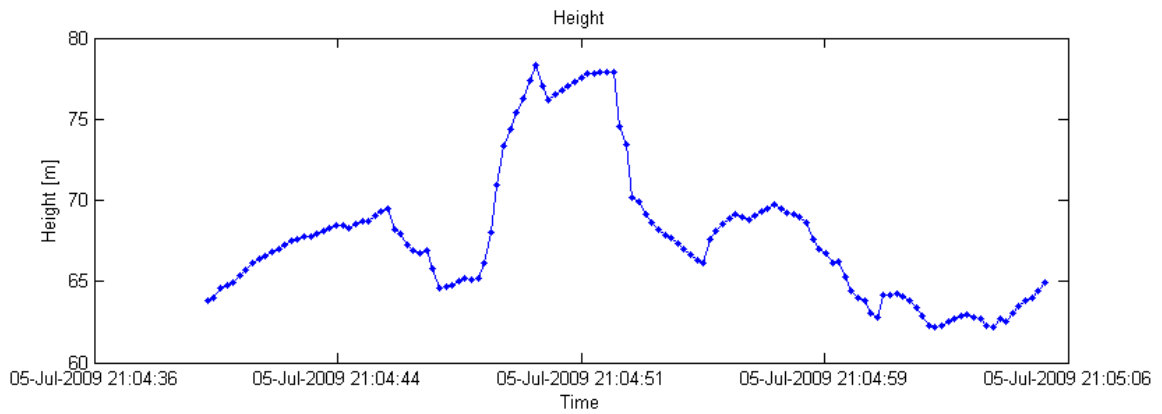
Figure 42, Kite height data obtained with the GPS data logger. Selected sample of three sweeps.

It is noted that the height signal obtained with GPS does not have a high accuracy. Even though the kite is flown at the same height in each sweep the signal shows large variations in height. In reality the variation in height is estimated at plus or minus two meters. More accurate height recordings could be valuable to check the height of the kite during each sweep.

6.4.2   Load cell logger data

Three load cells are used to determine the tension in the lines. Load cell 1 measures tension in the left hand steering line, load cell 2 in the right hand steering line. Load cell 3 measures the combined tension of the two middle (or depower) lines. The sum of all load cells is also plotted. The sample rate is 10 Hz.
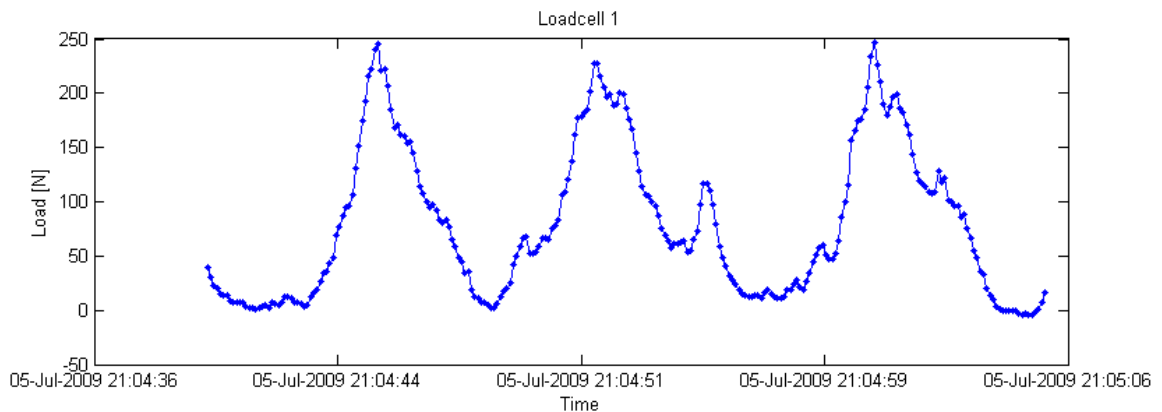
Figure 43, Line tension of the left steering line (load cell 1), measured by the load cell logger. Selected sample of three sweeps.
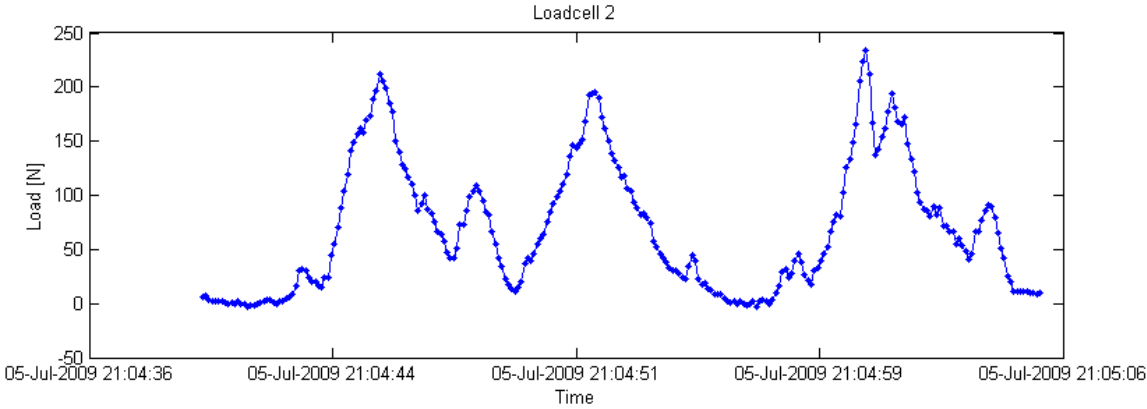
Figure 44, Line tension of the right steering line (load cell 2), measured by the load cell logger. Selected sample of three sweeps.

It is noted that the signal of load cells 1 and 2 clearly shows three large peaks during the three sweep motions. In between the three largest peaks also a smaller peak can be found. The small peaks are introduced by steering inputs. Between the first and second peak tension is applied on load cell 2 to turn the kite. Between the second and third sweep tension is applied on load cell 1.
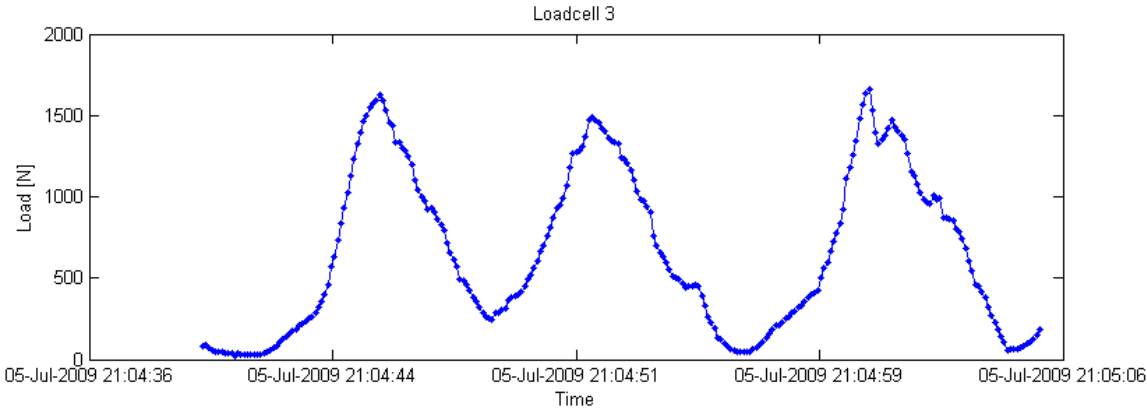
Figure 45, Combined line tension of the front lines (load cell 3), measured by the load cell logger. Selected sample of three sweeps.
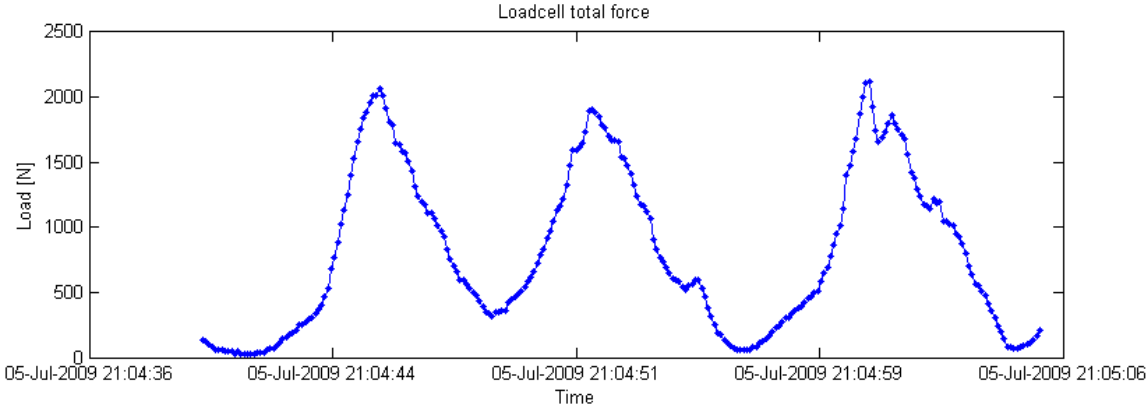
Figure 46, Total Line tension, Load cell 1 + load cell 2 + load cell 3.

Combining the three load cell signals in a total load cell force, results in maximum forces around 2000N.

6.4.3   Wind Sensor Data

The wind sensor measures wind velocity, direction and temperature. The sample rate is 1.876 Hz. The wind velocity is found to vary between 4.3 m/s before the first sweep and 5.3 m/s before the last sweep. This indicates how much variation the wind velocity can show, these variations require careful consideration while processing the data.
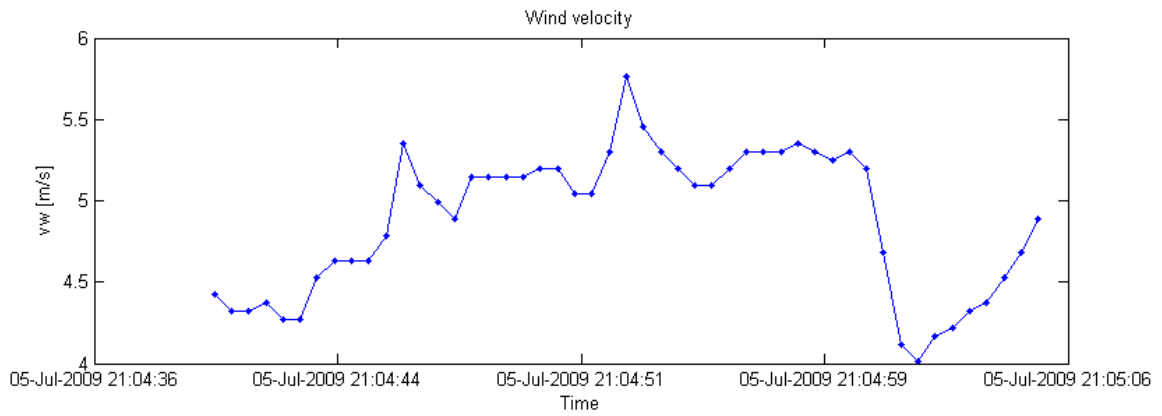
Figure 47, Wind velocity data during the three selected sweeps, measured by the wind sensor.

The wind direction varies between 59 and 67 degrees over the three sweeps.
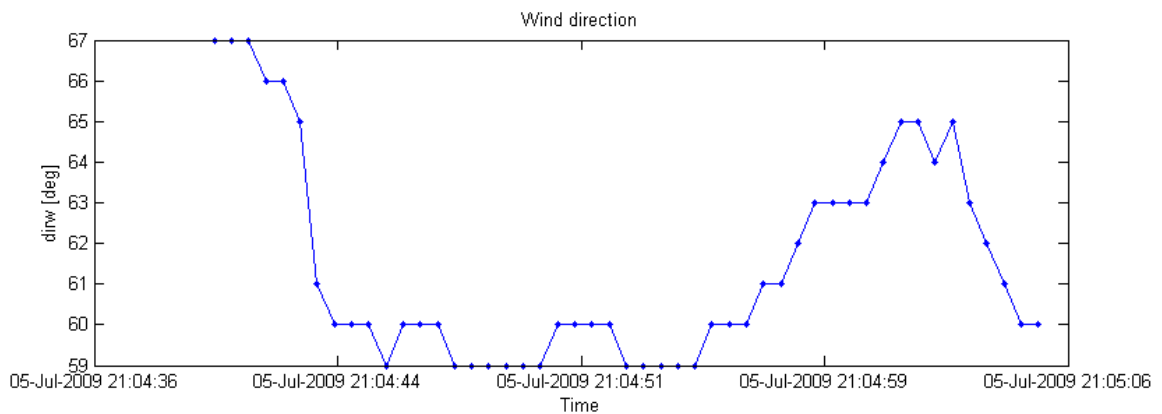
Figure 48, Wind direction data during the three selected sweeps, measured by the wind sensor.

The air temperature remains constant at 18.5˚C.
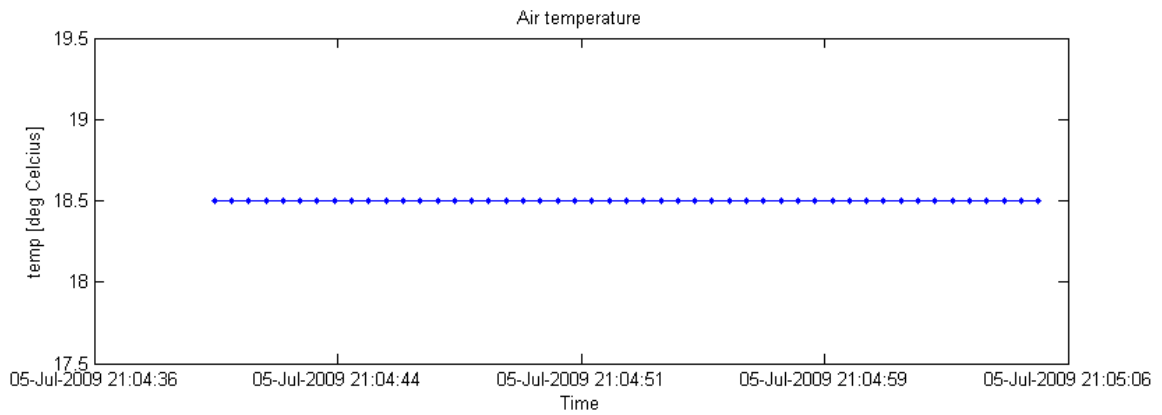
Figure 49, Air temperature, measured by the wind sensor.

In the next paragraph it is explained how the measured signals are processed into the final results.

6.5 Data Analysis

In the last paragraph it was shown how the different parameters are obtained. Here it will be explained what methods are used to process the data into usable results.

6.5.1 Wind data

The main target in this paragraph is to obtain a method to process the wind data. As the true wind velocity is not obtained at exactly the position of the kite it needs to be determined whether the measured wind is representative for the wind at the position of the kite.

If it could be assumed that the wind velocity is constant over the whole field of the experiment and constant over time it could be simply stated that the wind at the location of the sensor always equals the wind at the location of the kite. The validity of this assumption can be discussed by looking at an average sample of measured wind data.
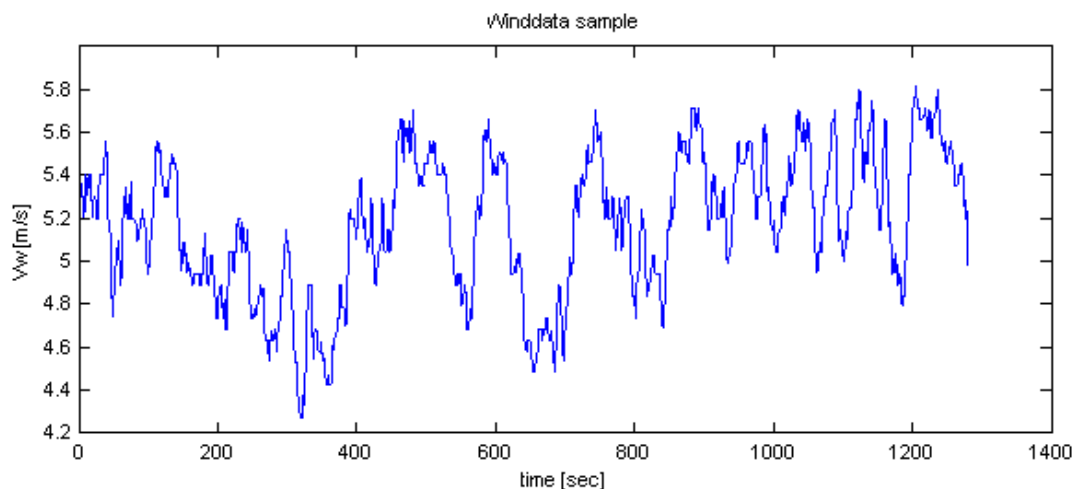
Figure 50, Wind velocity v_w sample at Scheveningen Beach, 6 m above the ground (date 14-4-2009).

The sample data in Figure 50 shows that the wind varies between 5.8 m/s and 4.3 m/s. The average velocity is estimated at 5 m/s.
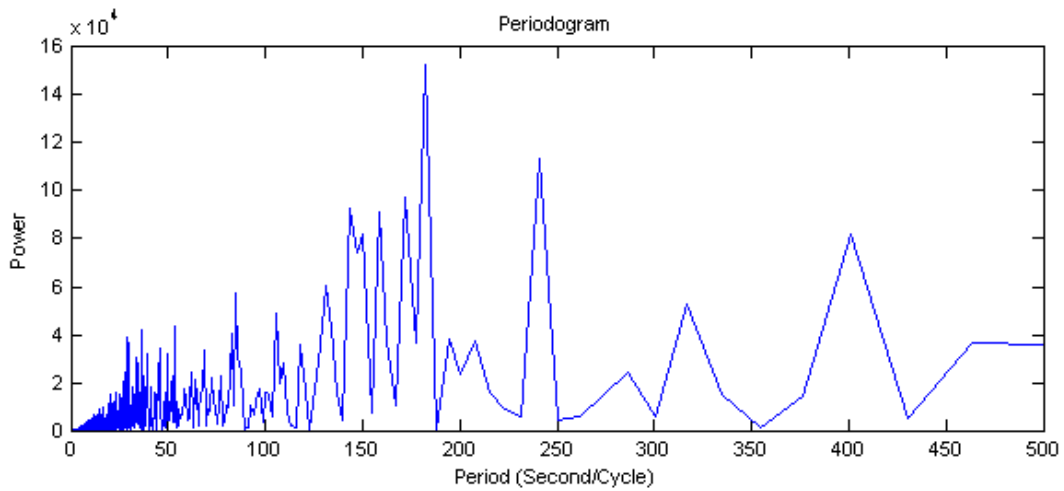

Figure 51, Periodogram of the wind velocity at Scheveningen Beach, 6 m above the ground (date 14-4-2009).

In the periodogram of Figure 51 it is attempted to find the periods that are most present inside the wind speed signal. There appears to be most energy between the 130 to 180 second periods. This indicates that many gusts are present that take around 2 to 3 minutes to complete.
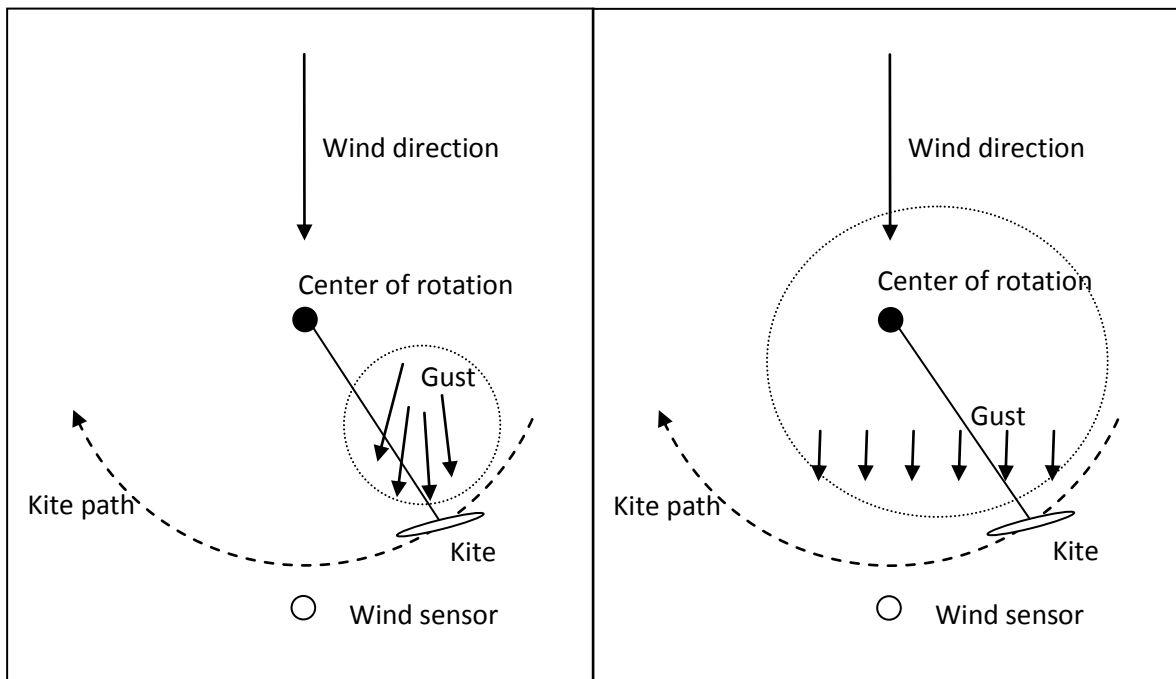

Figure 52, Top view of test field with two different gust sizes.

Looking at the top view of the test field in Figure 52 it can be seen how it is possible that a local gust is experienced by the kite while the wind sensor does not experience this higher wind speed yet. As a result of this it can be said that the smaller the distance between the kite and the wind sensor the more representative the wind data can be expected to be. Also it is noted that the wind can be seen as build up by wind variations at almost all levels. Variations can have a period of days to seconds to milliseconds. Wind gusts are the effect of turbulent eddy's in the atmosphere. These eddy's can be

visualized as more or less circular clouds (12). This explains that the gust period can be expected to correlate with the size of the gust. Gusts with a large period affect a large area and a short period gust affects a small area.

The question that needs to be answered now is: How can this be quantified?

It is first noted that it can be expected that the period of the gusts is an important factor here. This will be explained first. With a typical testing wind speed of around 5 m/s and 50 meter line length it takes 10 seconds for a gust to travel over the entire test field. As can be seen in Figure 50 the shape of the gusts is approximately sinusoidal. With the kite in the most downwind position and the wind sensor 5 meters downwind of the kite the gust will arrive at the sensor 1 second after arriving at the kite. This indicates that gusts with a large period (say larger than 120 seconds) are accounted for with a phase difference of less than 1/120 of the gust period. A gust with a small period of 1 second would have a phase difference of a full period.

In order to quantify the effect that gusts have on the wind data it is assumed that gusts have a circular shape. Figure 52. Now assuming that the gust moves straight across the wind sensor at true wind velocity v_t, the relation between the period and the size would be:

$$Gust\ diameter = v_w * Gust\ period$$

(6.1)

It cannot be assumed that every gust moves straight across the wind sensor. So it can be expected that the real gust size is slightly larger than described in equation 6.1. The gusts run at random positions over the wind sensor. To take this into account the gust diameter is increased by a correction factor.
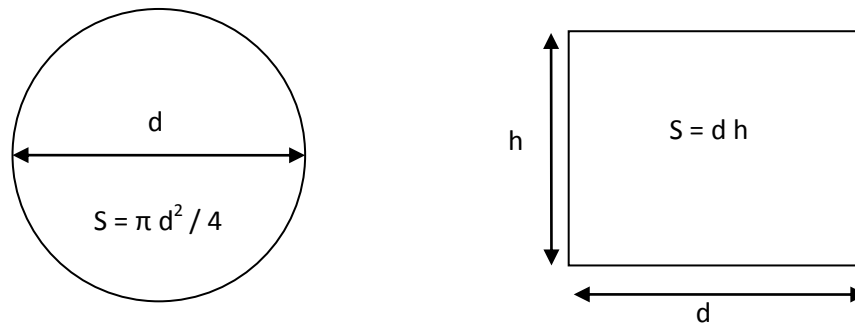
Figure 53, It is assumed here that gusts will have a more or less circular shape. This relates the recorded gust period and velocity to a gust diameter. Statistically a gust with diameter d will have an expected recoded wavelength of d*π/4.

For a gust of diameter d it can be expected that the mean recorded gust diameter is h = π d / 4. This is why a correction of 4/π is added to formula 6.1.

$$Gust\ diameter = v_t * Gust\ period * 4/\pi$$

(6.2)

Now looking at the test setup with 50 meter line length, it is assumed that gusts with a diameter smaller than 50 meter are too small to assume that the gust is experienced both at the location of

the kite and the location of the sensor. It is thus concluded that gusts with a period of less than 8 seconds cannot be accounted for due to the distance between the kite and the sensor:

$$Gust\ period = \frac{50\pi}{5*4} = 7.8 \approx 8\ sec$$

(6.3)

It is concluded that the wind velocity v_w that is used for kite analysis will be calculated with a running average over 8 seconds. With a sample period of 533ms this means that 15 samples are symmetrically averaged to determine the wind velocity at each moment in time. The resulting maximum error in the measured wind velocity is estimated to be ± 0.2 m/s for an average wind velocity of 5 m/s. This results in a 4% error due to the difference in location of the kite and the wind sensor.

Also the wind direction changes during a gust. The later described data processing method is not depending on exact measurement of the wind direction so it is not expected that this affects the accuracy of the results.

Inspecting the data it was discovered that the wind velocity is sometimes affected by the kite that sweeps past the wind sensor. This sometimes results in a sudden increase in the signal and sometimes in a sudden decrease. As the used wind information is a running average of 8 seconds the disturbance of the wind data is already averaged out and shall not introduce a large error.

6.5.2   Used crosswind models

This paragraph explains in detail which model assumptions were required and illustrates how the data is processes into results. In order to be able to process the obtained data, a theoretical model of the situation is required. The model has to describe the relations between wind velocity, kite velocity and resulting forces. First it is noted that with velocities not higher than 60 knots (≈ 30 m/s), the experiment can be treated as a low speed aerodynamic experiment.

No mass and no tether drag

Firstly a simple form of a crosswind sweep model will be introduced. For this model both kite and tether mass as well as tether drag will be neglected. This model serves as a reference to check the more complicated models and to illustrate the influence of neglecting mass and tether drag.
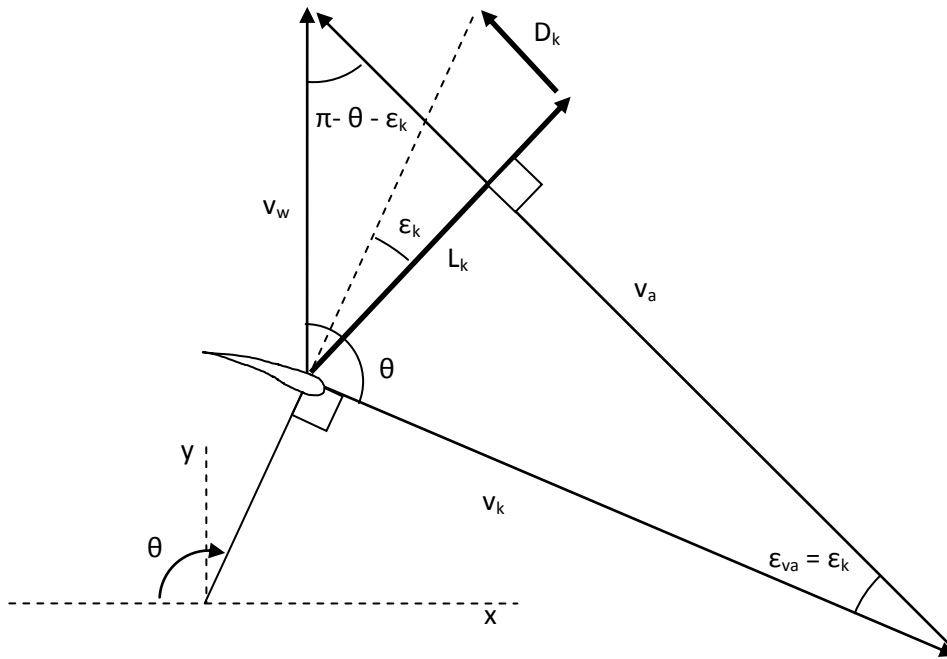
Figure 54, Schematic representation of the crosswind sweep. Including used vectors and angles.

In Figure 54 it is illustrated how the kite sweeps around the origin. The wind direction v_w is defined as always in the positive y direction. With the kite lift L_k always perpendicular to the apparent wind v_a and kite velocity always perpendicular to the kite lines, it can be seen that the angle between v_a and v_k equals the glide ratio of the kite: $\varepsilon_{va} = \varepsilon_k$.

Using the sine rule it is possible to calculate the ratio between the kite velocity v_k and the true wind velocity v_w as a function of the sweep angle θ.

$$\frac{v_k}{v_w} = \frac{\sin(\pi - \theta - \varepsilon_k)}{\sin(\varepsilon_k)}$$

(6.4)

Similarly it is possible to write the ratio between the apparent wind velocity v_a and the true wind velocity v_w as a function of θ.

$$\frac{v_a}{v_w} = \frac{\sin(\theta)}{\sin(\varepsilon_k)}$$

(6.5)

Here

$$\varepsilon_k = \tan^{-1}\left(\frac{D_k}{L_k}\right)$$

(6.6)

With above formulas it is possible to investigate the location of the highest velocity by differentiation. It is found that:

$$\left[\frac{v_a}{v_w}\right]_{max} = \frac{1}{\sin(\varepsilon_k)} \qquad \text{For...}\, \theta = \pi\!\!\diagup\!\!2 \qquad (6.7)$$

and

$$\left[\frac{v_k}{v_w}\right]_{max} = \frac{1}{\sin(\varepsilon_k)} \qquad \text{For...}\, \theta = \pi\!\!\diagup\!\!2 - \beta_k \qquad (6.8)$$

So maximum apparent wind and thus maximum lift force will be experienced straight downwind from the line attachment to the ground at sweep angle θ = π/2. The maximum speed will be experienced a few degrees before the kite is straight downwind.

It has to be noted that even though the events take place at different moments, the magnitudes of the maximum apparent wind speed and maximum kite speed are equal to each other in this mass less assumption.

Also note that the ratio between the kite velocity and true wind velocity is approximately equal to the lift to drag ratio of the kite. This only counts for small values of ε_k, so only for high lift to drag ratios. For L_k/D_k = 5 a maximum velocity ratio of 5.10 is found.
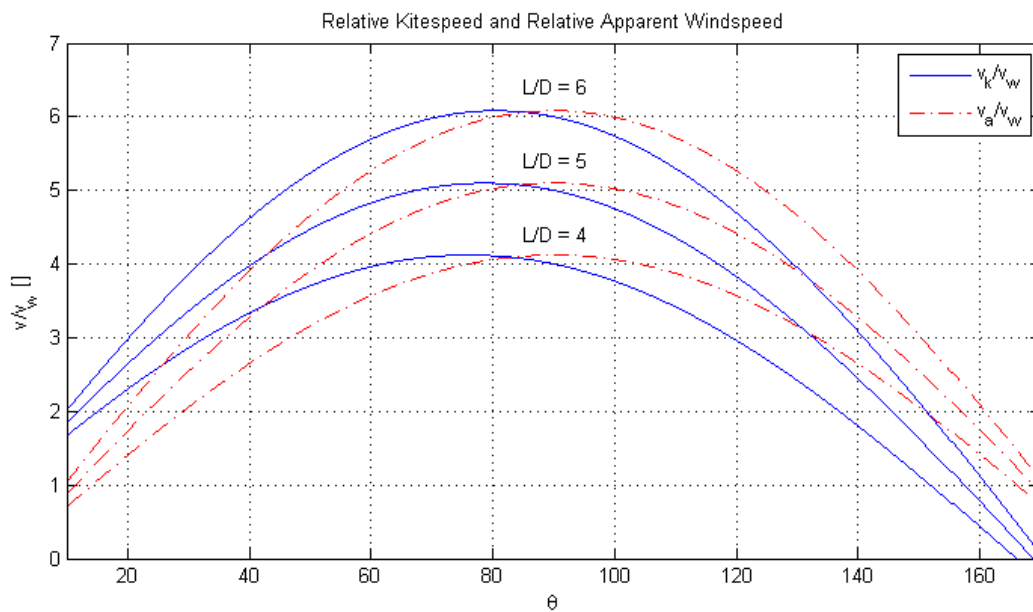

Figure 55, Kite velocity and apparent wind velocity as a function of sweep angle θ and lift to drag ratio.

Using this model the L_k/D_k can be obtained for each sweep. First the maximum kite velocity v_k and related wind velocity v_w are obtained for each sweep. 77 sweeps were extracted from the experimental data.
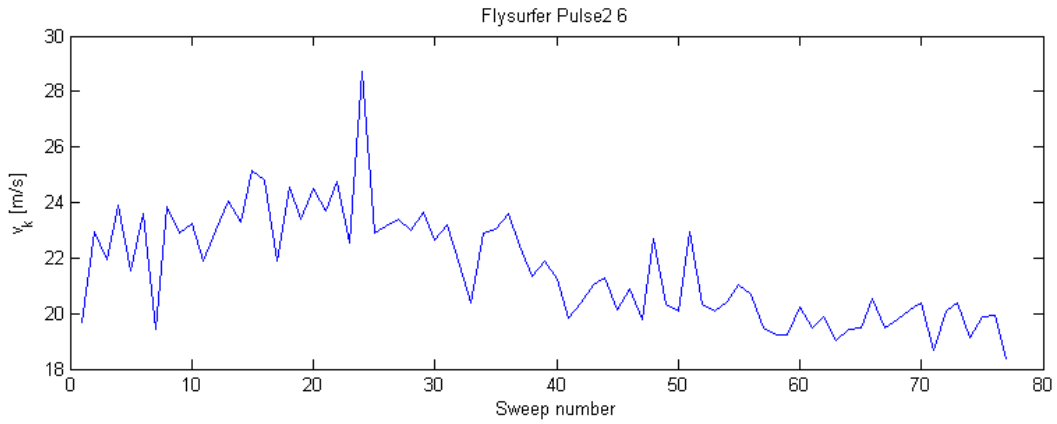
**Figure 56, Maximum kite velocity v_k for each sweep.**

Figure 57, Wind velocity related to each sweep.

A first estimate of the lift to drag ratio obtained for each sweep are given by:

$$\left[\frac{L_k}{D_k}\right]_i = \frac{1}{\tan(\sin^{-1}(\frac{1}{\left[\dfrac{v_k}{v_w}\right]_{\max,i}}))} \tag{6.9}$$
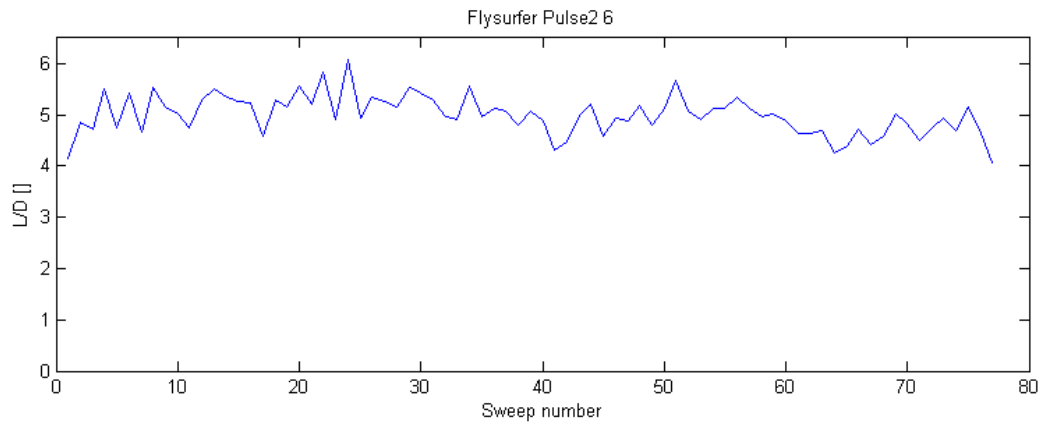

Figure 58, First estimate of the lift to drag ratio related to each sweep.

Note how the lift to drag ratio shows a more or less constant saw tooth like shape. The kite flies from one side to the other and then back. One possible explanation for the saw tooth shape is that the kite has a different lift to drag ratio while flying from left to right than when flying from right to left. Another explanation could be that it is not the kite that shows asymmetry but other conditions like the wind being slightly stronger on one side than on the other. It is left for further research to learn more about this phenomenon.

It is first explained how a first estimate of the obtained lift, drag and resultant force coefficients can be obtained. After that, corrections taking the line drag and centrifugal force into account are required to improve the results.

The maximum total line tension $[T_{tot}]_{max}$ of each sweep is first presented.
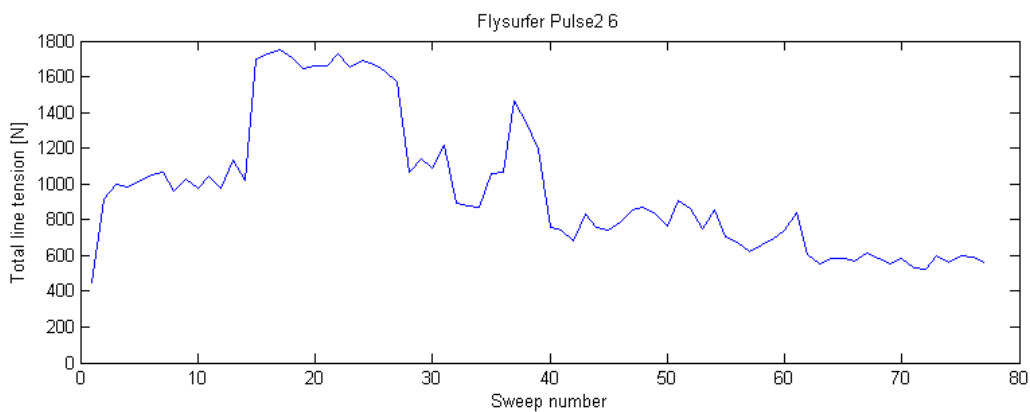

Figure 59, Maximum total line tension for each sweep.

A first estimate of the aerodynamic resultant force coefficient C_R can be obtained for each sweep using:

$$C_{Rk,i} = \frac{2[T_{tot}]_{max,i}}{\rho_{air}[v_k]_{max,i}^2 S_k}$$

(6.10)

A first estimate for the lift coefficient can then be obtained as:

$$C_{Lk,i} = \sqrt{\frac{C_{Rk,i}^2}{1 + \left[\dfrac{L_k}{D_k}\right]_i^{-2}}}$$

(6.11)
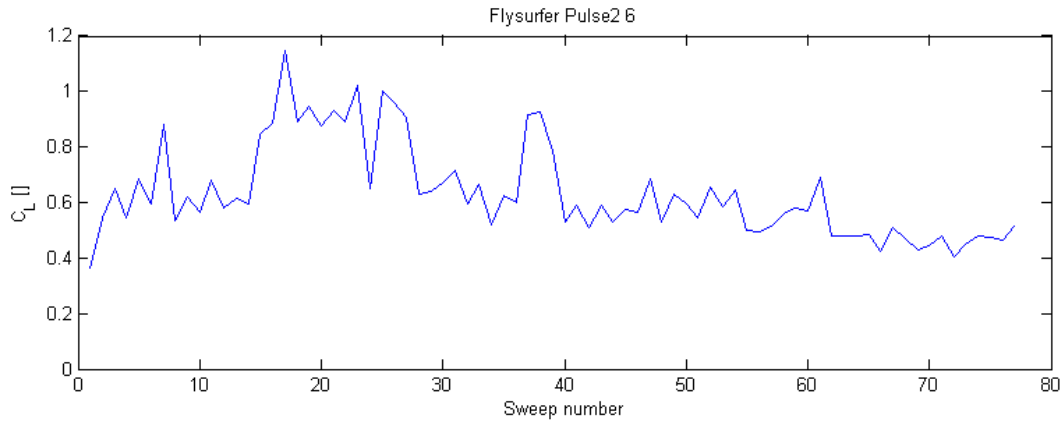
Figure 60, First estimate of the lift coefficient (with respect to projected area) related to each sweep.

The drag coefficient first estimate is calculated using:

$$C_{Dk,i} = \frac{C_{Lk,i}}{\left[\dfrac{L_k}{D_k}\right]_i}$$

(6.12)
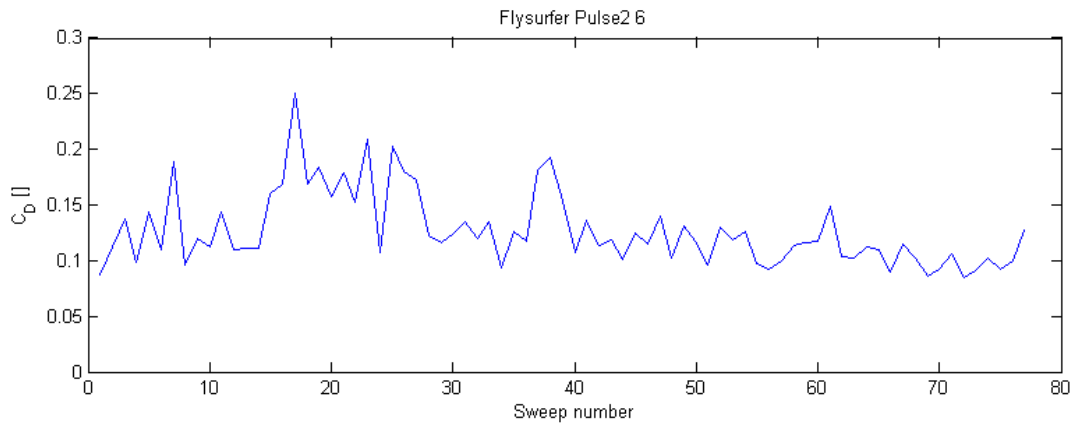
Figure 61, First estimate of the drag coefficient (with respect to projected area) for each sweep.

6.5.3 Correction for line drag

In reality it is not only the lift to drag ratio of the kite that determines the maximum velocity obtained by the kite. The lines are adding drag to the system that should not be accounted to the kite. A line drag compensation is required. As explained in chapter 4, the line drag can be estimated using a line drag coefficient related to the kite velocity. A line drag coefficient referring to the line drag force acting on the kite $C_{D,line}$ = 0.31 was estimated.

The kite drag coefficient can be corrected by subtracting the line drag surface divided by the kite surface.

$$C_{Dkl} = C_{Dk} - C_{D,line} \cdot \frac{S_{line}}{S_k} = C_{Dk}\left(1 - \frac{C_{D,line} \cdot S_{line}}{C_{Dk} \cdot S_k}\right)$$

(6.13)
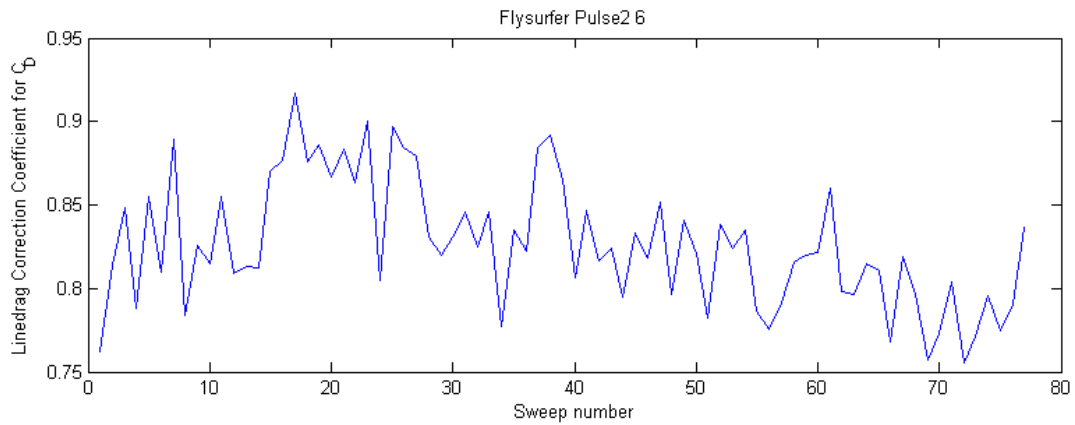
Figure 62, Correction coefficient to subtract the line drag from the kite drag.
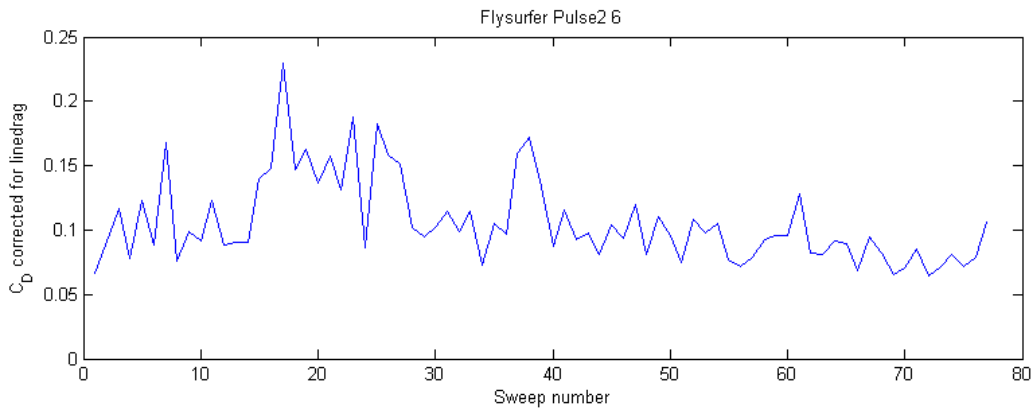

Figure 63, Fully corrected kite drag coefficient (with respect to projected area).

The lift coefficient remains unchanged by this correction. The L/D however is corrected in a similar way.

$$\left[\frac{L_k}{D_k}\right]_{l,i} = \left[\frac{L_k}{D_k}\right]_i \left(1 - \frac{C_{Dline}S_{line}}{C_{Dk,i}S_k}\right)^{-1} \tag{6.14}$$

6.5.4 Correction for centrifugal force

As the kite moves through the sweep it describes a circular path. As the mass of the kite moves through this path a centrifugal force is introduced into the lines that should not to subscribed to the aerodynamic forces produced by the kite. In order to correct for the centrifugal force a correction factor is obtained. It is first noted that the centrifugal force is given by:

$$F_{cent} = \frac{m_k v_k^{\,2}}{r} \tag{6.15}$$

Where:

m_k = Kite mass including the mass of the air inside the kite. The line mass could be included, but as both the mass and the velocity of the kite are dominating this equation, the line mass is neglected. [kg]

v_k = Kite velocity. [m/s]

r = Distance between the anchor point of the kite and the center of mass. This includes a length from sandbag to the actual Dyneema lines and the length of the kite bridles. [m]

Now the lift coefficient can be corrected as:

$$C_{Lkc,i} = C_{Lk,i} \left(1 - \frac{F_{cent,i}}{[T_{tot}]_{max,i}} \right)$$ (6.16)
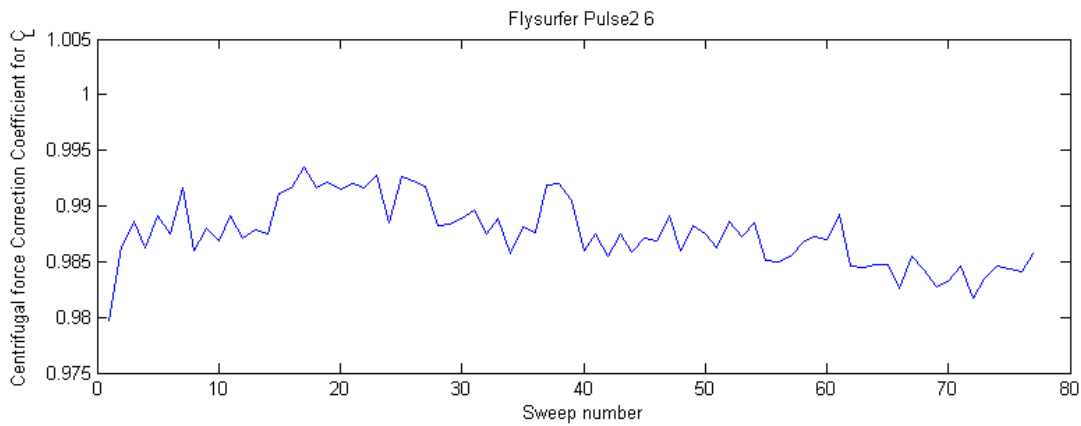

Figure 64, Correction coefficient to subtract the centrifugal force from the aerodynamic lift force.
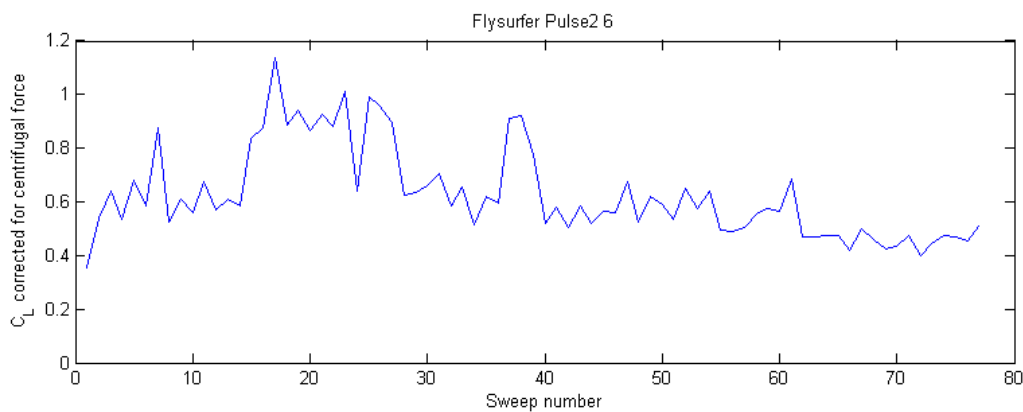

Figure 65, Fully corrected kite lift coefficient (with respect to projected area).

The lift over drag can be corrected with the same factor.

$$\left[\frac{L_k}{D_k} \right]_{l,i} = \left[\frac{L_k}{D_k} \right]_i \left(1 - \frac{F_{cent,i}}{[T_{tot}]_{max,i}} \right)$$ (6.17)

The fully corrected lift to drag ratio of the kite becomes:

$$\left[\frac{L_k}{D_k}\right]_{l,i} = \left[\frac{L_k}{D_k}\right]_i \left(1 - \frac{F_{cent,i}}{[T_{tot}]_{max,i}}\right)\left(1 - \frac{C_{Dline}S_{line}}{C_{Dk,i}S_k}\right)^{-1}$$ (6.18)
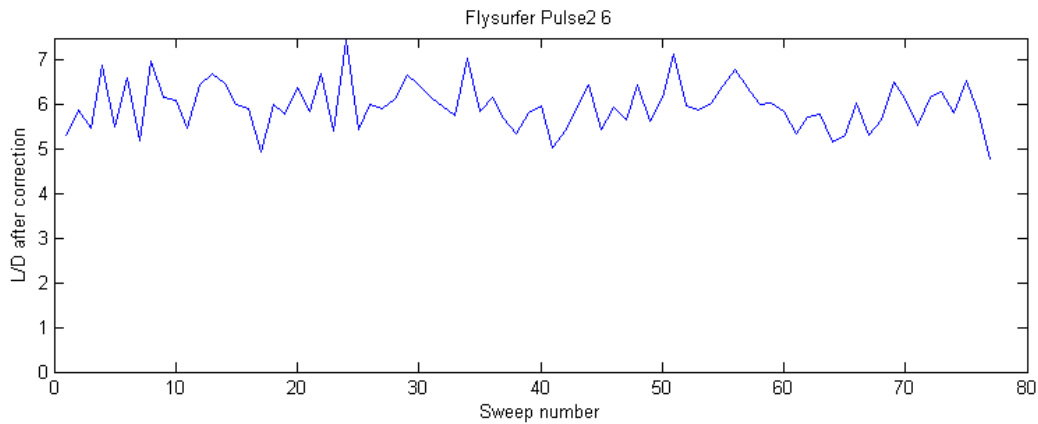

Figure 66, Corrected Lift to drag ratio of the kite obtained for each sweep.

6.5.5 Inertia effects

The proposed model is based on the assumption that the tested kite has zero mass. This assumes that the kite is always flying at its equilibrium velocity. The zero mass assumption is supported by the argument that the resulting aerodynamic forces are much larger than the kite mass multiplied with its acceleration. As the kite does have a mass and constantly accelerates and decelerates it is required to investigate the difference between the used model and reality.

To quantify the difference three dynamic simulations where compared to each other. The first simulation is based on the method used to process the data. It assumes zero mass and so is always instantaneously in balance with the aerodynamic forces. The line drag regarded as integrated into the lift to drag ratio of the kite.

In the second simulation a mass is added to the kite and a reasonable initial velocity had to be estimated. Both simulations assume a constant kite lift coefficient of 1.0 and constant lift to drag ratio of 5.2 throughout the sweep. The true wind velocity is set to 4.4 m/s. Using 0.05 second time steps, the resulting force is calculated for each step. Using a kite mass of 1.6 kg the acceleration is calculated throughout each step.

Trying different initial velocities it was found that the initial velocity has almost no influence on the finally obtained velocity.

In Figure 67 the difference is shown between the no mass assumption and including the mass. It is found that the difference in maximum kite velocity is less than 0.1%. The location of maximum velocity moves to a slightly higher sweep angle.
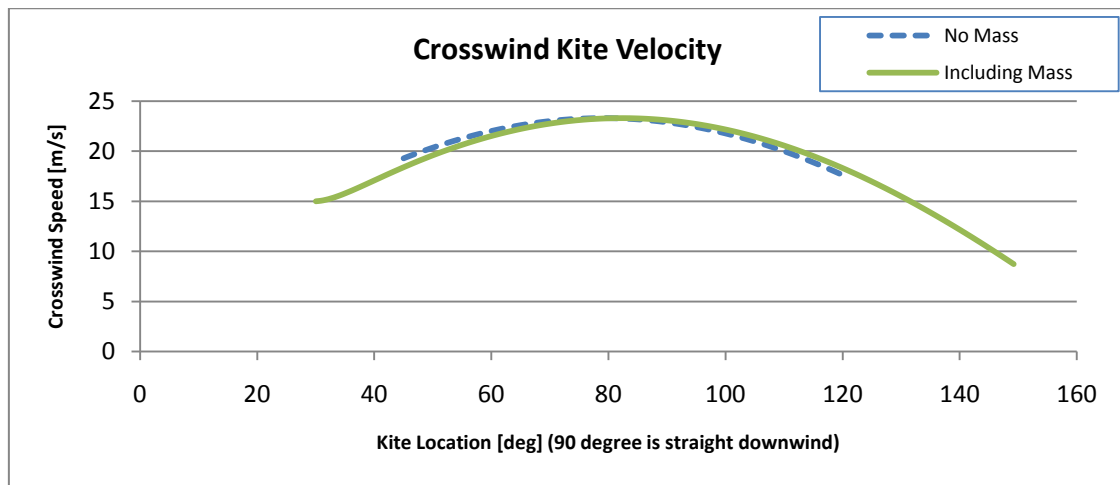

Figure 67, Kite velocity in dynamic simulation of a crosswind sweep with and without mass. [mass = 1.6 kg, v_w = 4.4 m/s, Cl = 1.0, L/D = 5.2].

In Figure 68 it is shown how the apparent wind velocity is affected by including a mass. It is found that the maximum apparent wind velocity is less than 1% higher after including the mass. The small increase in apparent wind is due to the fact that the introduced inertia slightly delays the moment of maximum velocity. Due to this, the kite velocity is higher while moving in upwind direction after the passing the straight downwind position.
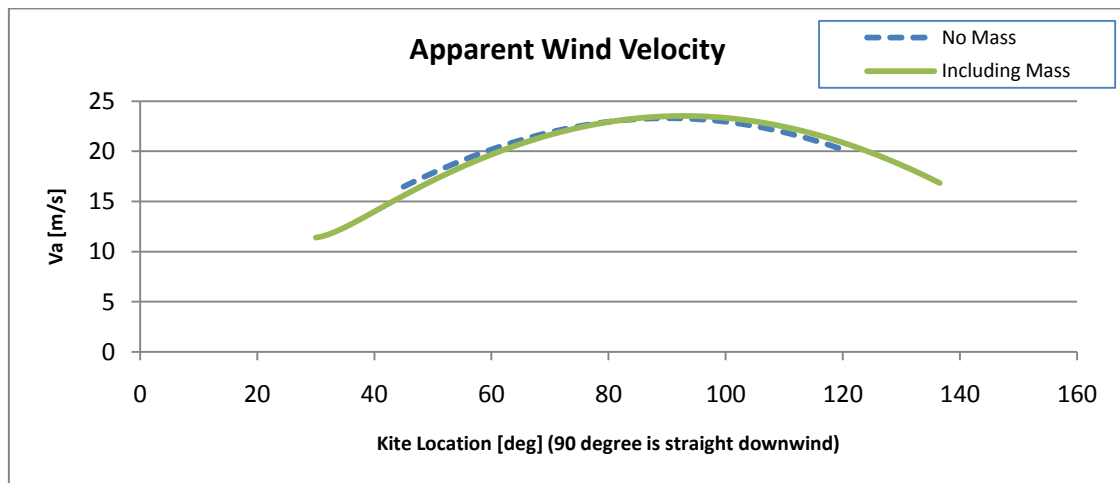

Figure 68, Apparent wind velocity in dynamic simulation of a crosswind sweep with and without mass. [mass = 1.6 kg, v_w = 4.4 m/s, Cl = 1.0, L/D = 5.2].

Figure 69 shows how the line tension is affected by taking the mass of the kite into account. It is found that the maximum tension is 1.8% larger after including the mass. This increase in tension is due to the shown increase in apparent wind.
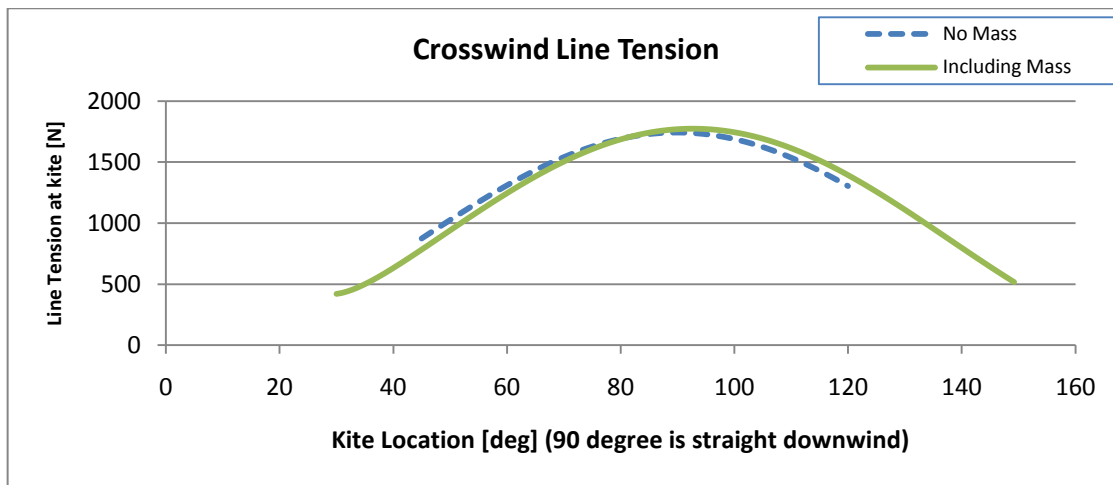

Figure 69, Line tension in dynamic simulation of a crosswind sweep with and without mass. [mass = 1.6 kg, v_w = 4.4 m/s, Cl = 1.0, L/D = 5.2].

It can be expected that using longer lines for the crosswind sweeps reduces the inertia effects. A drawback is then that the line drag is increased. The findings of the dynamic simulation indicate that the effect of inertia is small. It was decided not to correct the obtained results for the presence of inertia.

6.5.6   Angle of attack

In aerodynamic experimentation one of the most common variables is the angle of attack. The angle of attack is defined as the angle between a reference line on a body (the chord line in the case of an airfoil) and the free-stream direction of the flow that passes this body.

Defining the angle of attack of a kite is not straight forward. Comparing a standard surf kite to an average airplane wing it is noted that the kite has a remarkably large anhedral angle and a large amount of wing twist towards the tips. For most airplanes the wing twist is positive and results in a lower angle of attack at the wing tips than at the wing root. For all kites that were tested during this research the twist could rather be expected to be negative than positive, although determining the twist was not part of this thesis.

It should also be noted that the kite is not a rigid wing, the twist of this wing will visibly vary when changing the angle of attack. Also when steering the kite it is clearly visible that the rate of twist changes and becomes asymmetric. This asymmetry is what causes the kite to change direction. The extreme deformation that is possible is illustrated in Figure 70.

Figure 70, Extreme steering situation to illustrate the extreme spanwise variations in twist.

Clearly there is a lot to be said about the angle of attack of a kite. Assuming symmetric flight and defining the angle of attack with reference to the root chord could be used to determine the angle of attack during an aerodynamic experiment. It has to be said that the obtained data should be interpreted with care; large deformations could initiate unexpected results. In the crosswind kite test described here it was decided that the angle of attack could not be determined accurately enough in the available time. It was decided that it is more useful to first investigate what accuracy can be obtained without this information.

It would be interesting and useful to investigate whether an accurate wind sensor could be mounted on the kite to measure both angle of attack and apparent wind velocity.

An alternative for using the angle of attack could be to use the ratio between the tension on the front lines and the back lines. This will be discussed in the next paragraph.

6.5.7 Back line percentage

In this experiment the angle of attack could not be accurately obtained. An alternative for the angle of attack could be useful. Stevenson(8) uses the ratio between the back line load and the total line tension as the major parameter to analyze the data obtained in his tests. He calls this ratio the back line percentage. (Back lines are also frequently called break lines or steering lines.) Stevenson argues that the variation of the back line percentage is the only control that a flyer has over the performance of the kite. With the use of load cells in both front and back lines the back line percentage is readily available in this experiment.

$$Back\ line\ percentage\colon \mathrm{BL\%} = \frac{T_{back}}{T_{total}}$$

$$(6.19)$$

Still the parameter should be used with care. As shown in the example of Figure 71 the back line percentage is not necessarily linearly linked to the angle of attack. A variation in angle of attack could theoretically result in both a variation in lift over drag and a variation in lift coefficient in such a way that the back line percentage remains constant. Having said this, back line percentage is still expected to have a large influence on the performance of a kite. The back line percentage remains a valuable parameter and has shown to be useful in this experiment. In general a higher back line percentage results in a higher angle of attack.
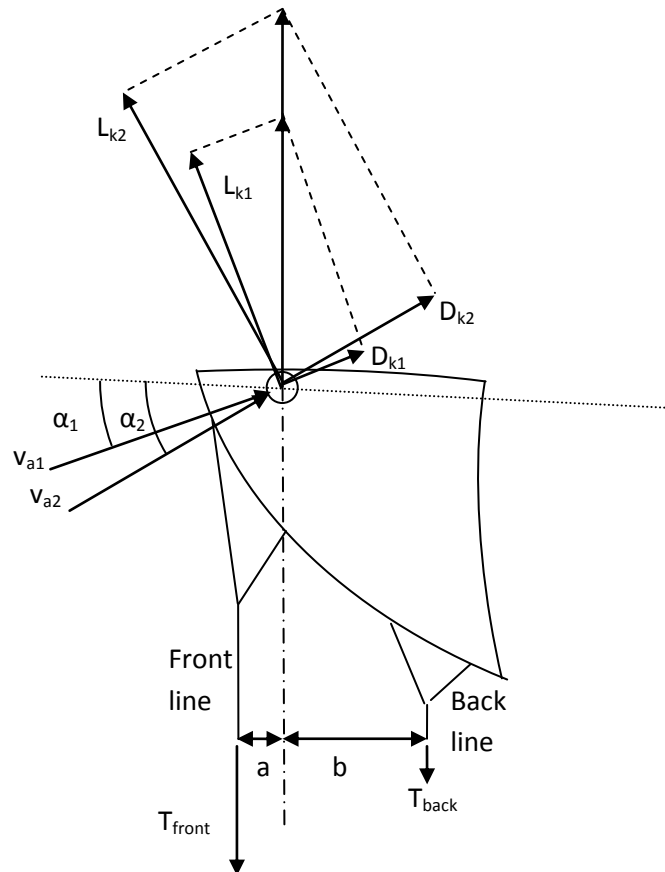
Figure 71, A different angle of attack doesn't necessarily mean a different distribution of forces over the front and back line T_{front}/T_{back}.

There is a second thing that needs to be kept in mind when using either the angle of attack or the back line percentage. When performing an aerodynamic experiment, the shape of the object under consideration normally remains constant while changing the attitude of the object with respect to the flow. In the case of most kites changing the back line percentage not only changes the overall angle of attack but also changes the shape of the kite. This means that in reality a differently shaped object is being tested. This could cause unexpected results. Changes in aerodynamic loading could also result in a changing geometry. This should be kept in mind when trying to understand to aerodynamic behavior of a kite.

Determining how a kite deforms under different loads is not easy. Each kite can be expected to react in its own way. In the work of de Wachter (10) it is illustrated how a so called ram air inflated kite (also called foil kite) deforms with respect to the power setting of the lines and with respect to the velocity of the oncoming flow. Different wind tunnel tests are performed and with the use of

photogrammetry and laser scanning the shape of the kite is recorded. Pulling both steering lines increases the overall angle of attack of the kite. It is shown that this has a much larger local effect at the tips of the tested kite than at the middle section. This even results in early stalling behavior at the tips while the flow is nicely attached in the middle section. Deformations due to different wing loadings are less profound, but are definitely present and have to be taken into account.

The aerodynamic force on any object can be expected to be constant when the next condition is applied: constant geometry, constant attitude, constant dynamic pressure and no hysteresis effects (different force and moment coefficients at increasing or decreasing angles of attack).

In general it can be expected that for each back line percentage in combination with its angle of attack and for each total aerodynamic loading there will be only one certain kite geometry. Neglecting hysteresis effects, this means that in general it can be expected that each back line percentage in combination with each dynamic pressure results in a unique aerodynamic force.

It should be noted that hysteresis effects could provide unexpected results. As the kite moves from one side to the other it moves through different velocities and possibly different angles of attack. This could result in hysteresis and in less accurate results. Careful inspection of the test data should give insight in the importance of this effect.

Plotting the obtained lift coefficient against the back line percentage shows the trend of higher lift at higher back line loading.
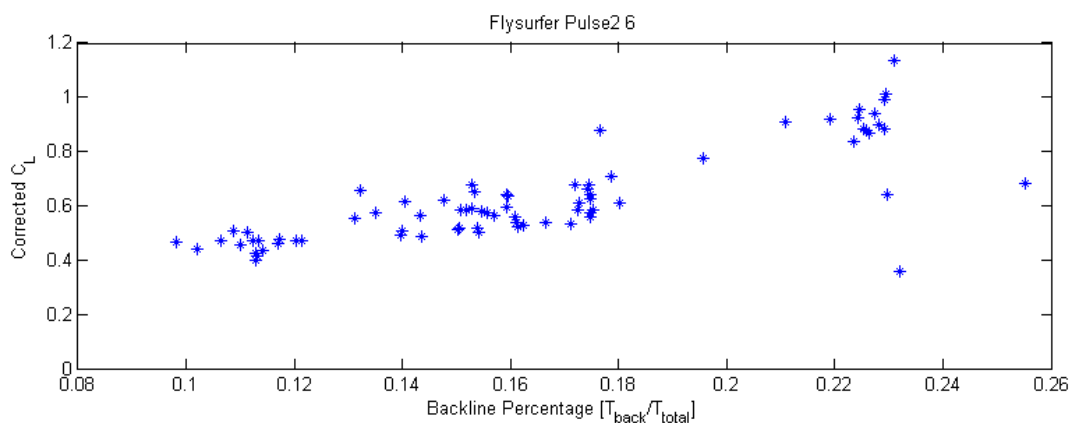
Figure 72, The corrected lift coefficient plotted against the back line percentage.

The drag also increases upon increasing the backline loading.
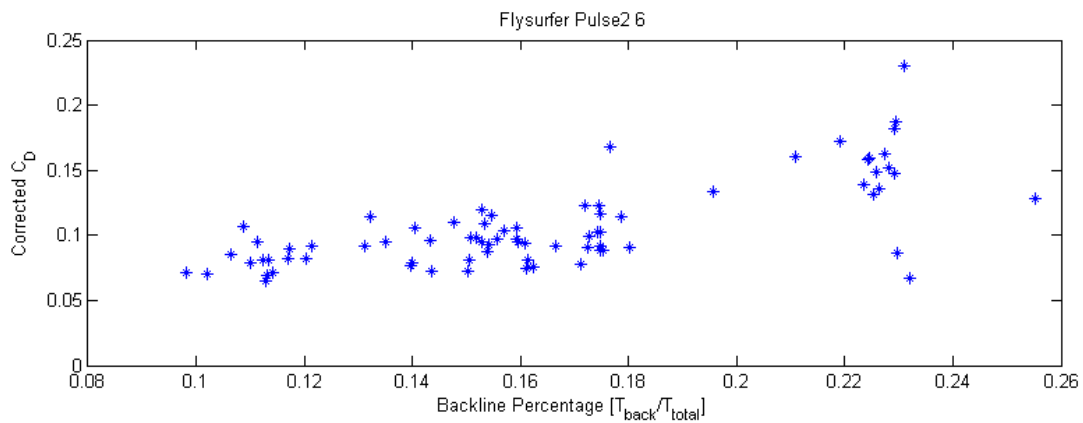
Figure 73, The corrected drag coefficient plotted against the back line percentage.

The lift to drag ratio is found to remain fairly constant on changing the backline loading.
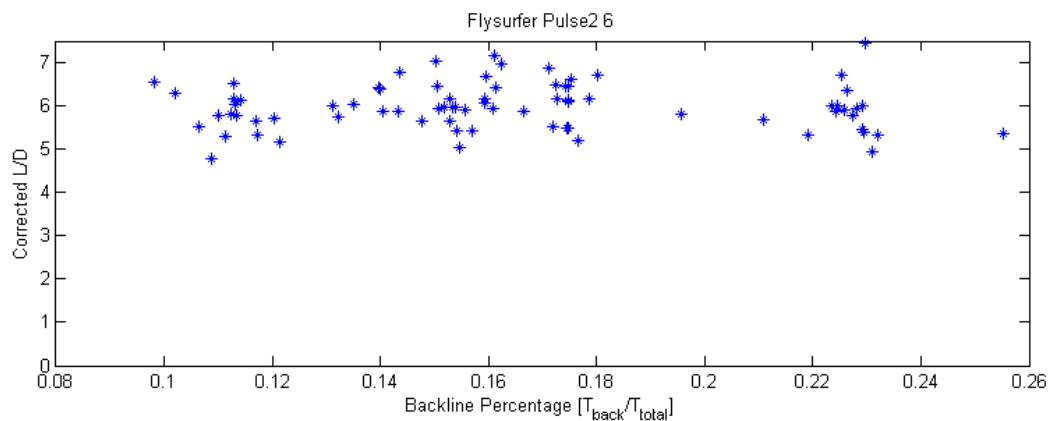
Figure 74, The corrected lift coefficient plotted against the back line percentage.

6.5.8   Point for point method

The foregoing subparagraphs of paragraph 6.5 have explained what methods were used to process the obtained data. This last subparagraph contains a short explanation of a second approach, which was investigated. This approach did not show a higher accuracy than the already explained method and was found to only add complexity. It was thus decided not to include the method in this report. As it is expected that future research could benefit from the obtained experience, is was decided to mention the method here.

It was noted that by using only the peak velocities and peak loads a lot of data remained unused. It was investigated if more data points around the peaks could be included in the analysis and provide a set of aerodynamic properties on each data point. This is why the method is referred to here as point for point method.

In order to process the signal for each data point a more accurate schematic representation of the kite in crosswind sweep was required. This representation is shown in Figure 75.
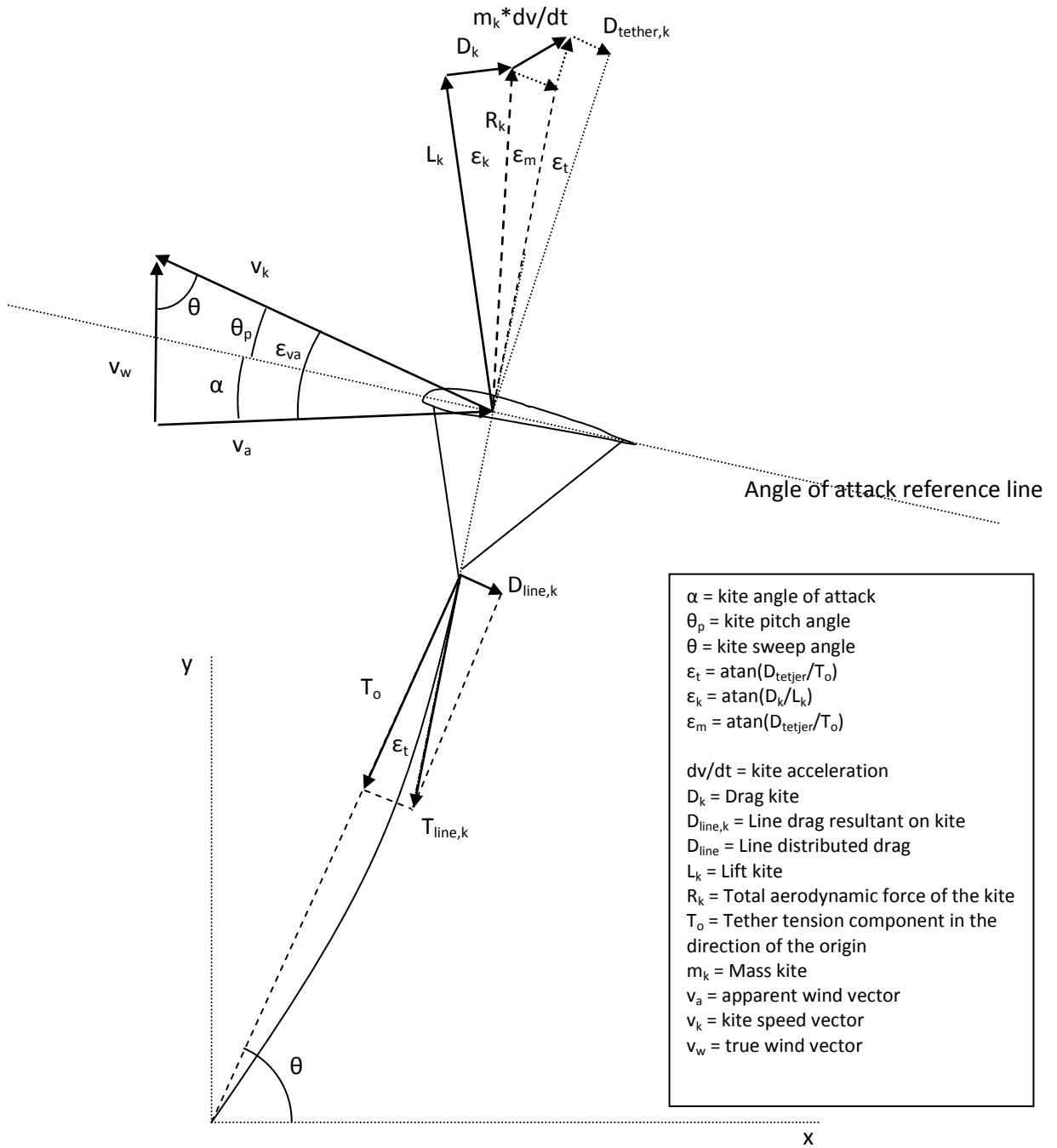
Figure 75, 2D representation of a kite in crosswind sweep.

The general balance of forces during a crosswind sweep can be written as:

$$m\frac{d\underline{v}_k}{dt} + \underline{T}_{line,k} + \underline{R}_k = \underline{0}$$

(6.20)

By satisfying this equation for each obtained track point one can obtain continuous information on both the lift and drag coefficient. Accelerations can be obtained by differentiating the available GPS velocity data. Accurate time stamps on both velocity and load cell data was required to be able to match each velocity to a load. Both magnitude and direction of the velocity signal where required in order to be able to calculate the apparent wind velocity.

It was found that using this approach accurate determination of the apparent wind velocity vector is critical to obtain accurate results. For this accurate determination of both wind direction and kite position are required.

It was found that the available data was not accurate enough to allow this approach. It is recommended to further investigate the possibilities to include more of the available data points.

6.6 Results

This paragraph serves to present the relation between the obtained lift and drag coefficients. Assuming a parabolic relation between lift and drag it is expected that the relation between the kite's lift coefficient and the drag coefficient is given by:

$$C_D = C_{D_0} + \frac{C_L^2}{\pi e AR} \tag{6.21}$$

Where C_{D_0} is the zero lift drag coefficient, e is Oswald's efficiency factor and AR is the kite's aspect ratio.
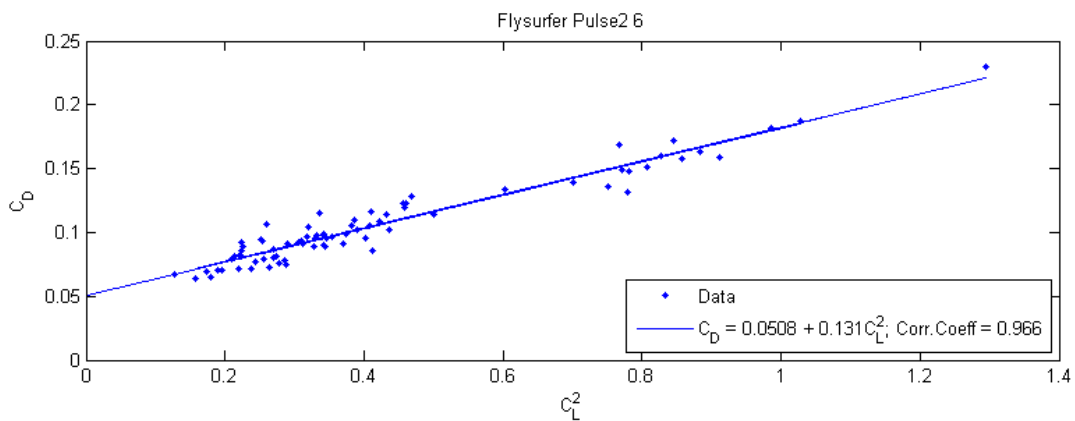
Figure 76, Relation between the kite drag coefficient and the lift coefficient squared. Each dot represents the corrected result from one of the sweeps.

It can be seen from the linear fit that $C_{D_0} = 0.0508$ and $\frac{1}{\pi e AR} = 0.131$. The Flysurfer Pulse 2 has an aspect ratio of 3.85. So the Oswald factor in this case is e = 0.63.

The maximum lift over drag value is now given by (13):

$$\left(\frac{C_L}{C_D} \right)_{max} = \frac{1}{2} \sqrt{\frac{\pi \cdot AR \cdot e}{C_{D_0}}} = \frac{1}{2} \sqrt{\frac{1}{0.0508 \cdot 0.131}} = 6.13 \tag{6.22}$$

The relation between the obtained lift coefficients and lift to drag ratio is plotted in Figure 77. It is concluded from this graph that the lift to drag ratio varies roughly between 5 and 6.1 in normal use.
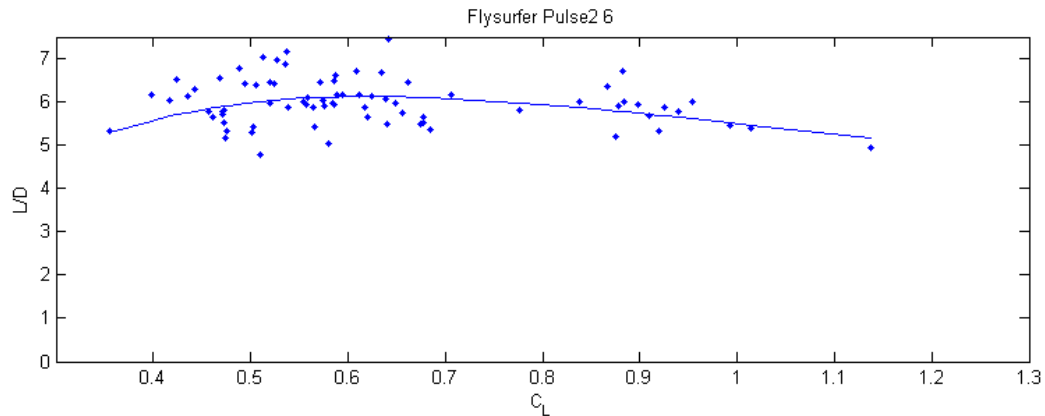
**Figure 77, Relation between the obtained lift coefficients and the lift to drag ratio.**

The obtained maximum lift to drag ratio is now compared to the values found by de Wachter (10). It is noticed that the maximum lift to drag ratio, of around 7.8 at 16 m/s flow velocity and with minimal load applied to the break lines, that was found by de Wachter was not found in this experiment. At a flow velocity of 12 m/s a maximum L/D of around 6.5 was found by de Wachter. This would be in better agreement to the results presented here.

There could be different explanations for the differences that are found. In de Wachter's work wall effects, slightly disturbing the tip vortices, could result in a higher L/D. Also it must be mentioned that de Wachter tests up to a flow velocity of 16 m/s while the flow velocity in the test presented here is around 25 m/s. The next paragraph serves to highlight possible sources of error involved in this testing method.

The described procedure was followed for different kites and on different days. In the process of fine tuning the testing procedure some kites were tested more accurately then others. It was decided to present the obtained results of a second kite, the 2008 Airush Flow 5, in appendix A.

6.7 Sources of Error

There are a number of possible sources of error involved in the described experiment. This paragraph will present a list of possible sources of error, followed by a small discussion about the magnitude of each error.

Load cell logger

The load cell logger was developed especially for this project. The logger was carefully calibrated before testing. Calibration showed a stable reading and a linear relation between the reading and the actual force. The accuracy of the obtained data depends mostly on the accuracy of the calibration. The error was estimated at 1%.

GPS

The accuracy of the kite velocity measurement is based on the accuracy of the used GPS. The GPS Doppler velocity is rated to have an accuracy of ± 0.05 m/s. At 25 m/s velocity this results in an error of 0.2%. Compared to the other sources of error this is a small error.

Wind sensor

The accuracy of the wind sensor data is rated at 5% of the measured wind velocity. Added to this error is the error introduced by the difference in location between wind sensor and kite, which was rated at 4%. This results in an estimated combined error of: $\sqrt{5^2 + 4^2} = 6.4\%$. This is seen as the largest source of error involved in the experiment. Possibilities to improve the accuracy include using multiple wind sensors and using a wind sensor with a higher accuracy.

Line Drag

It was shown how the data is corrected for the influence caused by the aerodynamic drag of the lines. The correction was shown to be in the order of 10 to 20%. The resulting accuracy depends on the accuracy of the used model to estimate the drag. The error in this model is estimated to be around 10%. This results in an estimated maximum error of 2% due to the line drag correction.

Centrifugal force

It was shown how the data is corrected for the influence caused by the centrifugal force on the kite. The correction was shown to be in the order of 1%. A possible error of 20% involved in this correction would result in a 0.2% error in the final result. Comparing to other errors involved, this error can be neglected.

Inertia

An error due to neglecting inertia effects is probably present. As explained in paragraph 6.5.5 the expected error is around 1% of the apparent wind velocity and 2% of the resulting aerodynamic force.

Difference between 2D and the actual 3D situation

Processing the results it was assumed that the situation during the sweeps can be seen as a 2D situation. The reason for this is that the kite sweeps are performed at such low height (6m) that the actual difference between 2D and 3D are very small. With 50m line length the expected resulting error is in the order of 0.7%.

Steering input during sweep

While steering the kite trough the path of the sweep steering input from the person steering can influence the outcome of the sweep. Each steering input is expected to reduce the velocity of the kite. It is difficult to quantify this effect, so it is recommended to focus further research on finding a method to reduce the uncertainty caused by this effect.

Related to this is a possible error due to vertical variations in the path of the kite. It is attempted to steer the kite in a path at 6 meters above the ground by aiming to fly at the height of the wind sensor. Deviations from this height could result in an error due to the existence of a wind gradient.

6.8 Conclusions and recommendations

The first objective of this chapter was to obtain an experimental method to obtain the aerodynamic properties of a kite. Different possible testing concepts were described and a concept referred to as crosswind kite testing was selected as the most appropriate for this thesis. A detailed description of the testing procedure was given and the required equipment was described.

The second objective was to describe the obtained experimental results. The obtained test data was described. The used method to process the obtained data into usable results was described and results were presented. It was shown that for the tested kite the lift to drag ratio varies roughly between 5 and 6.1.

After performing the described crosswind test a number of recommendations can be done to improve the described test method.

Accurately search for the minimum and maximum lift coefficient

Before testing a certain kite, it is not obvious at which setting the kite flies at its minimum or maximum lift coefficient. By adjusting the line setting during the test it becomes clear at which settings the kite will lose its ability to fly properly. By investigating these boundaries the maximum and minimum lift coefficient can be found.

Use an anemometer that is mounted on the kite

In order to obtain more accurate measurements of the apparent wind velocity, it can be recommended to mount an anemometer to the kite. When doing this, care has to be taken not to place the anemometer in the zone where the wind velocity is influenced by the kite. A GPS or other accurate timing method needs to be included in this sensor, to be sure that the measured values can be linked to the obtained velocities and line tensions. The measured signal has to be synchronized with millisecond accuracy.

Include an accelerometer in the kite

The extra information obtained from an accelerometer can be used to improve the velocity signal and to describe the path of the kite more accurately.

Increase the number of wind sensors on the beach

By monitoring the wind velocity at more than one location on the beach and possibly at different heights, more detailed information on the existing wind situation will be available.

Point for point method

It would be interesting to extend the method by using all data instead of only the peaks of each sweep. It should be possible to constantly track the aerodynamic coefficients. Some work in this direction has been done in an effort to increase the accuracy of the presented results, so far this has not lead to a satisfying improvement.

7 Component 4: Board

Figure 78, Author in action during the PKRA world cup in Walvis Bay, Namibia. (Final rank: 2nd) Source: Helena Darvelid.

The components Line, Rider and Kite have been treated in the previous three chapters. The last component that needs to be studied is the board. Due to its interaction with the surface of the water this is probably the most complex part of the system. Strong winds, that are required for high velocities, transform the water surface into a rough landscape with bumps and holes everywhere. In these conditions, speed kiteboarding can be compared to pushing a formula one car to its limits, on an off road track.

In this chapter the board properties are studied using both theory and experiment. In the first paragraph an experiment is described that serves to give a realistic indication of the lift to drag ratio and total drag force of a kiteboard. In the second paragraph the components building up the obtained drag force are studied. In the third and last paragraph of this chapter the board's lift coefficient is studied.

7.1 On the water kiteboarding test

The availability of theory that could help to identify the hydrodynamic properties of a kiteboard is limited. Available theory does treat the subject of planing plates. These plates are always positioned horizontally on the water. This is understandable as most theory was produced with either planing boats or water-based aircraft in mind. These crafts require mainly a vertical force to oppose their weight. A kiteboard needs to deliver both a vertical force (mainly to oppose the weight of the rider) and a large lateral force to oppose the force of the kite. This is why a kiteboard cannot be described as a horizontal planing plate with a pitch angle. A kiteboard is seen as a rolled, yawed and pitched planing plate.

It was decided to start this investigation with an experiment that should give a rough idea of both the direction and magnitude of the hydrodynamic force. It should be noted here that chapter 0 already gave an indication of the magnitude of the expected hydrodynamic force. It was found that for an expected total line tension between 600 N and 800 N the expected contact force between board and rider is between 700 N and 1000 N. The hydrodynamic force is more or less equal to the contact force between board and rider.

In this experiment both the line tension and the position of the kite with respect to the sailing course are determined. For this experiment the load cell logger, including the steering bar with 50 meter lines that was used during the kite experiment, could be used again. Both handheld GPS loggers, which were used during the kite analysis, could also be used again. Before entering the water, one GPS (the GT-31) was mounted on the rider's body, the other (the Q1300) was mounted to the kite.

Velocities positions and line tension where measured during a kitesufing session on the 8th of april 2009. The test location was Scheveningen beach, The Hague. The wind velocity at the moment of the experiment was 8m/s. The used kite was a 2008 Airush Flow 10. The used board is a custom race board. The conditions did not provide a speed record scenario; the wind was too light to set real records. Still this is seen as a test that can give an indication of the situation during a record attempt. Even in light wind it is possible to obtain a line tension that is a good indication of the line tension during a record attempt. The reason for this, is that the line tension is mostly the result of how the rider positions his center of gravity with respect to the board. This means that when the rider uses his full body weight and full strength to oppose the tension of the lines, the resulting line tension can be expected to be of the same order as when doing a speed run. Then the rider also uses all his strength.

The total line tension that was measured during this session is shown in Figure 79. It is seen that for this example the line tension ranges between 500N and 800N. This is roughly between 60 and 95% of the weight of the rider. This result confirms the conclusion drawn from the photo analysis of the rider in chapter 0.
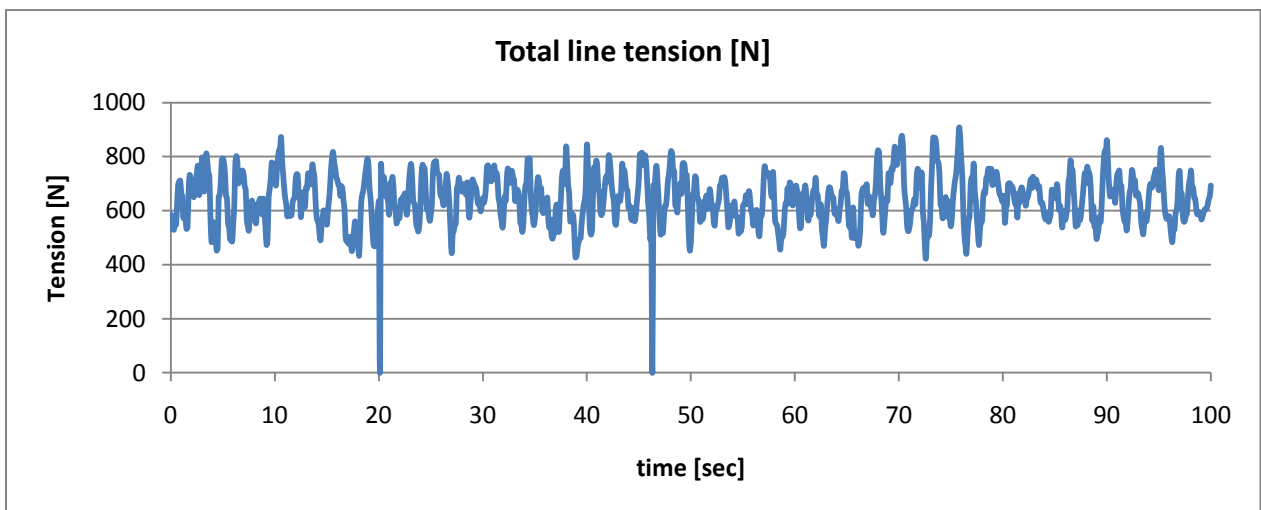

Figure 79, Line tension of the total of all 4 kite lines during a kitesession in Scheveningen. Windspeed 8m/s. Rider weight 80 kg, Kite, 10m Airush Flow 2008. Sailing on a close reach (75 degrees to true wind).
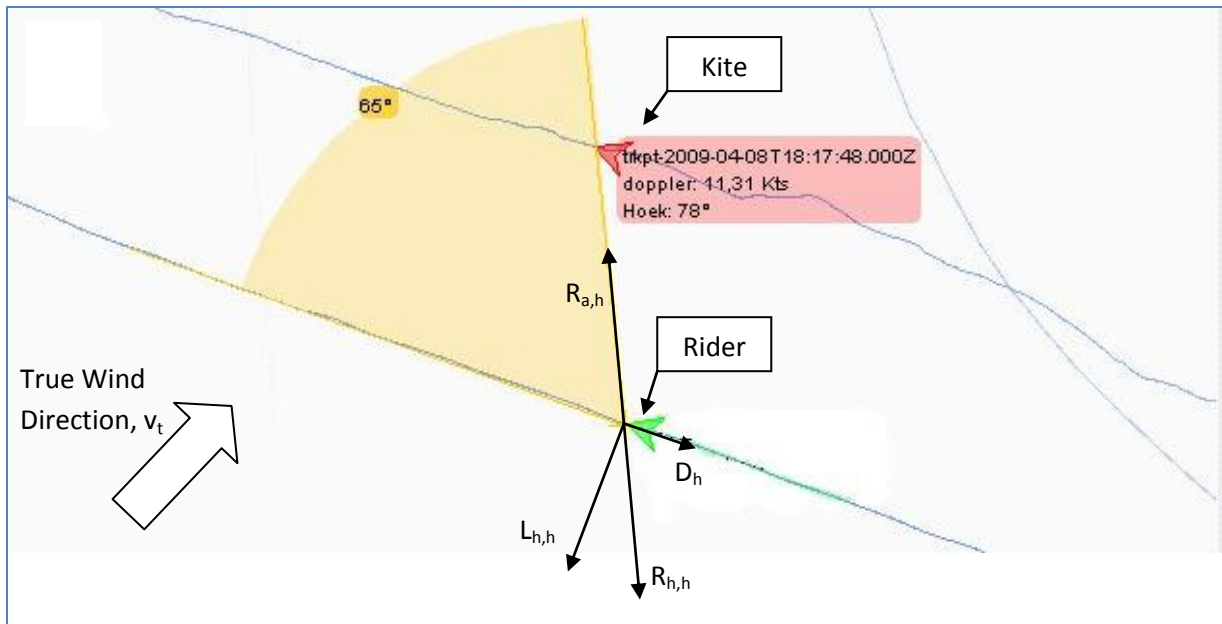
Figure 80, Sailing situation with one GPS logger in the kite and one on the body of the rider. Sailing direction from right to left. The kite is positioned slightly in front of the rider at an angle of 65degrees to the sailing direction. The arrow in the upper left corner points to the north. The wind direction is at 214 degrees. The course is slightly upwind, 74 degrees to true wind.

In Figure 80 the GPS track of both the kite and the rider is shown. The track was analyzed and it was found that the angle between the kite position and the sailing path remains constant at 65 degrees +- 2 degrees throughout this course. The position of the kite with respect to the rider indicates the direction in which the kite pulls. Also on other courses it was found that the angle between the kite position and the sailed course remained between 60 and 70 degrees.

This information can now be used to obtain a first estimate of the lift to drag ratio of the board. With both the direction and magnitude of line tension known the system can be cut into two pieces. On one end there is the kite with its aerodynamic force including the lines, on the other end there is the combination of board and rider. As this only serves as a crude indication of what can be expected from the hydrodynamic force, the drag force of the rider is conveniently neglected. It is assumed that $T_{line} = R_a$.

Looking at Figure 10 in chapter 3 explains how the horizontal component of the aerodynamic force $R_{a,h}$ needs to be balanced with the horizontal component of the hydrodynamic force $R_{h,h}$. Reversing the direction of vector $R_{a,h}$ directly indicates the direction of $R_{h,h}$.
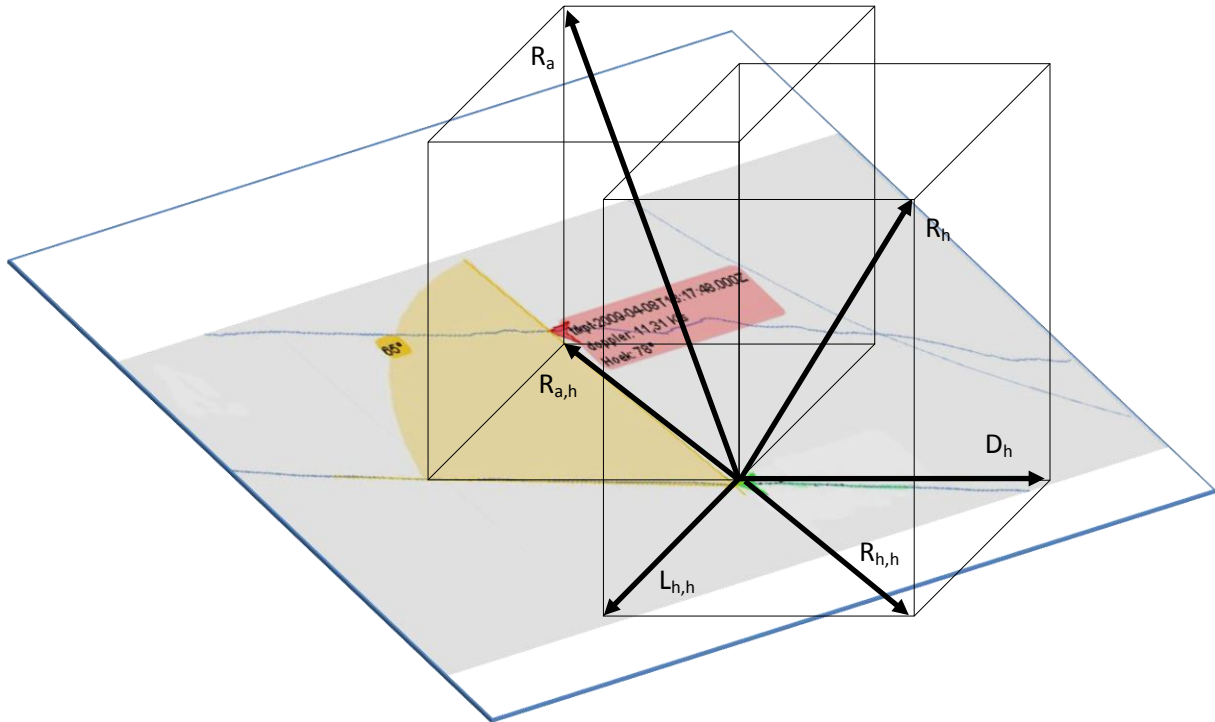
Figure 81, 3D representation of the the aero- and hydrodynamic relultant vectors R$_a$ and R$_h$ and their horizontal components.

Now for the obtained 60 to 70 degree angle between the kite lines and the travelled path the 2D hydrodynamic lift to drag ratio can be given. The board has a lift to drag ratio projected on the horizontal plane of $L/D = \tan(60\deg) = 1.7$ to $L/D = \tan(70\deg) = 2.7$. For the average airplane this would be a very low lift to drag ratio.

The average line tension was given to be 650N, it is estimated that the kite was flown at a height of 10 meter above the water and the used line length was 25 meter. The estimated hydrodynamic drag force is calculated as:

$$D_h = T_{line} \cos\left(\arcsin\left(\frac{KiteHeight}{LineLength}\right)\right) \cos(65\deg) =$$
$$650N \cdot \cos\left(\arcsin\left(\frac{10}{25}\right)\right) \cos(65\deg) = 250N$$

(7.1)

7.2 Kiteboard Drag

The total drag force of a kiteboard can be divided into a part lift induced or pressure drag and a part friction drag. For designing purposes it is important to know which part of the total drag force is produced by either the induced or the friction drag. A large friction drag could be reduced by trying to reduce the surface roughness or the wetted area. A large induced drag could be reduced by sailing under a lower angle of attack, and so by increasing the wetted area or the aspect ratio. In the first sub paragraph the friction drag will be studied. In the second sub paragraph the induced drag is addressed.

7.2.1 Friction Drag
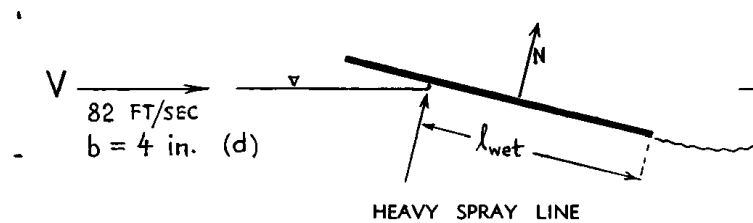
Figure 82, Lift coefficient on a flat rectangular planing surface as a function of wetted length. Source: (5)

In order to be able to estimate the friction drag of a kite board, it is first required to estimate the Reynolds number. The reference length that will be used to calculate the Reynolds number is the wetted board length. This is indicated by l_{wet} in Figure 82. The wetted length of a speed kiteboard is normally in the order of magnitude of 1m. This means that the expected Reynolds number at record speed of 25 m/s in 15°C water is around:

$$\mathrm{Re}_l = \frac{\rho_w v_s l}{\mu} = \frac{1025 \cdot 25 \cdot 1}{1.11 \cdot 10^{-6}} = 2.25 \cdot 10^7$$

(7.2)

An estimate of the board's friction drag can be obtained with the use of Schoenherr's practical from empirical formula (5). Where for Reynolds numbers between 10^6 and 10^8 it is given that: K = 0.044 and m = 6:

$$C_f = K / \mathrm{Re}_l^{1/m} = 0.044 / 2.25 \cdot 10^{7^{1/6}} = 0.0026$$

(7.3)

In order to be able to estimate the friction drag force it is also required to estimate the total wetted surface. The estimation of the total wetted surface is not as straightforward as it might seem. The question arises whether the wetted surface consists of only the part of the board that is truly below the surface of the water or if the wetted surface should include the spray that wets the part of the board that remains above the water surface. This is illustrated in Figure 83. The wetted area below the water surface is estimated at about half the wetted area including the area wetted by spray.

Figure 83, Looking at the bottom surface of the board during a speed run, it is clear that not the whole board is in contact with the water. Also next to the surface area that is below the water surface, there is an additional wetted area due to the spray above the surface. Picture: Graig Kolesky

Also it needs to be mentioned that the wetted area is by no means constant during a speed run. The board bounces over small waves and sometimes even completely loses contact with the water. The best that can be done here is to give a crude indication of the average wetted surface.

Due to the lack of literature on rolled planing plates an assumption needs to be made here. It is assumed that the friction drag depends on the wetted area including the area wetted by the spray. The reality is thought to lie somewhere between the two cases. The spray flows over the free bottom surface of the board but gradually loses some of its velocity and thus friction force. The induced drag and the lift force however are assumed to depend on only the board area that is below the water surface.

For a more or less triangular estimated wetted area of 0.5 x 1 m x 0.20 m = 0.10 m² this friction coefficient results in a friction drag force of:

$$D_{friction} = \frac{1}{2}\rho_w v_s^{\,2} C_f S_{wet} = \frac{1}{2} \cdot 1025 \cdot 25^2 \cdot 0.0026 \cdot 0.10 = 83N$$

(7.4)

Comparing this to the estimated total drag of 250N, it can be estimated in the current example that about 30% of the total drag force is due to friction drag. The resulting 70% (167N) is then due to induced drag. It has to be mentioned here that the estimates only serve as rough indication. A more detailed investigation is required to obtain more reliable results.

7.2.2 Induced Drag

This paragraph serves to indicate which formula could be used to relate the induced drag to the obtained lift.

Available theory only treats planing plates without any roll angle. Most theory was produced with either planing boats or water-based aircraft in mind. It has to be questioned whether the available theory is valid for the case of a kiteboard which is not planing in a horizontal manner but always with a certain angle of roll and yaw. In kitesurfing rolling the board is normally referred to as edging the

board. By rolling, the edge of the board is pushed into the water in order to keep the board from sliding sideways.

In reference (14) Shuford explains that, neglecting the airflow over the top surface of the board, the induced drag of a planing plate is purely related to the pressure on the bottom surface of the plate. The induced drag of a planing plate $C_{D,S}$, based on the wetted area, is given by the lift coefficient $C_{L,S}$ times the tangent of the board angle of attack τ:

$$C_{D,S} = C_{L,S} \tan \tau$$

(7.5)

The situation is sketched in Figure 84. For the situation of a rolled and yawed planing plate the same assumption applies. The airflow over the top surface can still be neglected. This means that rolling and yawing the board does not affect the above stated formula. Lift and pressure drag are simply two components in which the surface pressure forces can be decomposed. It is left for future research to further investigate this relation.
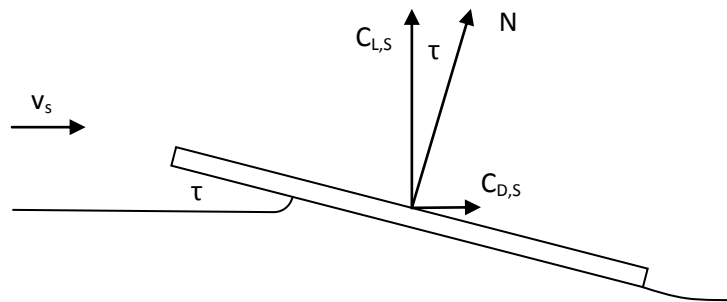
Figure 84, The induced drag coefficient $C_{D,S}$ is based on the lift coefficient $C_{L,S}$ and angle of attack τ.

7.3 Kiteboard Lift

The literature that was found on the subject of planing surfaces only covers the application of horizontal planing surfaces. A horizontal planing surface (flat or with an angle of deadrise, also called V bottom) only produces a vertical lift force, while for kitesurfing also a horizontal component of lift is required. In kitesurfing this horizontal component of lift is obtained by rolling the planing surface up to a roll angle of more than 45 degrees.
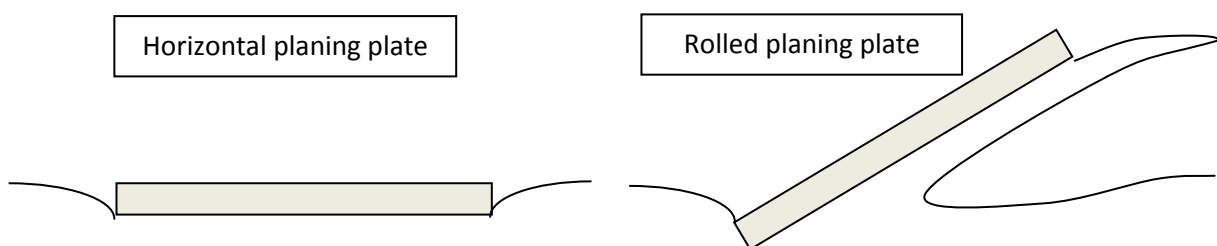
Figure 85, Horizontal and rolled planing plate seen from behind. The plate moves straight into the paper.

It is expected that the lift coefficient for a horizontal planing plate as obtained in literature (14) is always higher than the lift coefficient of a rolled planing plate. The reason for this is that in the rolled situation the water contacting the surface of the plate can easily be pushed upward to the water surface while in the flat planing situation the water is deflected down and sideways into the mass of water.

Possibly a rolled kiteboard could be best compared to one half of a planing plate with a V shaped bottom surface, or as Shuford (14) calls it, an angle of dead rise. Shuford proposes a formula to calculate the total lift of a horizontal planing plate with a certain angle of dead rise for different angles of attack:

$$C_{L,S} = \frac{0.5\pi AR\tau}{1+AR}\cos^2\tau\left(1-\sin\beta_e\right)+\left(C_{D,c}\right)_{\beta_e=0}\cos^3\tau\sin^2\tau\cos\beta_e \qquad \textbf{(7.6)}$$

Where $C_{L,S}$ is the lift coefficient based on the principal wetted area bounded by the trailing edge, the chines (intersection between bottom and sides of a flat or V bottomed boat) and the heavy spray line (not accurately defined, equivalent of the stagnation line).

$(C_{D,c})_{\beta=0}$ is the crossflow drag coefficient for a cross section having a flat bottom surface. Shuford determined this value to be 4/3 for models with a sharp chined or sharp edged plate.

β_e [rad] is the dead rise angle, the angle between the v shaped bottom surface and the horizontal.

AR is the aspect ratio defined as the b/l_m = the beam over the mean wetted length (distance from aft end of the planing surface to the mean of the heavy spray line.)

τ [rad] is the trim angle or angle of attack, defined as the angle between the bottom surface and the direction of travel. A kite board has a curved bottom surface; this makes it unclear how to compare the lift from a kiteboard to literature.

Shuford's formulas for lift and drag could be used in future research to further investigate the properties of the board. It was decided to choose the hydrodynamic force as one of the output parameters of the model. It was shown how the estimate the necessary parameters of the components line, rider and kite. Using sailing velocity, sailing direction and wind velocity from experience, it is possible calculate the hydrodynamic force that is required for equilibrium. The obtained results are presented in the next chapter.

8 Results

This report has shown how a kiteboarder was recognized as a sailing system with four components, lines, rider, kite and board. Using both theory and experiment each component was studied. The influence of each component on the velocity of the total system can only be explained while regarding the complete system. The main purpose of this chapter is to investigate what can be learned when the obtained knowledge is combined.

In order to combine the obtained knowledge two steady state models where build. The first one aims to estimate parameters for a known sailing velocity. The second model serves to predict the obtained velocity when all parameters are known. The second model can be used to predict the obtained sailing velocity after improving one of the components.

Using a steady state model is seen as a valid approach as at maximum speed velocity constant. There might be ways to obtain a higher peak speed by using what could be called dynamic maneuvers. For example it might be possible to increase the top speed by waiting for a gust and steering the kite up or down while bearing off downwind. Even though this is a perfectly valid way to obtain high velocities this type of maneuver is not taken into account in this thesis.

A model of the situation of a kitesurfer being propelled by the wind can be helpful to understand the situation better, but a model is only as good as you build it. There will always be phenomena that are not taken into account. Also those parameters that are taken into account will always have an uncertainty. These simplifications introduce errors into the model. The challenge of making a useful model is to leave out all insignificant parameters while ensuring that the link with reality stays as close as possible.

Results obtained from both models will be illustrated with the use of two cases. Two real life scenarios are sketched that have been obtained during speed kitesurfing competitions in 2008.

Scenario 1, Port St Louis

The first case played in April 2008 during a PKRA speed world cup competition in Port Saint Louis, France. The extremely strong wind during this competition allowed the competitors to obtain remarkably high speeds. Still the sailing direction, dictated by the local conditions, was too close to 90 degrees to break the world record. The author obtained a second rank in this competition. The best average 10 second run was obtained from GPS recordings and used as the first case.

Scenario 2, Luderitz

The second case played in October 2008 in Luderitz, Namibia. A group of kiteboarders had planned a full month of chasing records at a location that is known for its strong winds and flat water. The main reason for the higher velocities of this case can be found in the fact that the sailing direction was about 26 degrees more downwind. During this event both the Outright World record and the magical 50 knot barrier where broken. The author was able to break the Dutch National Record, 47.36 knots over 500m. The fastest 10 seconds during this run, obtained from GPS recordings, are used in to form the second case.

Variable	Port St. Louis	Luderitz
Average 10 second Sailing speed	21.6 m/s	25 m/s
Sailing direction	115 deg	141 deg
Wind velocity at 10m above the ground	23 m/s (9 Bft.)	22 m/s (9 Bft.)
Roughness length	0.005 m	0.005 m
Temperature	14 ˚C	17 ˚C
Air pressure	1000 hPa	1000 hPa
Humidity	50%	50%
Kite brand, type and size	Airush Flow RDLE 7m^2	Airush Flow 7m^2 2008
Kite projected area	5.2 m^2	5.2 m^2
Kite height above the ground	10 m	10 m
Kite L/D	5.2	5.2
Line length	25 m	25 m
Line thickness	1.3 mm	1.3 mm
Total tension in the kite lines	800 N	800 N

Table 9, Two cases are used to visualize the obtained modeling results. The input parameters of both cases are displayed in this table.

Results that were obtained using the parameter estimation model are presented in the first paragraph of this chapter. Results obtained using the speed prediction model, are presented in the second paragraph.

8.1 Parameter estimation results

Two cases have been described and were fed into a steady state model. The information given in Table 9 was required as input. The model uses this information to ensure a steady state situation. Obtained results are presented in Table 10.

Variable	Port St. Louis (% of total drag)	Luderitz (% of total drag)
Aerodynamics		
Apparent wind at the kite	24.0 m/s	15.9 m/s
Total Aerodynamic Force	803 N	782 N
Kite Drag Force	151 N (20%)	151 N (21%)
Kite Lift Force	786 N	785 N
CL kite (w.r.t. projected surface)	0.43	0.99
Line Drag Force	42 N (6%)	20 N (3%)
Rider Drag Force	133 N (18%)	92 N (13%)
Aerodynamic L/D (with respect to v_a at 10m)	2.2	3.0
Aerodynamic L/D 2D horizontal plane	2.0	2.7
Angle between 2D and 3D aero Aero	25 deg	25 deg
Hydrodynamics		
Total Hydrodynamic Force	964 N	944 N
Hydrodynamic Drag Force	483 N (56%)	458 N (63%)
Hydrodynamic Lift Force	834 N	826 N
Hydrodynamic L/D 3D	1.73	1.80
Hydrodynamic L/D 2D horizontal plane	1.16	1.20
Angle between 2D and 3D Hydro	48 deg	48 deg

Table 10, Two cases where described. Modeling results obtained for each case are given in this table.
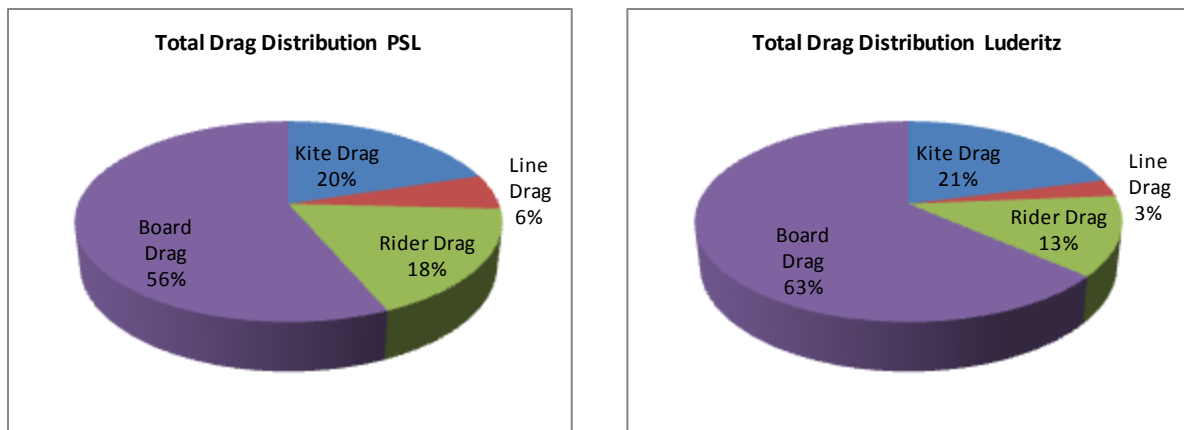
Figure 86, Distribution of the drag over the system components, for both cases.

Looking at the results from both cases it becomes clear that in this system the board is the largest source of drag. This gives a strong indication that an attempt to improve the board's efficiency could lead to a significant improvement of the sailing velocity.

It is remarkable that in Port St Louis the rider drag is almost equally important as the kite drag. In Luderitz the rider drag has a slightly smaller share, but can definitely not be neglected. Also the percentage line drag is much larger in Port St. Louis than in Luderitz. The smaller percentages rider and line drag in Luderitz are due to the sailing direction. Sailing more downwind in Luderitz reduces the apparent wind velocity. This reduction in apparent wind halves the line drag and reduces rider drag by 25%. Looking at the required lift coefficient, to produce the 800N line tension that was inserted in both cases, it becomes clear that the used lift coefficient in Luderitz was more than twice as large as the one used in Port St. Louis.

As explained in chapter 4 the lines where divided into 9 equally sized sections. Looking at how the total line drag is distributed over the lines indicates how the wind gradient influences both cases.
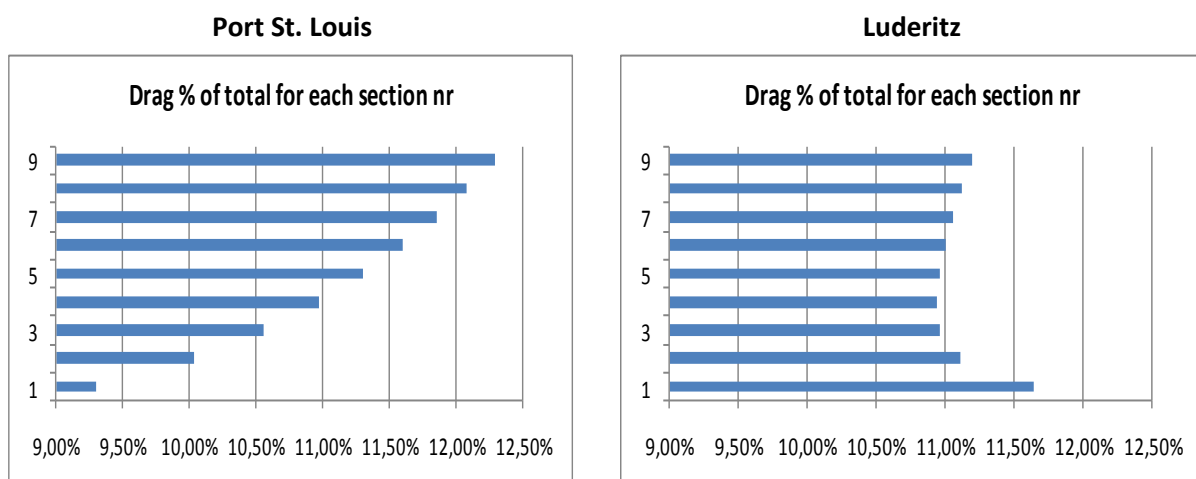
Figure 87, Percentage of the total drag on each line segment. Line segment 1 starts at the rider en line segment 9 ends at the kite. True wind varies with height and so does the apparent wind, this results in a different drag on each line section.

It is remarkable that in Port St. Louis the highest line drag component is found close to the kite, this is the location of highest apparent wind velocity. Racing on a more downwind course in Luderitz causes the highest apparent wind velocity to be near the rider and the lowest apparent wind velocity, and thus line drag, at line section 4.

Looking at the drag distribution over the different body parts of the rider a similar situation is found. Racing more downwind in Luderitz, creates a lower drag percentage on the head than in Port St. Louis.

Port St. Louis

Drag % per body part

Luderitz

Drag % per body part
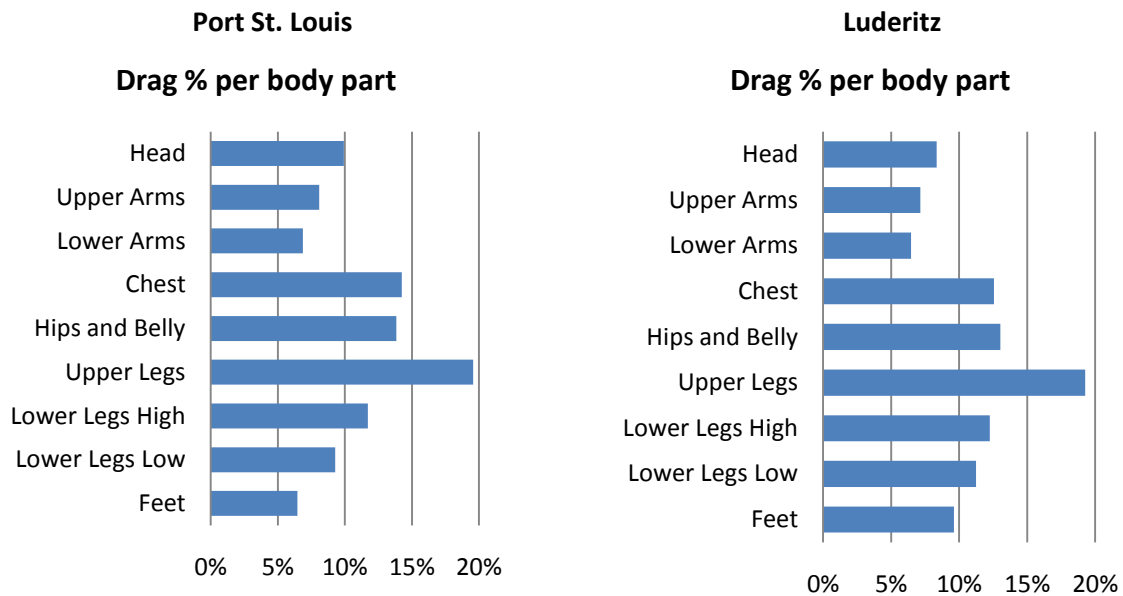
Figure 88, Percentage drag on each body part of the rider. In Port St. Louis a higher percentage drag is found near the head than in Luderitz.

Looking at Table 10 it is noted that the board lift to drag ratio is included in the list of output parameters. Building the model it was found that the board properties were the most inaccurate to estimate. Knowing which sailing velocities are reasonable it was decided to calculate the board properties as a function of all other parameters. The hydrodynamic force results after adding all aerodynamic forces. Projecting the hydrodynamic force on the horizontal plane, a horizontal lift to drag ratio can be found. In Port St. Louis this ratio is estimated at 1.16 and in Luderitz at 1.20. This remarkably low lift to drag ratio (compared to experience in the aerodynamic field) explains the high drag percentage that was found for the component board. Using Schoenherr's formula to estimate the friction drag of the board as explained in chapter 7, it was found that in Port St. Louis 31% of the board drag is due to friction. In Luderitz 36% is due to friction. The resulting drag is pressure drag.

After presenting the drag distribution results, that were obtained using the parameter prediction model, the effect of improving the system components is investigated in the next paragraph. For this the so called speed prediction model is used.

8.2 Speed Prediction and Improvement Strategy

In the previous paragraph it became clear how the involved drag is distributed over the different components. In this paragraph attention will be paid to which effect improvements to the system will have. In order to predict the obtained velocity it was necessary to build a second model. This model is called the speed prediction model. After improving one of the parameters, the model will find a new equilibrium by varying the system velocity. Being able to change parameters and predict the velocity, a number of optimization routines could be build around the model. Results obtained by improving and optimizing components are presented below.

Parameter Improvement		Velocity Improvement	
Parameter	**Improvement**	**Port St. Louis**	**Luderitz**
Kite L/D	+10%	1.55%	1.06%
Board L/D	+10%	3.36%	2.42%
Line drag	-10%	0.52%	0.16%
Rider drag	-10%	1.64%	0.73%

Table 11, Optimization results.

Line length optimization

Being able to predict the velocity it becomes possible to investigate different settings and see if the velocity can be increased. The line length is an interesting parameter to investigate, as it takes only a small effort to adjust the line length. As shown in the previous paragraph the drag contribution of the lines is limited. Shortening the lines could decrease the drag and thus increase the sailing velocity. With shorter lines the kite will also fly at a lower altitude. Due to the assumed wind gradient the true wind velocity will be lower at lower altitudes, so shortening the lines could also decrease the sailing velocity. Probably an optimal line length can be found. It was attempted to find the optimal line length for both described cases.

Optimizing the line length in the Port St. Louis case, results in a 35 meter line length and an increase in velocity of 0.55%. The increase in line length from 25 to 35 meter, shows that apparently the benefit of stronger wind at higher altitude outweighs the benefit of less frontal line area.

Optimizing the line length in the Luderitz case, results in a 109 meter line length and an increase in velocity of 7.79%. The benefit of stronger wind at higher altitude is even larger in this case. It still needs to be investigated if the large line length of 109 meters is practically possible. Long lines are known to reduce the feeling with the kite, due to damping of steering inputs.

Sailing direction optimization

Looking at the two described cases it can already be seen that the highest velocity is obtained on a course that is most downwind. The sailed course is for a large part defined by the angle between the wind direction and the used beach. Sailing with offshore wind it is favorable to stay as close to the beach as possible. In strong wind waves develop within a short distance, the larger the distance from the beach, the larger the waves. It is still interesting to investigate the optimal course.

Optimizing the sailing direction in the Port St. Louis case, results in a 152 degree course. The velocity would then increase by 29.3%. This clearly illustrates that the sailing direction in Port St. Louis was far from optimal.

Optimizing the sailing direction in the Luderitz case would result in a 154 degree course. The velocity would then increase by 3.28%. Also in Luderitz it would be beneficial to sail a more downwind course.

It is concluded that optimizing the line length and sailing direction has a large influence on the obtained velocity. Further research is recommended on the possibilities of optimization.

9 Conclusions and recommendations

9.1 Conclusions

To recapitulate from the introduction:

This thesis aims to obtain a general understanding of what properties are of importance to obtain a high kiteboarding velocity and to understand how each component contributes to the finally obtained velocity.

Chapter 2 explained how a kiteboarder can be seen as a sailing system and how this system can be separated in four components: the lines, the rider, the kite and the board.

In chapter 3 the general performance of a sailing system was investigated. It is concluded that the properties 'wind velocity' and 'lift to drag ratio of the system' define the sailing velocity. It was shown how to calculate the sailing speed, when those two properties are known. There is a linear relation between the wind and the sailing velocity when the lift to drag ratio is constant. A higher wind velocity results in a higher sailing speed. The lift to drag ratio of the system is defined by the horizontal components of the hydrodynamic and aerodynamic lift to drag ratio. This means that in order to obtain a high sailing velocity, both these horizontal lift to drag ratios need to be high.

In chapter 4 to 7 the components of the system were taken apart and the aerodynamic performance of each component was investigated. For each component a method was given to estimate the total drag force.

In chapter 4 it is first shown how to model the line drag during sailing. In order to account for large variations in apparent wind velocity over height, the line is separated into different sections. Secondly it is shown how to model the line drag during the crosswind test. It is concluded that in order to apply a line drag correction to the test results, the line drag resultant on the kite can be estimated with a single drag coefficient. This drag coefficient is defined with respect to the line frontal area and the dynamic pressure at the kite. The coefficient is estimated at 0.31.

In chapter 5 it is shown how to model the aerodynamic drag on the rider. Similar to the modeling of the lines, the rider is divided into components to account for a variation in flow velocity over height. The magnitude of the mechanical contact forces, of the board and the lines acting on the rider, is estimated using a picture analysis. It is concluded that during a speed run, the line acts on the rider with a force between 70% and 95% of the body weight. The board acts on the rider with 85% to 116% of the body weight.

In chapter 6 an experimental approach is described that can be used to test kites. The experiment is based on flying a kite from one side to the other while recording its flying velocity and line tension. The results obtained for a tested kite are presented. It is shown that for the tested kite the lift to drag ratio varies between 5 and 6.1 in normal use.

In chapter 7 it is described how to estimate the board friction and pressure drag. It is concluded that the board lift and drag can best be estimated using a parameter estimation model. Sailing velocities

from experience in combination with the drag estimations of the components line, rider and kite, can be used to estimate the hydrodynamic lift and drag forces.

In chapter 8 the components were combined again and inserted into two different models. Two real life cases with record conditions were described in order to present the obtained results. It was discovered that the hydrodynamic drag force of the board generated the highest drag contribution, between 56% and 63% of the total drag. This indicates that improving the efficiency of the board could lead to a large velocity increment. The contribution of the kite is estimated between 20% and 21%. The lines contribute 3% to 6% of the total drag force and the rider 13% to 18%. It was also shown that optimization of line length and sailing direction could result in a large improvement of the sailing velocity.

The obtained knowledge can be used as a basis to improve the performance of the kiteboarder and provides a first step towards breaking the world speed sailing record.

9.2 Recommendations

Looking at the results from this thesis a number of recommendations can be done:

Board research

Looking at the large amount of drag produced by the board it is highly recommended to investigate the possibilities to improve the hydrodynamic performance. A separate research focused on the properties of the board could lead to large improvements.

Optimization

Looking at the easily obtained velocity increments by optimizing the line length and sailing direction, it is advised to further investigate the optimization possibilities. The practical limitations of these theoretical outcomes should be investigated.

Kite selection

It is advised to use the described kite test to select the best kite available on the market. Knowledge obtained from these test results can then be used in the design of even better kites.

Recapitulating the recommendations from the kite experiment of chapter 6:

Accurately search for the minimum and maximum lift coefficient

Before testing a certain kite, it is not obvious at which setting the kite flies at its minimum or maximum lift coefficient. By adjusting the line setting during the test it becomes clear at which settings the kite will lose its ability to fly properly. By investigating these boundaries the maximum and minimum lift coefficient can be found.

Use an anemometer that is mounted on the kite

In order to obtain more accurate measurements of the apparent wind velocity, it can be recommended to mount an anemometer to the kite. When doing this, care has to be taken not to place the anemometer in the zone where the wind velocity is influenced by the kite. A GPS or other

accurate timing method needs to be included in this sensor, to be sure that the measured values can be linked to the obtained velocities and line tensions. The measured signal has to be synchronized with millisecond accuracy.

Include an accelerometer in the kite

The extra information obtained from an accelerometer can be used to improve the velocity signal and to describe the path of the kite more accurately.

Increase the number of wind sensors on the beach

By monitoring the wind velocity at more than one location on the beach and possibly at different heights, more detailed information on the existing wind situation will be available.

Point for point method

It would be interesting to extend the method by using all data instead of only the peaks of each sweep. It should be possible to constantly track the aerodynamic coefficients. Some work in this direction has been done in an effort to increase the accuracy of the presented results, so far this has not lead to a satisfying improvement.

10 Bibliography

1. TheFreeDictionary. [Online] [Cited: 10 16, 2009.] http://www.thefreedictionary.com.

2. Dictionary.Com. [Online] [Cited: 10 16, 2009.] http://dictionary.reference.com/.

3. **WSSRC.** World Sailing Speed Record Counsil. [Online] 2009. http://www.sailspeedrecords.com/.

4. **Stull, R.B.** *Meteorology for Scientists and Engineers.* University of Britisch Columbia : Brooks/Cole.

5. **Hoerner, S.F.** *Fluid Dynamic Drag.* USA, 1965.

6. **Melkert, Joris A.** *Verslag van de eerste onderzoekingen aan de Stratow-configuratie.* Alphen aan de Rijn, 1992.

7. Matbase. [Online] [Cited: 9 9, 2009.] http://www.matbase.com/material/fibres/synthetic/dyneema/properties.

8. **Stevenson, J.C.** *Traction Kite Testing and Aerodynamics, PhD thesis.* University of Canterbury, 2003.

9. **Stevenson, J.C.** *Circular flight kite tests: converting to standard results.* The Aeronautical Journal, 2006.

10. **De Wachter, A.** *Deformation and Aerodynamic Performance of a Ram-Air Wing.* TU Delft, 2008.

11. **Barlow, J.B.** *Low-Speed Wind Tunnel Testing.* New York : John Wiley & Sons, Inc., 1999.

12. **Stull, Roland B.** *An Introduction to Boundary Layer Meteorology.* Vancouver, Canada : Springer Science + Business Media B.V., 2009. 978-90-277-2769-5.

13. **Ruijgrok, G.J.J.** *Elements Of Airplane Performance.* Delft : Delft University Press, 2004.

14. **Charles L. Shuford, Jr.** *A theoretical and experimental study of planing surfaces including effects of cross section and plan form.* Langley Field, Va : Langley Aeronautical Laboratory, National Advisory Committee for Aeronautics, 1956. 1355.

15. **Payne, P.R.** *Design of High-Speed Boats: Volume 1 Planing.* Fishergate, 1988.

16. **Van der Vlugt, R.** *Speed Kite Project.* Delft, 2008.

17. **Strganac, Donald T. Ward and Thomas W.** *Introduction to Flight Test Engineering.* Iowa, USA : Kendall Hunt Publishing Company, 1996.

18. **Loyd, Miles L.** *Crosswind Kite Power.* Livermore, Calif. : American Institute of Aeronautics and Astronautics, 1980. 80-4075.

19. **Marchaj, C.A.** *Aero- Hydrodynamics of Sailing.* : Dodd, Mead & Company, 1979.

20. **Payne, Peter R.** *Design of High-Speed Boats Planing.* : Fishergate Inc, 1988.

21. KNMI. [Online] http://www.knmi.nl/klimatologie/daggegevens/index.cgi.

Appendix A: Experimental results of the 2008 Airush Flow 5

This appendix contains the experimental results obtained for the Airush Flow 5 m^2. This is the same brand and type as the kites that were used in the described cases of chapter 8. In chapter 6 it was decided to present only the experimental results obtained for the Flysurfer Pulse 6 m^2. The Flysurfer was most accurately tested and results could be compared to the results obtained by De Wachter (10). The obtained relation between lift coefficients lift coefficients and lift to drag ratio is presented in the following two graphs:

The lift coefficient is calculated with respect to an estimated projected area of 3.75 m^2.
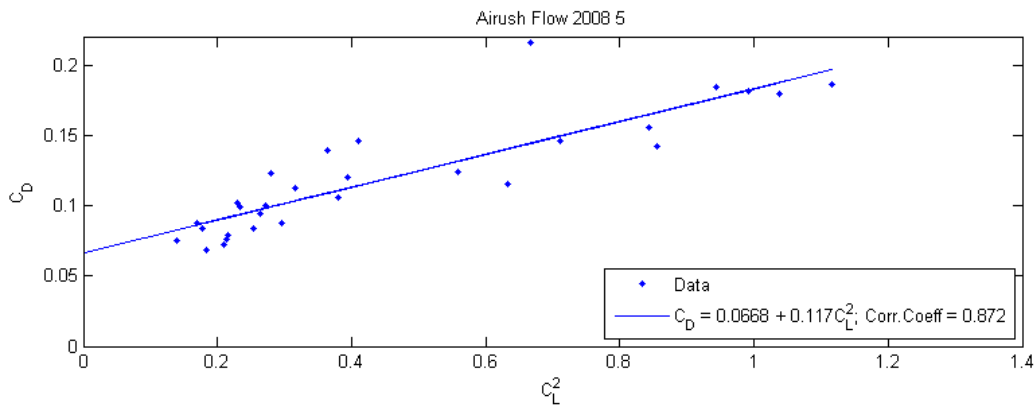
Figure 89, Experimentally obtained relation between the kite drag coefficient and the lift coefficient squared.
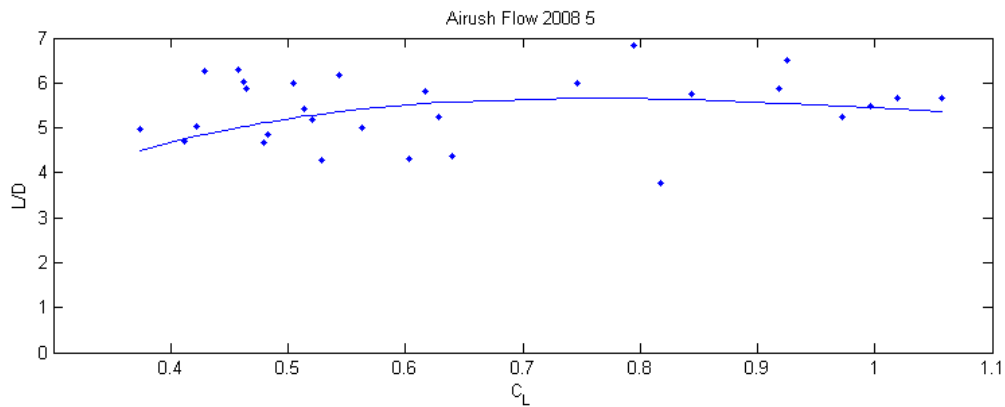

Figure 90, Experimentally obtained relation between the lift coefficient and the lift to drag ratio.